Structures of the deep bedrock in Gothenburg

A structural documentation of the GE1 drill core

Julia Ladefoged

Degree of Bachelor of Science
with a major in Earth Sciences
15 hec

Department of Earth Sciences
University of Gothenburg
2021 B-1138

UNIVERSITY OF GOTHENBURG

UNIVERSITY OF GOTHENBURG
Department of Earth Sciences
Geovetarcentrum/Earth Science Centre

Structures of the deep bedrock in Gothenburg

A structural documentation of the GE1 drill core

Julia Ladefoged

ISSN 1400-3821

B1138
Bachelor of Science thesis
Göteborg 2021

Mailing address	**Address**	**Telephone**	
Geovetarcentrum	Geovetarcentrum	031-786 19 56	Geovetarcentrum
S 405 30 Göteborg	Guldhedsgatan 5A		Göteborg University
			S-405 30 Göteborg
			SWEDEN

Abstract

Gothenburg Energy, SGU and Gothenburg University are currently investigating the possibilities of a deep geothermal energy plant in Gothenburg. In their first investigations there have been a 1 km drilling in Högsbo. The aim of this thesis was to provide a structural documentation of the rocks from the first 555m of the Gothenburg Energy 1 (GE1) drill core, as well as determining the rebound number and the P-wave propagation time through different lithologies of the drill core. The lithologies and radioactive isotope concentrations has been described by Hynynen (2021) and a combined log of the core will be included in both theses.

The foliation throughout the core is generally dipping gently to moderately to the south, southeast and north, relative to the orientation, however the foliation is changing with depth. The fractures of the core exhibit different dip and dip direction depending on depth, but most of the fractures are dipping moderately to gently to the east and southeast. There is no indication of increased number of fractures with depth. The angular relation between mean foliation sets and mean fracture sets indicate there are older fractures which have been folded with the foliation and younger fractures which cross the foliation.

Overprinting foliation and folded folds have been observed at several locations, implying at least two different deformation events have altered the bedrock.

Measured Lineations on fracture planes are mostly plunging steeply, indicating vertical movements. Lineations on foliation planes are plunging gently to the N-S and NW-SE, resembling the orientations of the intersection lineations from the observed overprinting foliations. They could therefore be interpreted as lineations with similar origin.

Further research is needed to draw any conclusions from the investigated mechanical properties. Similarly further investigations are needed to evaluate if Högsbo would be suitable for a deep geothermal energy plant.

Table of content

1. Introduction

In recent decades, the negative effects of human emissions have been recognized, and its large impact on the environment is a reality we are already facing. As a consequence, the demand for renewable energy sources is rapidly increasing and one such fossil free alternative energy source is deep geothermal energy.

Exploration projects of utilizing deep geothermal energy have grown in popularity of lately and advancements in drilling technology has made it possible to reach greater depths faster (Rosberg & Erlström, 2019). This could lead to lower costs and in turn make deep geothermal energy plants both environmentally and economically sustainable.

Deep geothermal energy is the heat generated from the earth's interior, primarily generated by the decay of radioactive isotopes and the residual heat from the accretion of the earth. The increasing geothermal gradient can be exploited by drilling to a depth where liquid can be heated to 70°C or 150°C for heating respectively electricity (Institute of seismology university of Helsinki, 2020). In the Fennoscandian shield where the geothermal gradient is quite low a drilling of approximately 6-9km is needed (Institute of seismology university of Helsinki, 2020).

The principle of utilizing deep geothermal energy revolves around injecting a liquid into the bedrock, either through a closed or an open system, where heat transfer from the bedrock to the liquid. The heated liquid can then be extracted from a second drill hole, see *Figure 1* (Institute of seismology university of Helsinki, 2020).

For large volumes of liquid to be stored and circulated through the bedrock, the permeability needs to be of moderately high levels, usually acquired through the accessibility of fractures. However, the permeability in crystalline rock decrease with depth, therefore the need of enhancing the permeability may occur, thus creating an enhanced geothermal heat production, EGS (Institute of seismology university of Helsinki, 2020). EGS is acquired by hydraulic stimulation, where large volumes of liquid are injected to the bedrock, expanding fractures and zones of weaknesses, consequently increasing the permeability (Leary et al., 2017). The objective is to create a consistent and sufficiently large fracture network, where the injected liquid has time to heat up. However, if the fractures expand too much the liquid circulation will go faster than the heat transfer, then he extracted liquid might not get sufficiently heated to be used for heating or electricity (Institute of seismology university of Helsinki, 2020).

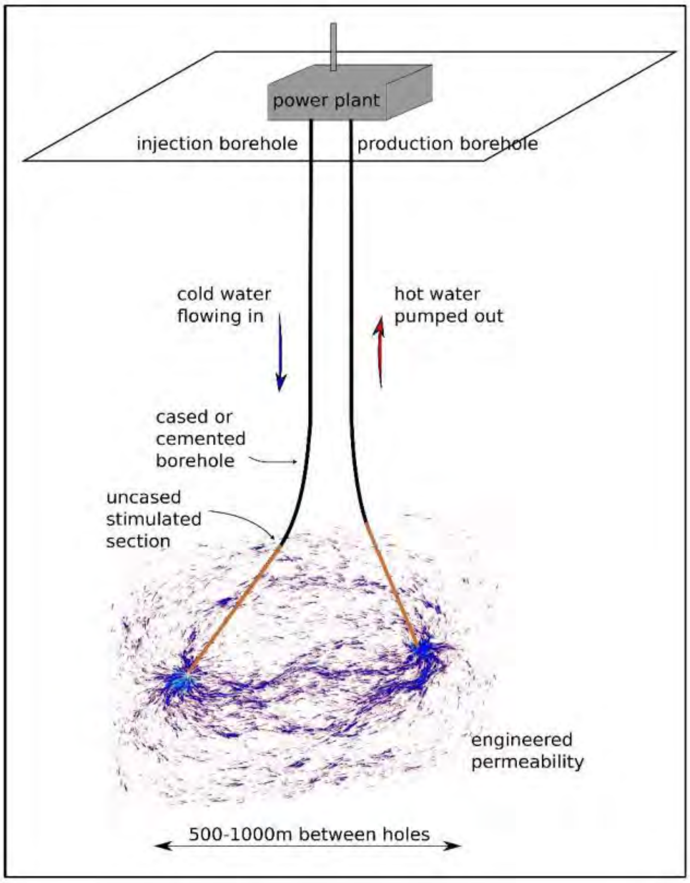

Figure 1. Illustration of a deep geothermal energy plant, where water is injected to the bedrock and connected fractures enable the water to flow from an injection drill hole to a production drill hole. (Institute of seismology university of Helsinki, 2020).

The Swedish geology is far from optimal for exploiting deep geothermal energy. The crystalline bedrock is making it more difficult to create a reservoir for storing heated liquid, compared to more permeable sedimentary rocks.

However, there is an ongoing deep geothermal energy exploration project in Finland, Espoo, with similar bedrock conditions as Sweden. Which poses the question, would this be possible in Sweden as well?

Gothenburg Energy, SGU and Gothenburg University are currently working with a deep geothermal exploration project in Gothenburg, where a 1 km deep bedrock drilling has been performed in Högsbo (57.655697, 11.951559), see *Figure 2*. This is the beginning of an investigation considering if Gothenburg could be suitable for a future deep geothermal energy plant.

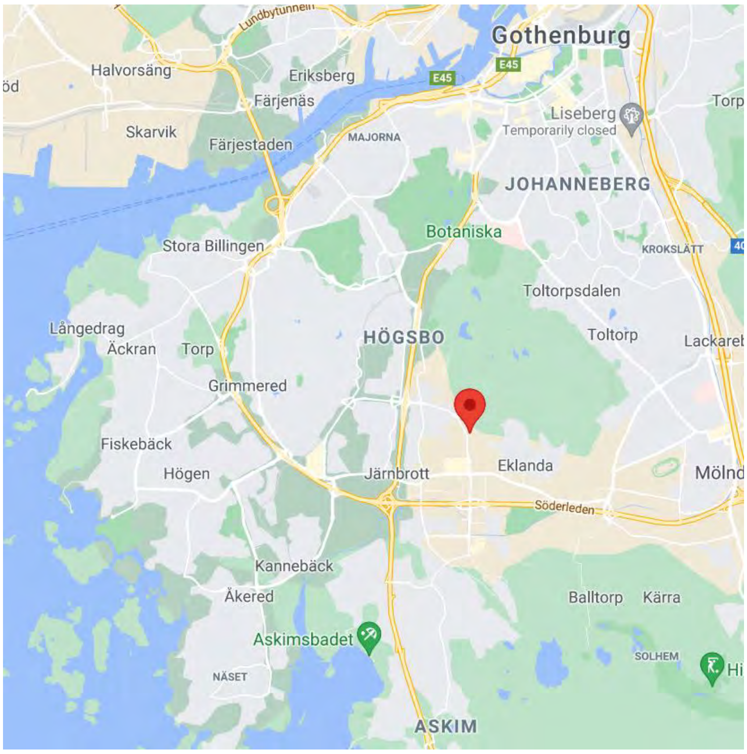

Figure 2. Overview of the GE1 drill core drilling location in Högsbo, 57.655697, 11.951559 (Google, n.d).

For a future deep geothermal energy system to work in the Gothenburg area there needs to be a sufficient geothermal gradient and enough fractures for liquid to be stored in the bedrock. Vertical fractures are of importance as they make it possible to transport water to deeper depths. However, to transport water from an injection drill hole to a production drill hole, the fractures also need to be connected, see *Figure 1*. This could be achieved by stimulating the bedrock or existing fractures. Therefore, it is important to know both the mechanical and structural properties of the bedrock.

1.1 Aim

The aim of this thesis is to provide a structural documentation of the rocks from the first 555m of the Gothenburg Energy 1 (GE1) drill core, as well as determining the rebound number and the P-wave propagation time through different lithologies of the drill core. The thesis will also briefly investigate the possibility of different fracture patterns and discuss structural features and their geological implications.

The documentation will contribute to an increased understanding of the deep bedrock in Gothenburg. Furthermore, the structures and mechanical properties can be used to assist a first evaluation if utilizing deep geothermal energy at the investigated area would be suitable, from a structural perspective.

The record of the first 555m will be presented in two separate theses, Hynynens *Lithological investigation and radioisotope concentrations in pilot borehole GE1, Högsbo - A first step towards geothermal energy in Gothenburg, Sweden* (2021), will describe the lithology and radioactive isotope concentrations, whereas this thesis will provide structural observations and some mechanical properties. Observations and measurements from both theses will be illustrated in a combined log, which will be included in both theses.

1.2 Regional Geology of Gothenburg

The bedrock of Gothenburg belongs to the Idefjorden terrane, which is a part of the Sveconorwegian province (Bingen et al., 2008). The Sveconorwegian province mainly formed during the Gothian orogeny, when the Fennoscandian shield started to grow towards the west (Gorbatschev & Gaál, 1987). The bedrock has then been further altered by the Gothian orogeny (1750-1550 Ma) and the Sveconorwegian orogeny (1200-900Ma) (Gorbatschev & Bogdanova, 1993; Gorbatschev & Gaál, 1987).

The Swedish regions of the Sweconorwegian province extends from the Protogin zone (PZ) in the east to the Swedish coastline in the west (Lundqvist et al., 2011). The Sveconorwegian province is divided into the Telemarkian terrane, the Bamble terrane, the Kongsberg terrane, the Idefjorden terrane (western- and median segment) and the Eastern segment, see *Figure 3* (Bingen et al., 2008).

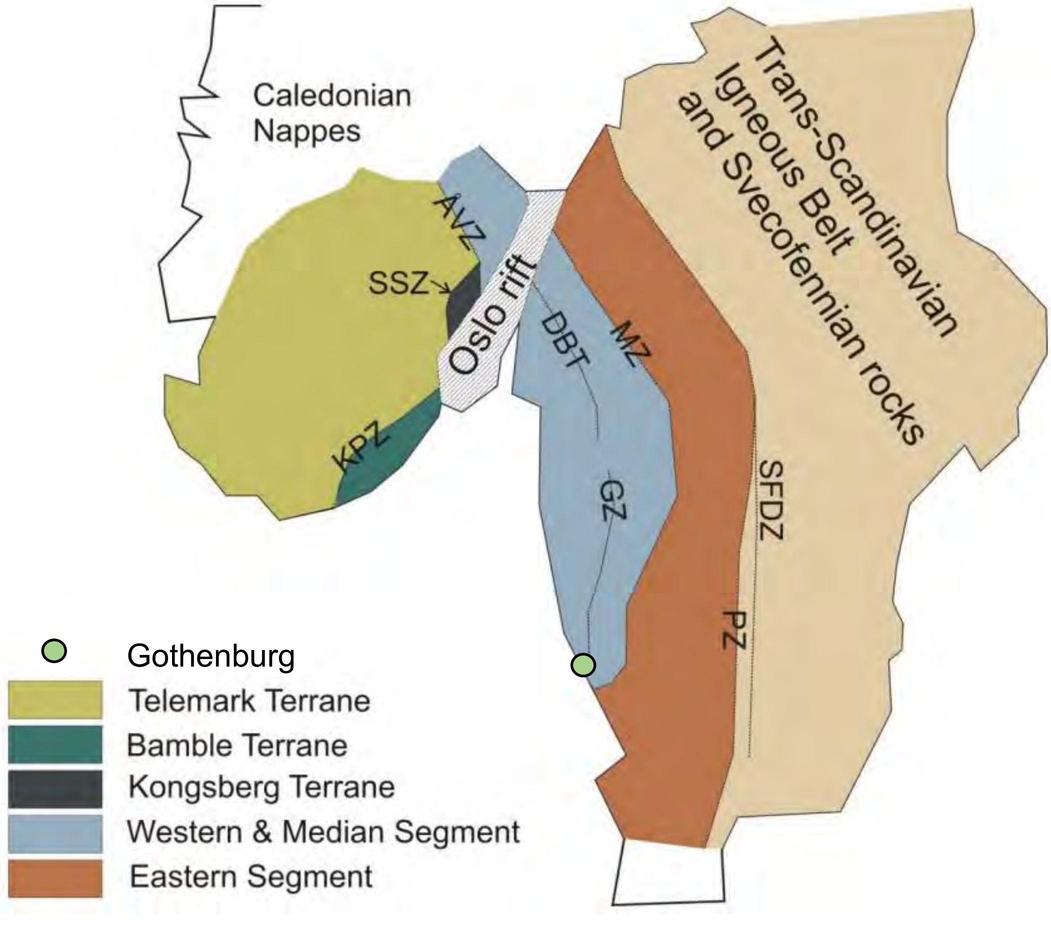

Figure 3. The different tectonic units of the Sweconorwegian province (Hegardt, 2010), modified with an approximate location of Gothenburg.

The Eastern segment and the Idefjorden terrane are separated by a west dipping fault zone, the Mylonite zone (MZ) (Lundqvist et al., 2011). The Idefjorden terrane further consists of the Stora Le Marsstrand formation in the west, followed by the Hissing suite (aka B-granite) and the Gotheburg suite (aka A-granite) to the east, see *Figure 4* (Åhäll & Connelly, 2008).

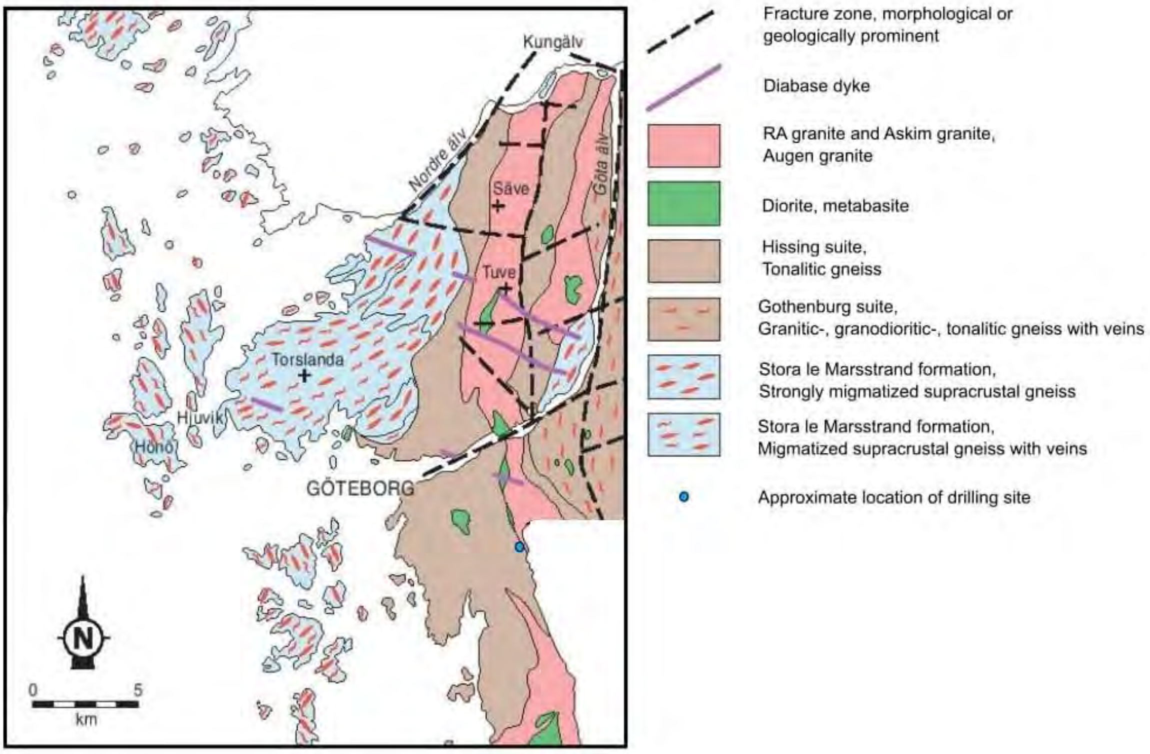

Figure 4. Modified geological map of the western segment (SGU, 2000).

The western parts of the Idefjorden terrane were formed approximately 1760Ma from a combination of sedimentation and volcanism (Åhäll & Daly, 1989). Sedimentary rocks were metamorphosed and folded by the Gothian and Sweconorwegian orogenesis, which resulted in the dominating Greywacke metasediments of the Stora Le Marsstrand group (Åhäll & Daly, 1989). 1634-1594Ma, during the Gothian orogeny, differentiated magma intruded the eastern parts of the Western segment and formed a bedrock with intermediate granitoid composition, which were later folded and deformed, today known as the Gothenburg suite (Åhäll & Connelly, 2008). At later stages of the Gothian orogeny, approximately around 1560Ma, another differentiated magma intruded the western segment, with a slightly greyer granitic-, granodioritic- and tonalitic composition, later deformed by the Sveconorwegian orogeny, the Hissing suite (SGU, 2006).

Between the Gothian and Sveconorwegian orogeny an intraorogen bimodal magmatism intruded the Western segment and resulted in north-south striking granitic bodies, such as the Askim granite (1336Ma) and the Kärra granite (1311Ma) (Lundqvist et al., 2011). These have been interpreted as rifting events or crust extension, between the Gothian and the Sveconorwegian orogeneses, therefore these intrusions have been used to distinguish deformations from different orogeneses, as they have only been altered by the Svegonorwegian orogeny (Park et al., 1991).

The Sveconorwegian orogeny deformed the western parts of the Idefjorden Terrane in a north-south trending orientation and close to the surface, most of the units generally dip medium steeply to steeply to the west (SGU, 2006). The orogeny also created the previously mentioned shear zones, the Protogin zone (PZ), the Mylonite zone (MZ) and the Göta älv zone (GZ).

The Protogin zone, the eastern boundary of the eastern segment mainly exhibit extensional shear zone structures (Bingen et al., 2008). Slightly further to the east the Sveconorwegian front deformation zone (SFDZ) mark the limit of where deformation from the Sveconorwegian orogeny can be observed (Bingen et al., 2008). The Mylonite zone, the eastern boundary of the Idefjorden Terrane, is a west dipping shear zone. Interpreted as a result of top to the southeast thrusting, followed by a more eastern movement, during a compression event of the crust (Viola, et al., 2004). Observed localised extensional shear zone structures, described by Berglund (1997), indicate the zone was reactivated during an east-west crustal extension (Viola, et al., 2004). The Göta älv zone, the boundary between the western and the median segment, show signs of similar thrust movements as the Mylonite zone (Park et al., 1991). However, in the coastal regions, as well as the Lysekil- Marsstrand area, north-south sinistral shear zones have been observed (Park et al., 1991). It is important to understand that the Göta älv zone is not a sole shear zone, there is a wide network of shear zones branching out from it, further described by Park et al. (1991).

Local measurements of structures in the Gotheburg area indicate that the foliation at the surface is dipping moderately to steeply to the west (SGU, 2006). Drill cores from the West link project also provide foliation measurements from central Gothenburg (approximately from Olskroken to Korsvägen), where the foliation is dipping shallowly to steeply (20-70°) to the west (Medan, 2015). Which apart from the dip angles coinsides with SGUs (2006) surface mapping. Measurements from the Götatunnel and the Nygårdstunnel also suggest that the foliation is dipping shallowly to the west, however is changing orientation with depth due to folding (Persson, 2007).

Fractures found in the West link project were divided into 5 different age groups depending on the mineral coatings of the fractures (Medan, 2015). Fracture group 1 was dipping steeply to the southwest; fracture group 2 was dipping to the south and the north, as well as reopening previous fracture set; fracture group 3 and 4 were dipping shallowly to the northwest and reopening previous fracture sets; fracture group 5 was reopened fracture sets. Generally the younger generation of fractures seemed to be less steep than the older generation of fractures. Identified fracture groups from the Götatunnel and the Nygårdstunnel were mainly dipping shallowly to the west and steeply dipping to the north and south (Persson, 2007).

In short, there is a great complexity to the geological settings of the Gothenburg area and further structural information from the deep bedrock could help to improve or strengthen already advanced theories of how the bedrock was formed and deformed.

1.3 Structures in drill cores

Structural information from drill cores can give us valuable knowledge of tectonic stresses and structural history (Chakraborty & Mukherjee, 2020). However, a fundamental problem with interpreting structures in drill cores is the cylindrical geometry of the core, combined with the drilling orientation, which complicates the geometry of already complex structures even further. Another difficulty is to recognize large scale structures, although small structures will often indicate the possibility of large-scale structures with associated attributes (Marjoribanks, 2010).

Planar features such as bedding, foliation, veins, fractures, etc. will be recognized as ellipses on the drill core surface, see *Figure 5*. A particular planar structure is mylonitic foliation, which is when the foliation spacing gradually get smaller and subsequently a stronger banding is created. This is due to high strain, which flatten and transform the rock and is usually associated with shear zones formed during plastic deformation (Fossen, 2010).

Linear structures can be observed along fracture planes or separated foliation planes, there can also be penetrative mineral lineations, which can be seen throughout the core (Marjoribanks, 2010).

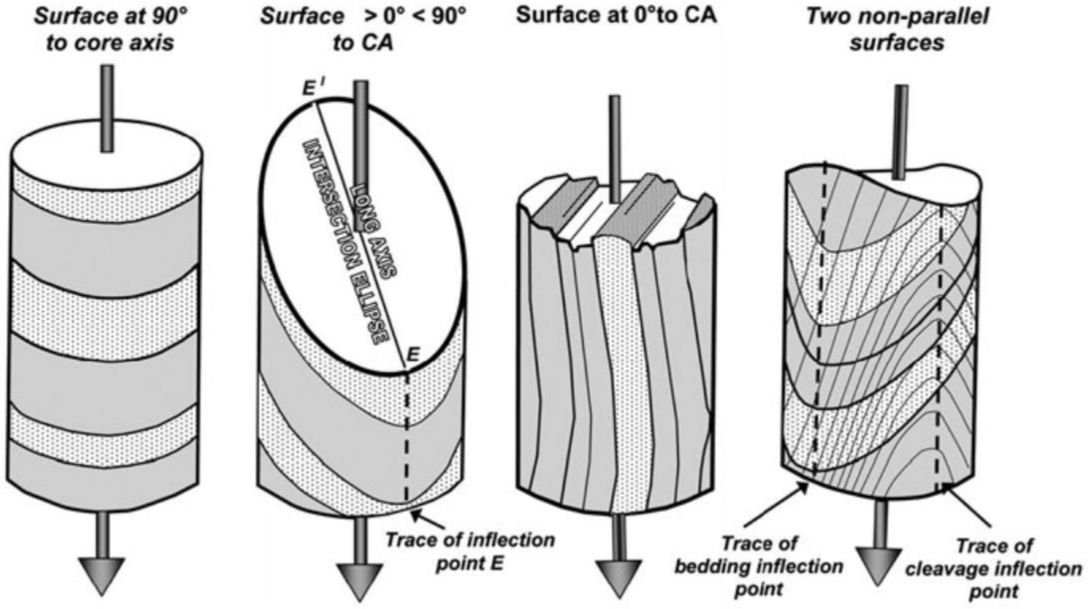

Figure 5. Planar structures in cylindrical drill cores (Marjoribanks, 2010).

Folds tend to have quite complicated appearances on the drill core surface and there are several different categories of folds. A widely known and well-established way of describing folds is Fleutys (1964) classification, where folds are divided according to the plunge of the hinge line and the dip of the axial surface, see *Figure 6*. The classification makes it easier to determine how different folds have been shaped.

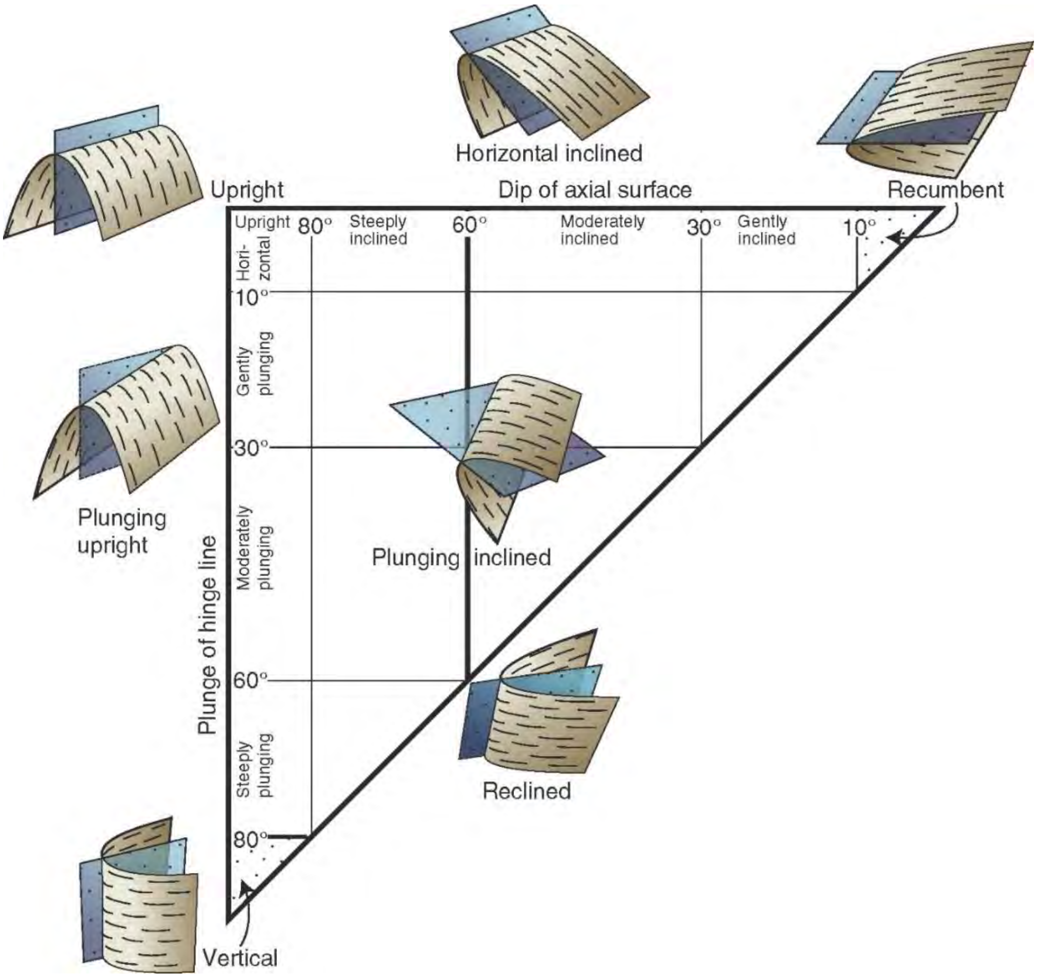

Figure 6. Fleutys (1964) classification of folds, illustrated by Fossen (2010).

2. Method

2.1 Documentation of rock structures

Structural features of the GE1 drill core were continuously documented and measured with a Kenometer and a protractor.

The drill core was initially photographed in both a wet and a dry state, the core was thereafter marked with a reference line, due to the core not being oriented. When core loss or non-continuous segments were encountered, a new reference line was marked.

Based on the assumptions that the foliation is unlikely to change direction at the end of each reference line and the foliation at the surface is generally dipping towards the west, the reference lines were oriented by turning the first foliation measurement from each reference line in the same direction as the last foliation measurement from the previous reference line. Furthermore, the first foliation measurements of the first 15m were oriented approximately to the west. However, these are not necessarily correct assumptions to make. Therefore, all orientations of this thesis need to be used with care. The dip is independent of the core orientation and can therefore be used without any assumptions. Henceforth all measurements will be oriented according to previous section and will further be referred to as oriented.

Foliations, veins, open fractures, sealed fractures, faults, folds, lineations and shear zones were documented. Discontinuities in the core with noticeable fracture minerals or any indication of weathering were interpreted as open fractures, while visible fractures in intact core segments were classified as sealed fractures.

The α- and *β* angle from the reference line was measured with a kenometer for the foliation, veins, open fractures and sealed fractures, as shown in *Figure 7*. The dip angle was calculated by subtracting the α angle from 90°. The lineations from 220-555m were documented and the pitch angle was measured with a protractor on foliation- or fracture planes, see *Figure 8*.

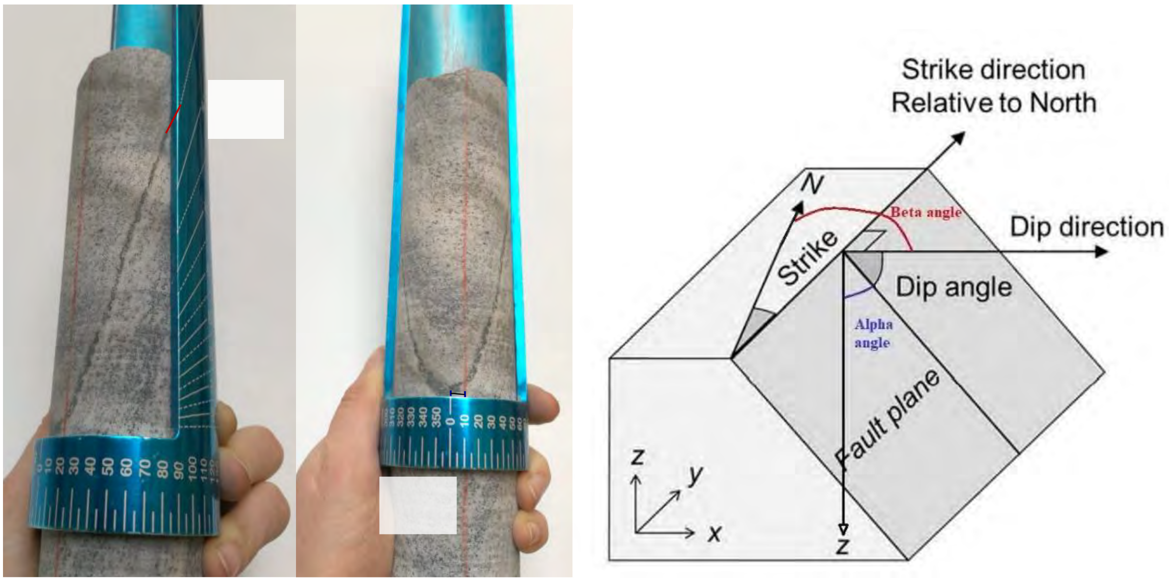

Figure 7. A) Right side of the kenometer showing the α angle. B) Bottom of the kenometer showing the β angle from the maxima of a structure to the reference line. C) Modified illustration by Markou & Papanastasiou (2018) showing the relations between α-, β angle, dip angle and dip direction.

Figure 8. Blue line showing the lineation and white line showing the fracture plane. Protractor used to determine the pitch.

2.2 Mechanical properties

The non-destructive SonReb method was intended to be used to determine the unconfined compressive strength. However, due to not being able to calibrate the method with lab measurements, that was not possible. Instead rebound value and P-wave propagation time was recorded, these measurements can be used to later calculate the rock strength.

The drill core was sampled approximately every 5 meters to include all prominent rock units. An L-Schmidt hammer was used in accordance with the ISMR (1978) standard method of determining the rebound value. However, the European standard (EN12504-2) of 9 impacts on each sample was used instead of ISMRs suggested 20 impacts. Furthermore, instead of ISMRs recommended steel cradle, for minimizing surrounding disturbances, two wooden strips were clamped to the base, as seen in *Figure 9*. The correction calculation of the obtained rebound number was done according to the ASTM (2000) standard.

Figure 9. Setup for the Schmidt hammer test, two wooden strips attached to a 30 kg steel base.

The Pundit 200 Ultrasonic pulse velocity instrument was then used to determine the P-wave propagation time through the core. Firstly, the 54kHz transducers were covered with a thin layer of adhesive and then pushed firmly against the core, with a constant distance and close to constant pressure. For each sample point a minimum of 10 readings were collected and an average used for the final measurement.

The obtained P-wave propagation measurements and the rebound values need to be calibrated with lab-based uniaxial compression tests. This calibration work is not part of this thesis.

2.3 Presenting rock structures and mechanical properties of the rocks

The GGU Stratigraphy program was used to continuously construct a log of general structural patterns, rebound value and P-wave propagation time, in combination with Hynynens (2021) documentation of lithology and radioactive isotope concentrations.

General structural patterns, structures continuing or reappearing for a minimum of 0,5 m, were continuously plotted in the stratigraphic program, more sporadic structures were also documented, however these were not included in the final log.

All fractures, lineations, foliations and large scale folds were plotted into separate stereonets, with the Stereonet 11.3 software (Allmendinger, 2020). The foliation measurements were compared to the open fractures, by visually selecting approximate foliation maximas and open fracture maximas for each 100m interval, thereafter their angular relationship could be determined.

In the GGU Stratigraphic program two stereonets were included for every 100m, one for the rock foliation and one for rock fractures.

3. Result

For concluded and combined log of structures, rebound hardness, P-wave propagation time, lithologies and radioactive isotope measurements, see Appendix A. For all documented structural information and uncalibrated unconfined compressive strength measurements, see Appendix B and D.

3.1 Foliation

The foliation dip is varying from 15-65° throughout the first 555m of the core, as seen in *Figure 10*. From 0-180m the foliations are generally between 20-50° with a maximum of 65°. From 180-420m the dip is mainly 30-40° and, locally 20-30° and 40-50°. Between 420-510m the dip is primarily 20-30°. From 510-530m the dip is generally ranging from 50-60° and from 530-555m the dip is mostly between 20-30°.

The foliation has an overall scattered orientation, however there is a clear tendency for south, southeast and north dipping foliations, relative to the orientation of the reference lines, see *Figure 11*.

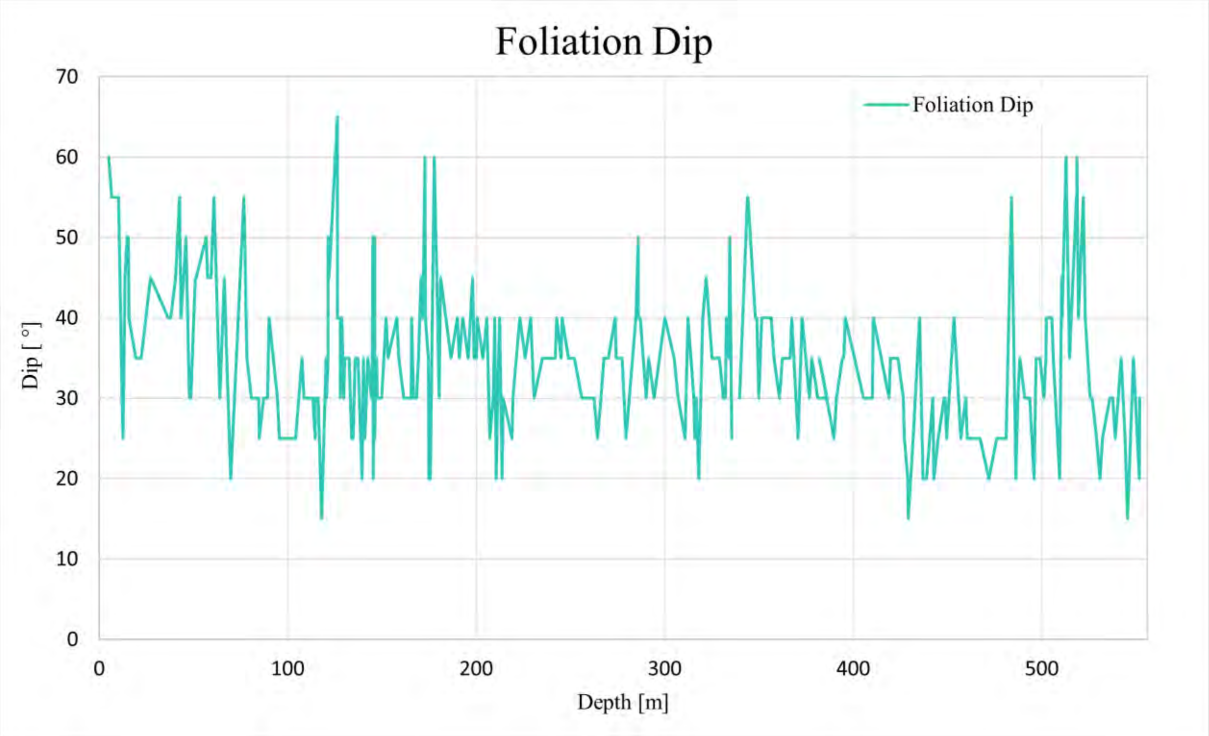

Figure 10. 293 measurements of the foliation dip from 0-555m of the GE1 drill core

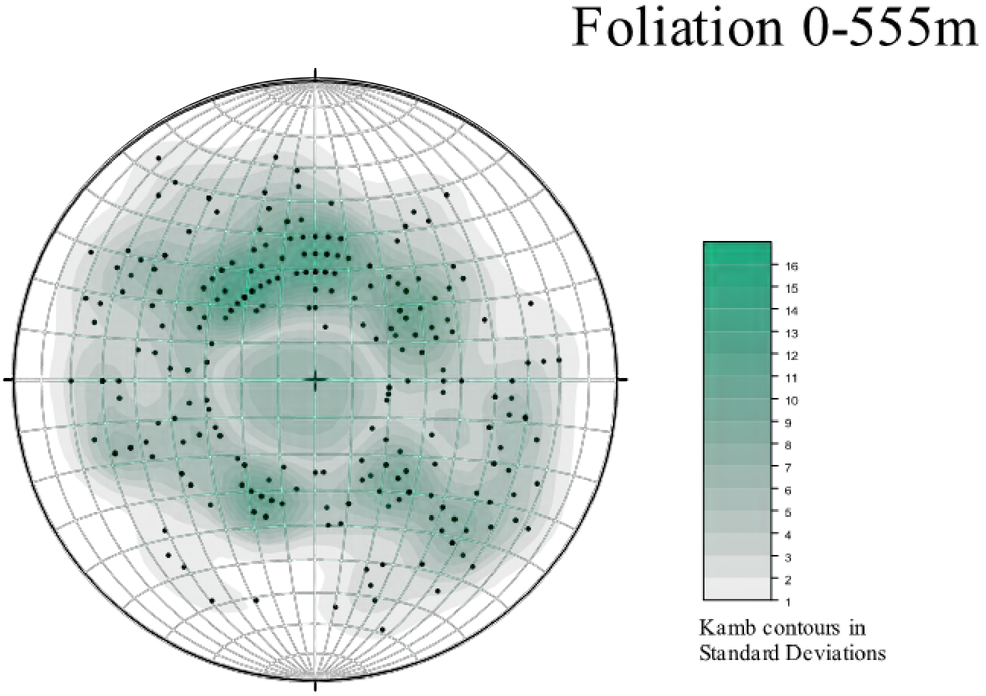

Figure 11. Stereonet contour plot of 293 foliation measurements from 64 reference lines of 0-555 m of the GE1 drill core. Orientation executed as described in section 2.1.

The foliation for each 100m interval display large differences of the foliation dip and orientation for different depths. From 0-100m and 100-200m the foliation is dipping moderately to gently (30-50°) to the southeast, see *Figure 12*. Between 200-300m the foliation is dipping distinctly to the north, with a dip of 20-40°. The foliation dipping directions from 300-400m are a bit more scattered, ranging from steep (60-70°) east dipping to shallow and moderate (20-50°) southwest dipping. From 400-500m there are two main steep (50-70°) dipping directions, northwest and southeast. At 500-555m the foliation continues to dip moderately to steeply (40-80°) to the northwest, without any southeast dipping directions.

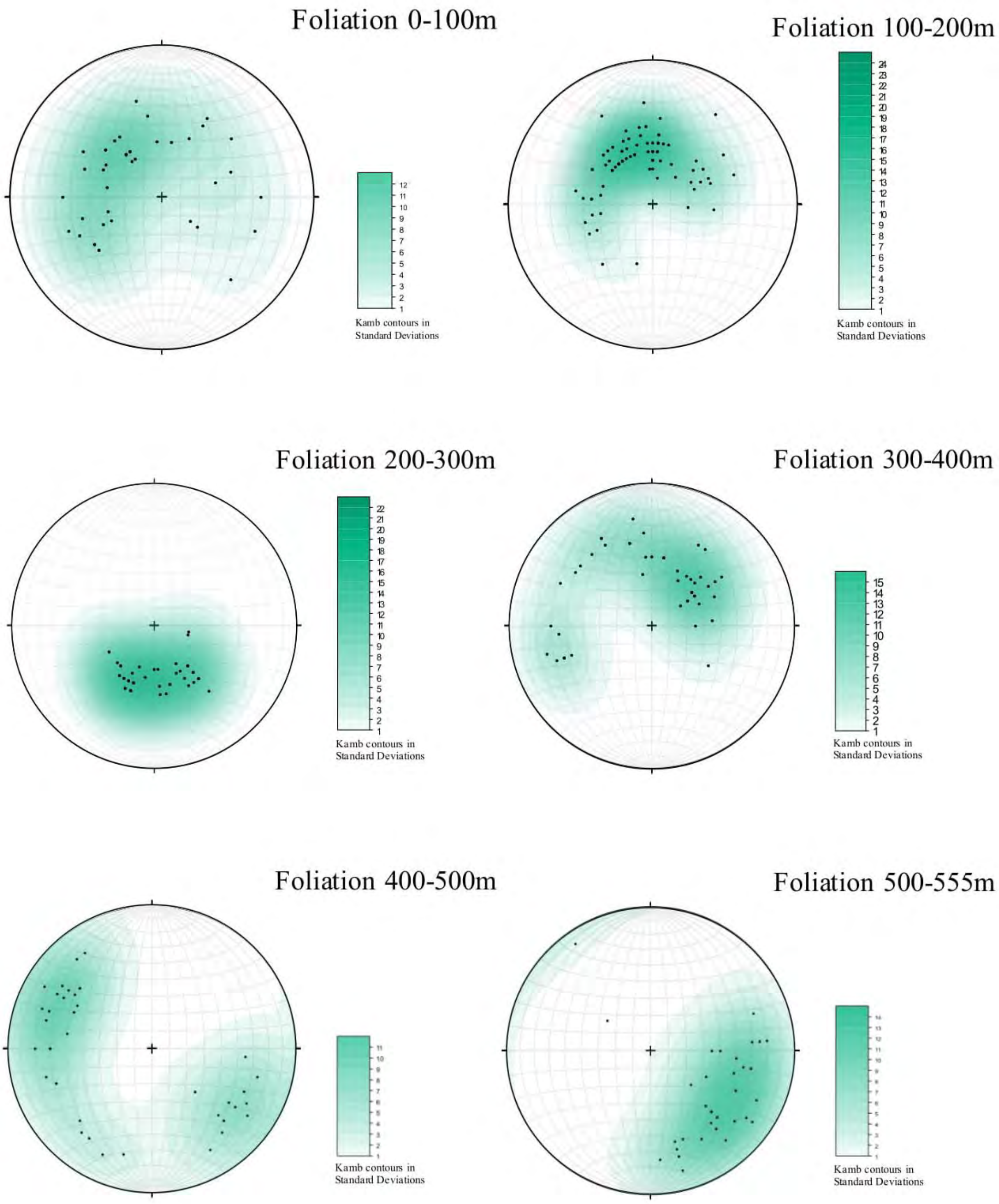

Figure 12. Stereonet contour plot of foliation measurements from 64 reference lines from 0-555m of the GE1 drill core, divided for each 100m interval. Orientation executed as described in section 2.1.

3.2 Fractures

The number of open fractures varies from 0-24 fractures per 5 meters, see *Figure 13*. At the depths of 95-145m, 165-190m and 395-410m the number of open fractures is somewhat larger than average, generally with more than 5-10 fractures per 5 meters.

95-145m is located within biotite rich tonalitic gneiss, see Appendix A. 165-190m extends over biotite rich tonalitic-, biotite rich granitic-, granodioritic-, as well as granitic gneiss. 395-410m initially consist of granitic gneiss, however from 402m the lithology changes to granitic gneiss with several large biotite zones.

Occasional increased numbers of open fractures are found at 345-350m, 365-370m, 485-490m and 495-500m. All of them located within biotite zones, granitic gneiss with biotite zones or biotite rich tonalitic gneiss, with the exception of 485-490m which is dominated by granitic gneiss.

At the depths of 190-240m, 415-470m and 520-555m the number of open fractures is generally very low, with less than 3 fractures per 5 meters. These depths all coincide with lithologies of granitic-, granodioritic-, tonalitic- or biotite rich granitic gneiss.

The sealed fracture frequency is relatively constant, rarely exceeding 5 fractures per 5 meters.

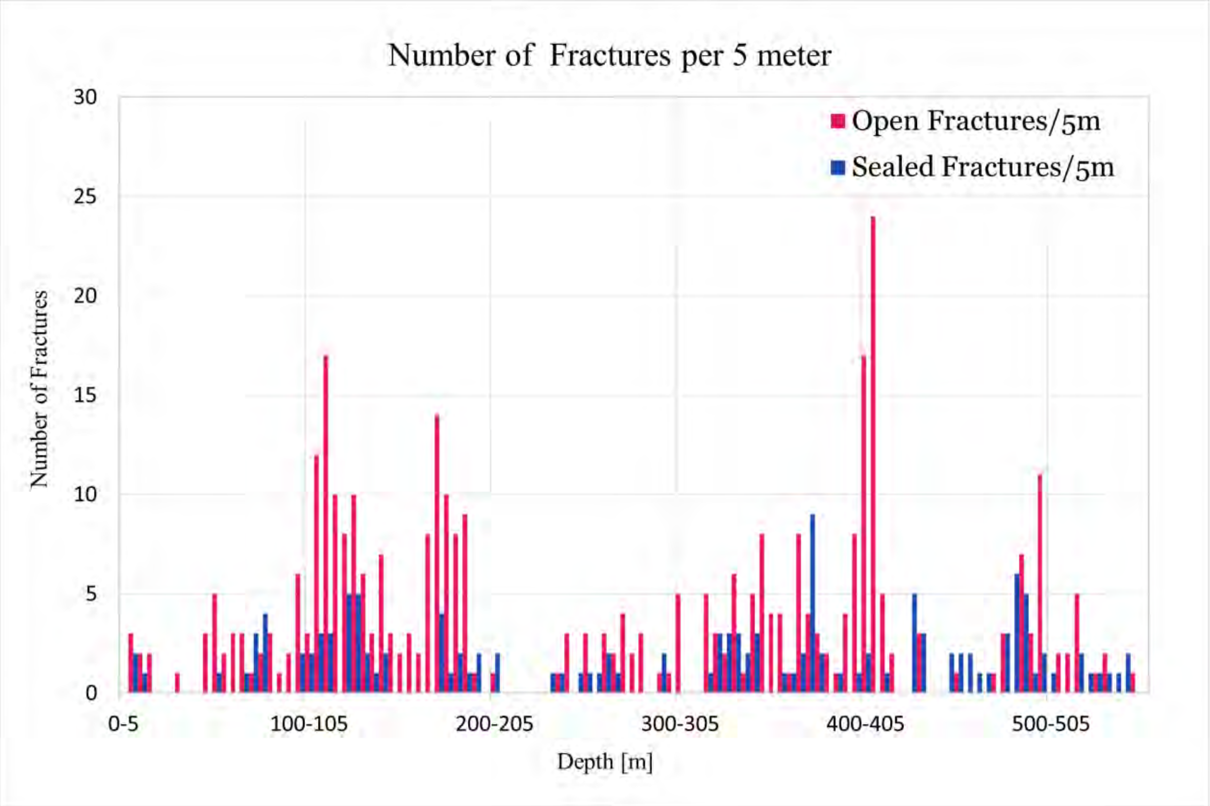

Figure 13. Number of open fractures and sealed fractures per 5 m, from 0-555m of the GE1 drill core.

The open fractures have an overall scattered orientation, however there is a clear tendency for moderate to shallow east and southeast dipping fractures, relative to the orientation of the reference lines, see *Figure 14*.

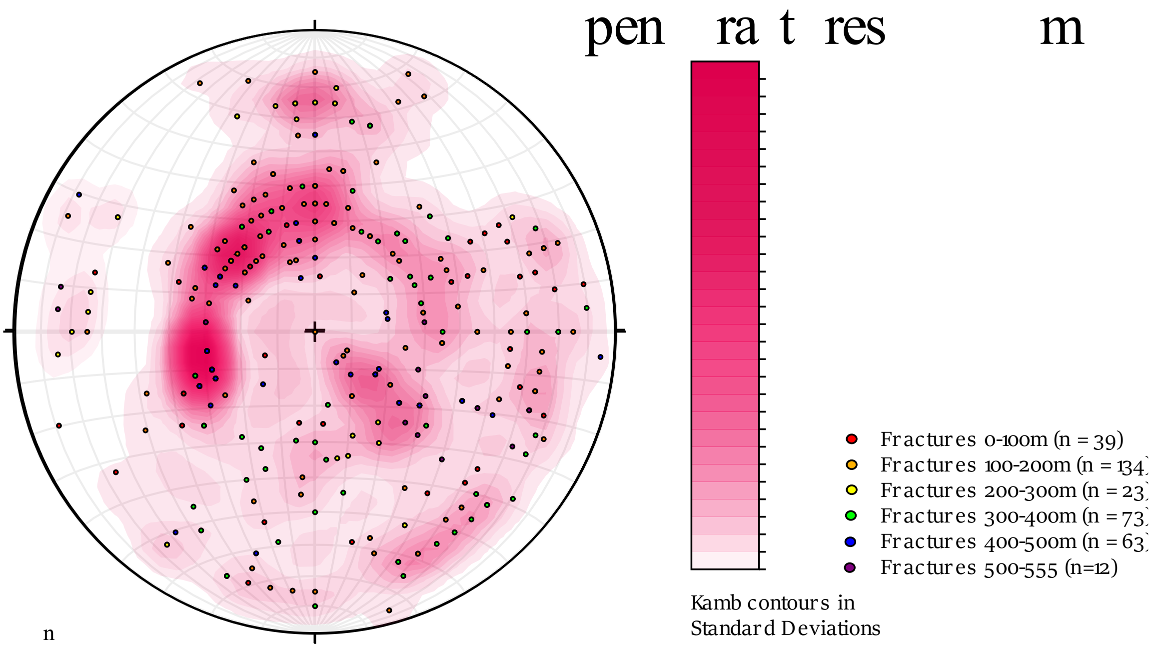

Figure 14. Stereonet contour plot of 344 open fractures from 64 reference lines from 0-555 m of the GE1 drill core. Orientation executed as described in section 2.1

The open fractures for each 100m interval display large differences of the dip and orientation for different depths. From 0-100m the main fracture group is dipping moderately to steeply (40-80°) to the west and a less widespread fracture set is dipping gently (10-30°) to the east, see *Figure 15*. From 100-200m the main fracture set is dipping gently to moderately (20-40°) to the southeast, with two less frequent fracture groups dipping moderately to steeply (50-70°) to the west and northwest. Fractures from 200-300m are dominated by three fracture sets, two of them dipping steeply (70°), to the south respectively the east, and one dipping moderately (30-50°) to the north. From 300-400m two fracture groups are dipping gently to moderately (25-45°) to the northeast respectively southwest and another fracture set dipping steeply (60-80°) to the northwest. At 400-500m there are two fracture sets, one dipping gently to moderately (20-40°) to the east, the other one gently to moderately (20-40°) to the northwest. From 500-555m the main fracture group is dipping moderately (35-55°) to the northwest.

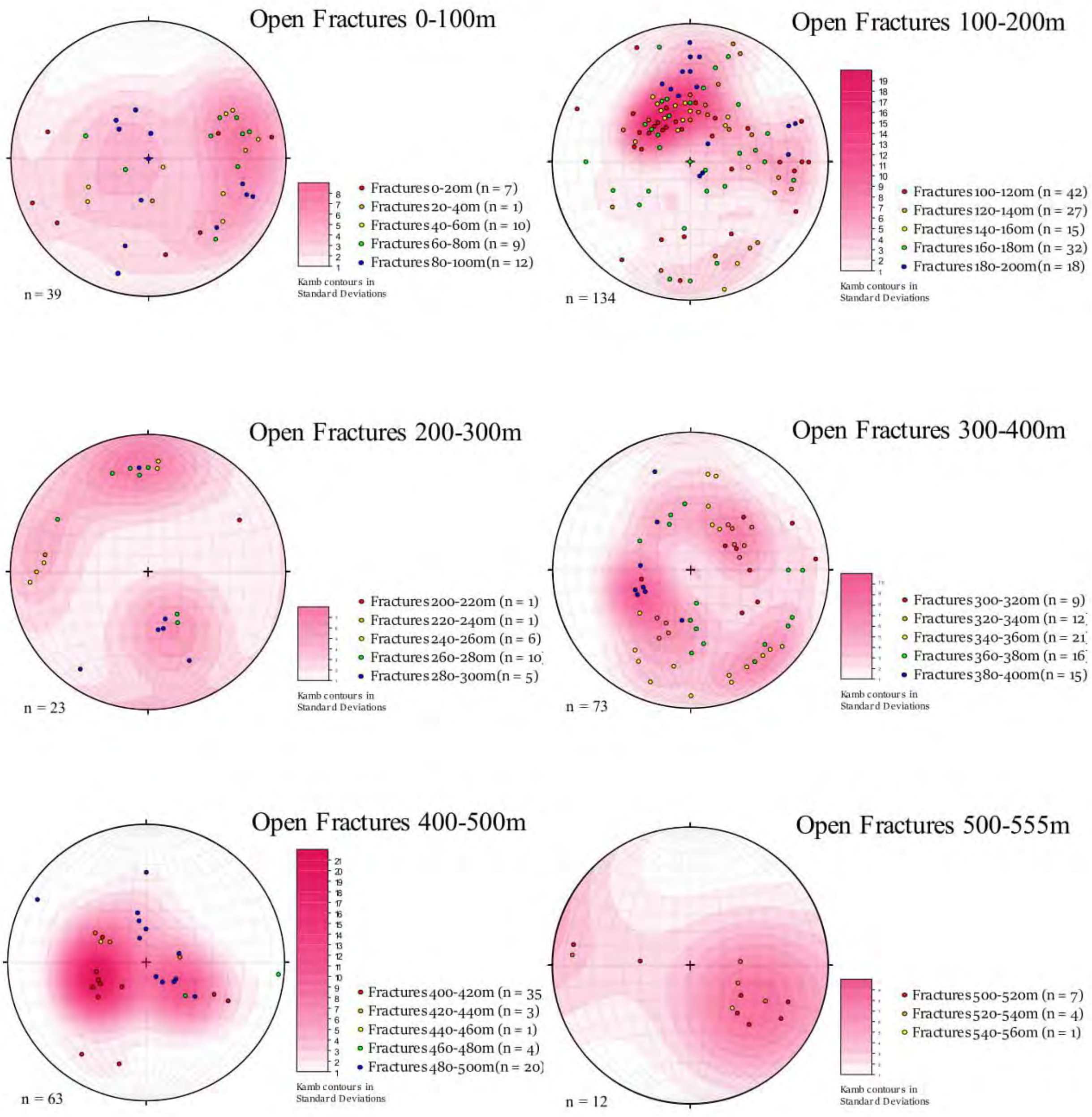

Figure 15. Stereonet contour plot of open fracture measurements for each 100m of 0-555m of the GE1 drill core. Orientation of 64 reference lines executed as described in section 2.1.

3.3 Foliation and fractures

Comparison of approximate mean foliation sets and fracture sets for each 100m interval can be seen in *Figure 16*.

From 0-100m the foliation set is dipping moderately (30°) to the southeast, wheras fracture set 1.1 is dipping moderately (60°) to the west and fracture set 1.2 dipping shallowly (10°) to the east. From 100-200m there is one fracture set (Fr 2.2) very similar to the foliation set, both dipping moderately (30-40°) to the south. Fracture set 2.1 and 2.3 are dipping steeply (60-70°) to the northwest respectively west. The foliation from 200-300m is dipping moderately (30-40°) to the north, similarly to fracture set 3.2. Fracture set 3.1 and 3.3 are dipping steeply (65-70°) to the south respectively east. From 300-400m there are two mean foliation sets, foliation

4.1 dipping moderately (60°) to the east and foliation 4.2 dipping moderately (35°) to the southwest. The orientation of fracture set 4.1 is similar to foliation 4.2 with a shallower (35°) dip and fracture set 4.2 is almost identical to foliation 4.1. From 400-500m there are two mean foliation sets dipping steeply (60-65°) to the southeast (Fol 5.1) respectively northwest (Fol 5.2). Fracture set 5.1 is dipping gently (30°) to the east and fracture set 5.2 is dipping gently (25°) to the northwest. From 500-555m the foliation is dipping moderately (60°) to the northwest and the fracture set moderately (45°) to the northwest.

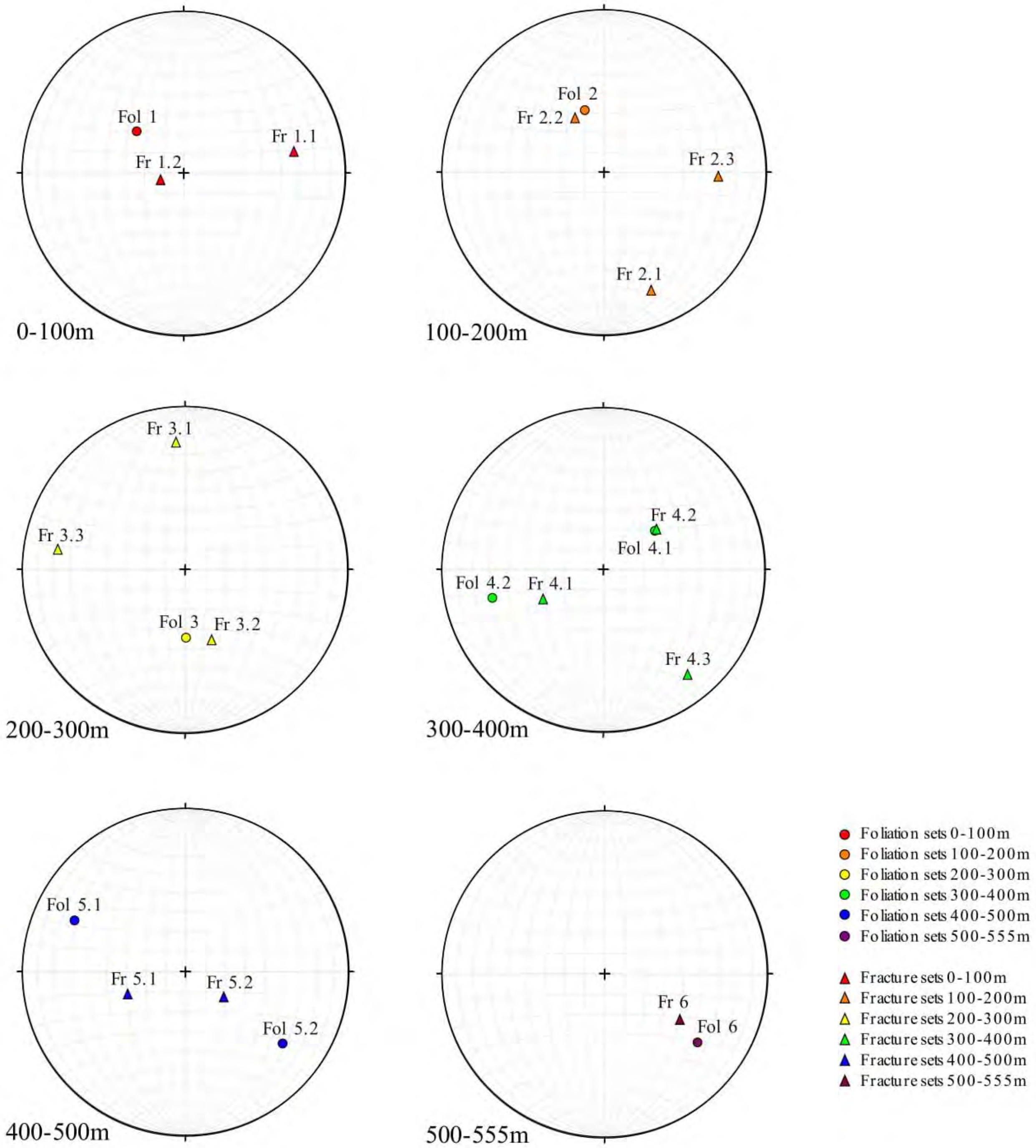

Figure 16. Approximate mean foliation sets and mean fracture sets separated for each 100m interval. Approximate mean orientation was selected visually from stereonets in Figure X and Y. Orientation of reference lines executed as described in section 2.1

The angles between the foliation sets and the fracture sets can bee seen in *Table 1*. The angular differences of fracture set 1.1, 2.1 and 3.1 relative to respective foliation is very similar, within a 1,6° difference. Similarly the angle difference of fracture set 2.3 and 3.3 relative to respective foliation, is 74,6° and 77,3°, a deviation of 2,7°. The angles between fracture set 1.2, 2.2 and 3.2 relative to respective foliation is ranging from 6,2-27,4°, a 21,2° difference.

The angle between fracture set 5.1 and foliation set 5.1 is quite similar to the angle between fracture set 5.2 and foliation set 5.2, furthermore the angle between fracture set 5.1 and foliation set 5.2 is very similar to fracture set 5.2 and foliation set 5.1.

Table 1. Table showing angles between foliation sets and fracture sets from Figure y. Separated for each 100m interval.

Angles between foliation and fractures

0-100m		100-200m		200-300m	
	Foliation 1		Foliation 2		Foliation 3
Fracture set 1.1	80,6°	Fracture set 2.1	80,1°	Fracture set 3.1	79°
Fracture set 1.2	27,4°	Fracture set 2.2	6,2°	Fracture set 3.2	12,4°
		Fracture set 2.3	74,6°	Fracture set 3.3	77,3°

300-400m			400-500m		
	Foliation 4.1	Foliation 4.2		Foliation 5.1	Foliation 5.2
Fracture set 4.1	66,7°	27,4°	Fracture set 5.1	45,8°	82°
Fracture set 4.2	1°	88,2°	Fracture set 5.2	86,8°	40°
Fracture set 4.3	73,9°	78,8°			

500-555m	
	Foliation 6
Fracture set 6	15,5°

3.4 Veins

The number of veins varies from 0-24 veins per 5 meters, as seen in *Figure 17*. The first 80m of the core have very few veins, ranging from 0-5 veins per 5 meters. At a depth of 80-100m the number of veins increase, followed by a decrease around 100m depth. Another slow increase of veins occurs around 300m, followed by an almost continuous vein frequency between 4-10 veins per 5 meters.

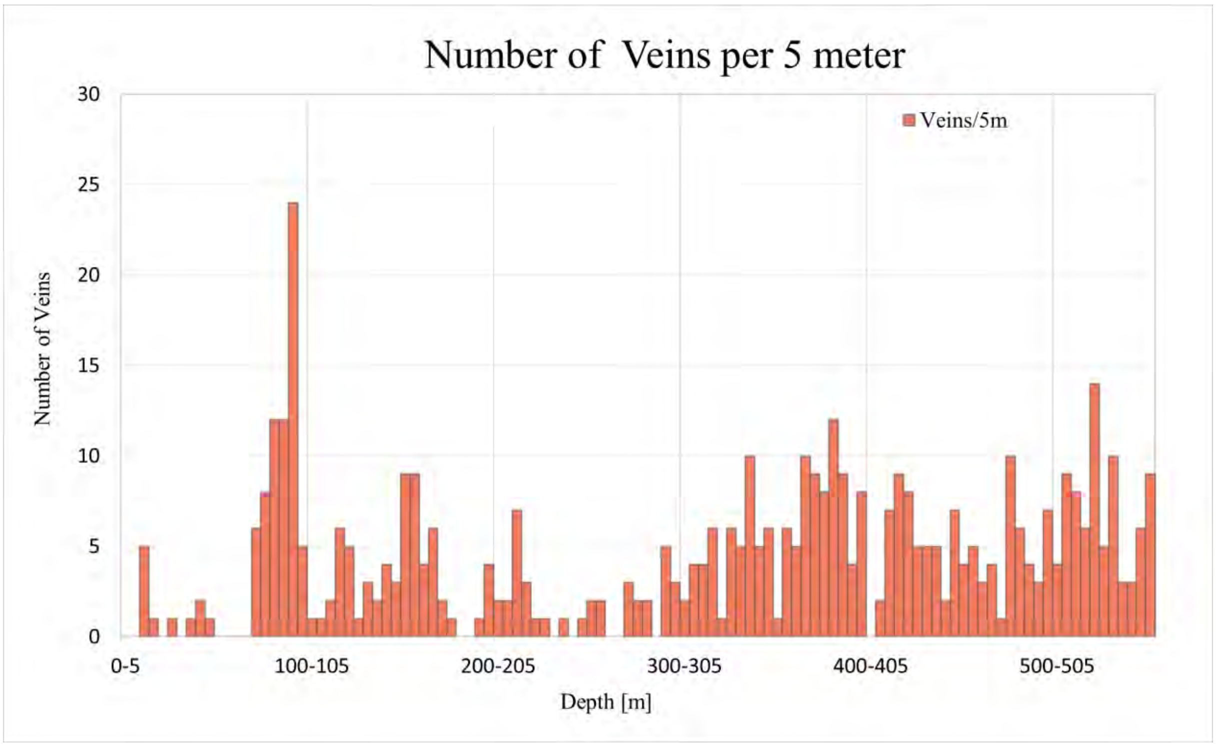

Figure 17. Number of veins per 5 m, from 0-555m of the GE1 drill core.

3.5 Folds

Several folds were documented in the core, see Appendix A and B for all documentations and depths. At 448,7-480,25m along reference line 50 a gradual 180° foliation change was observed. From the foliation measurements a fold axial plane and a fold axis were calculated, see *Figure 18*. The dip of the calculated fold axial plane was 36° and the plunge of the fold axis 54°, according to Fleutys (1964) classification a moderately plunging and inclined fold.

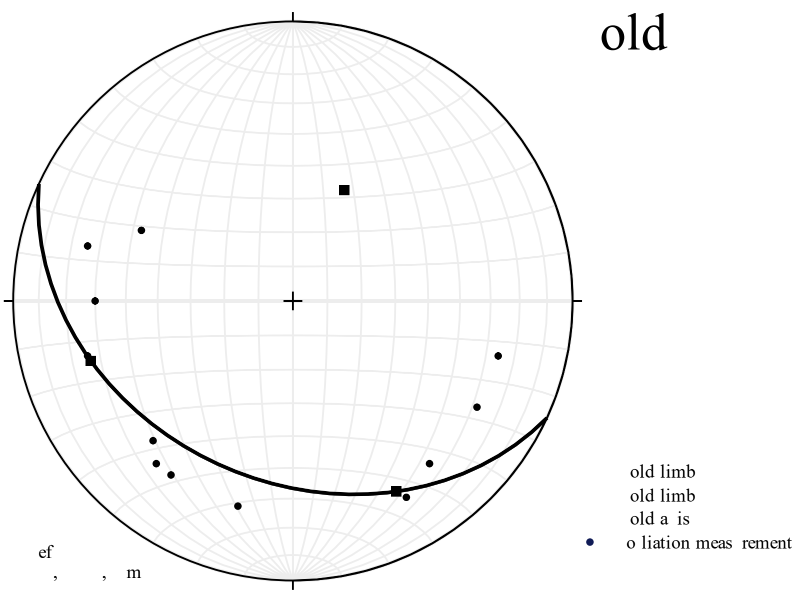

Figure 18. Calculated axial plane from foliation measurements of reference line 50. Orientation of reference line executed as described in section 2.1.

Another large fold was observed at 511m, see *Figure 19*. From foliation measurements on either side of the fold, a fold axial plane and a fold axis could be determined. The dip of the fold axial plane was 88° and the plunge of the fold axis 1,9°, according to Fleutys (1964) classification an upright horizontal fold.

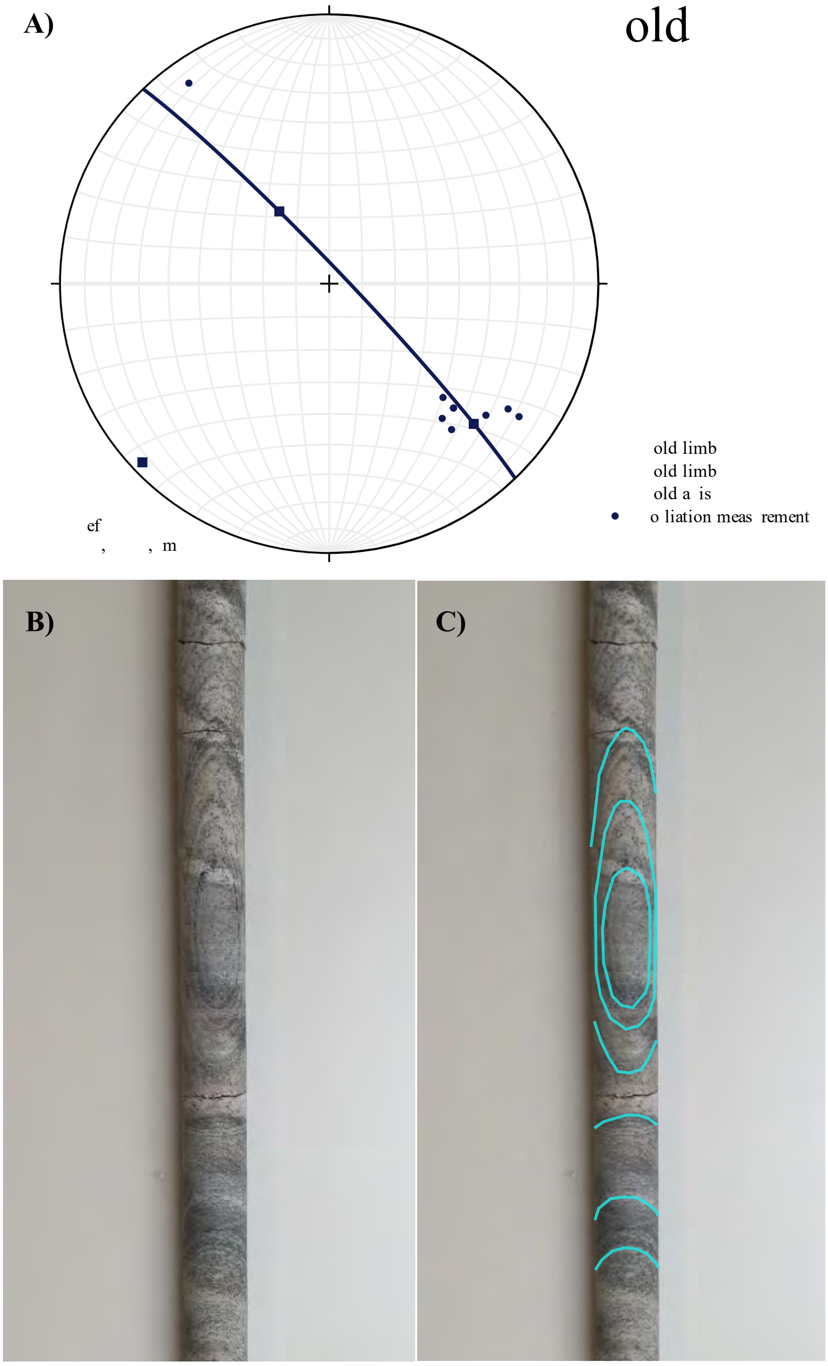

Figure 19. A) Calculated axial plane from foliation measurements between 510-512,6m of the GE1 drill core. Orientation of reference lines executed as described in section 2.1 B) Picture of core at corresponding depth. C) Highlighted foliation at corresponding depth.

The calculated foldaxes of the two observed folds from *Figure 18 & 19*, can be compared to the mean foliation sets for each 100m interval, see *Figure 16*. Notice that some of the foliation intersections are located very close to the calculated fold axes.

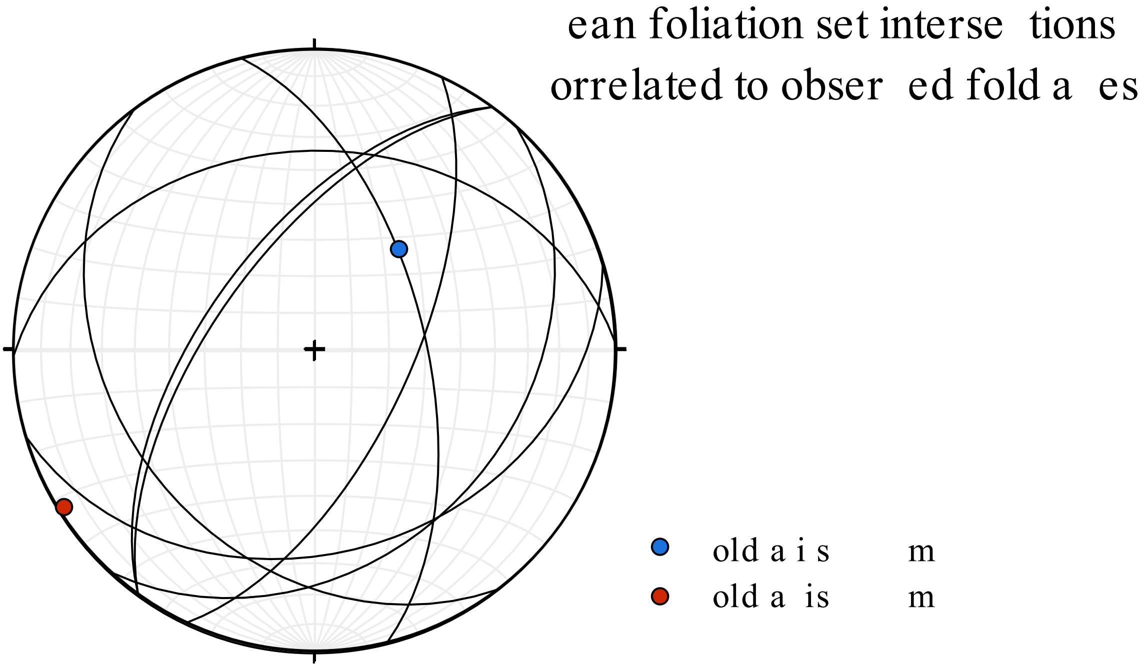

Figure 20. Mean foliation set intersections correlated to observed fold axes. Orientation of reference lines executed as described in section 2.1

3.6 Other rock structures

Two overprinting foliations were observed at depth 126,2 m and 518,63m, see *Figure 21*.

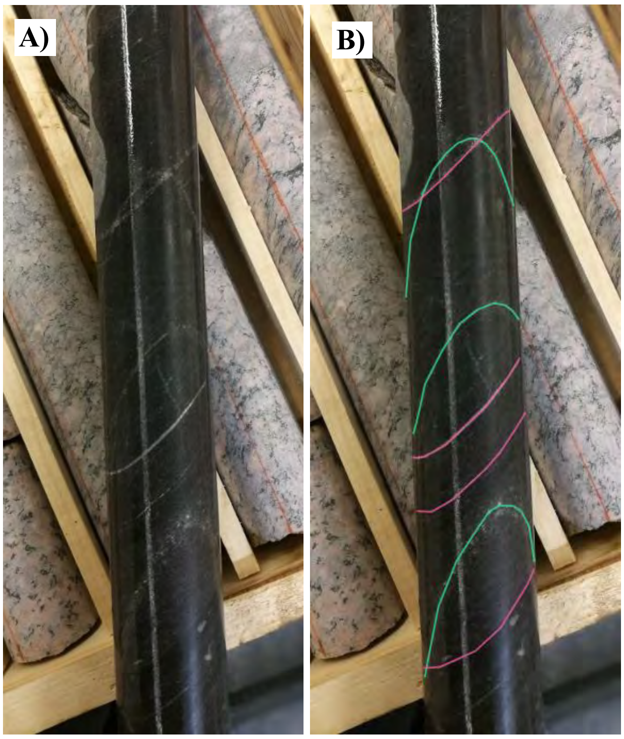

Figure 21. A) Overprinting foliation at depth 126,2m of the GE1 drill core. B) Highlited overprinting foliation at corresponding depth, where green is the older foliation and pink is the overprinting.

Various S-structures were observed in the core and several biotite zones exhibited mylonitic textures, where the foliation on both sides of the biotite zone was gradually getting stronger and the grains more elongated closer to the biotite, see *Figure 22*.

Figure 22. Biotite zone with mylonitic texture at 319,65m depth of the GE1 drill core.

At a depth of 447,2-448,9m 4 quartz veins with a dip of more than 70° were observed, see *Figure 23*.

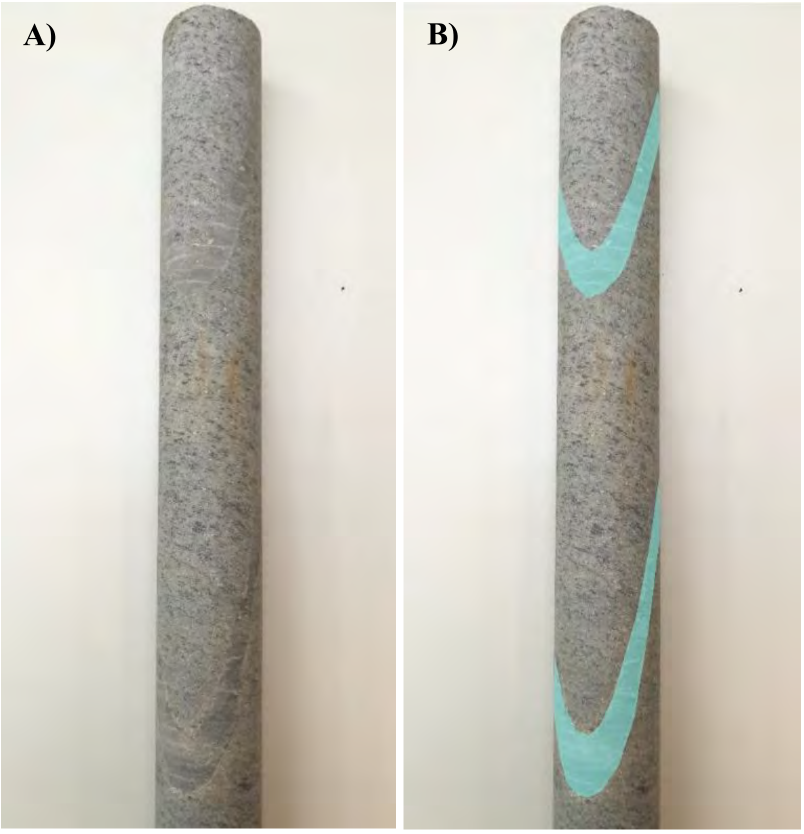

Figure 23. A) Two quartz veins at a depth of 448,37-448,6m in the GE1 drill core. B) Highlited quartz veins at corresponding depth.

3.7 Lineations

Nearly all measured lineations on fracture planes are plugning moderatly to steeply (60-80°), see *Figure 24*. There is only one exception at 342,09m where the plunge is considerably lower at 30°. The trends of the lineations are quite scattered, however most of them have a N, NW, SW or S trend.

Lineations on fracture planes

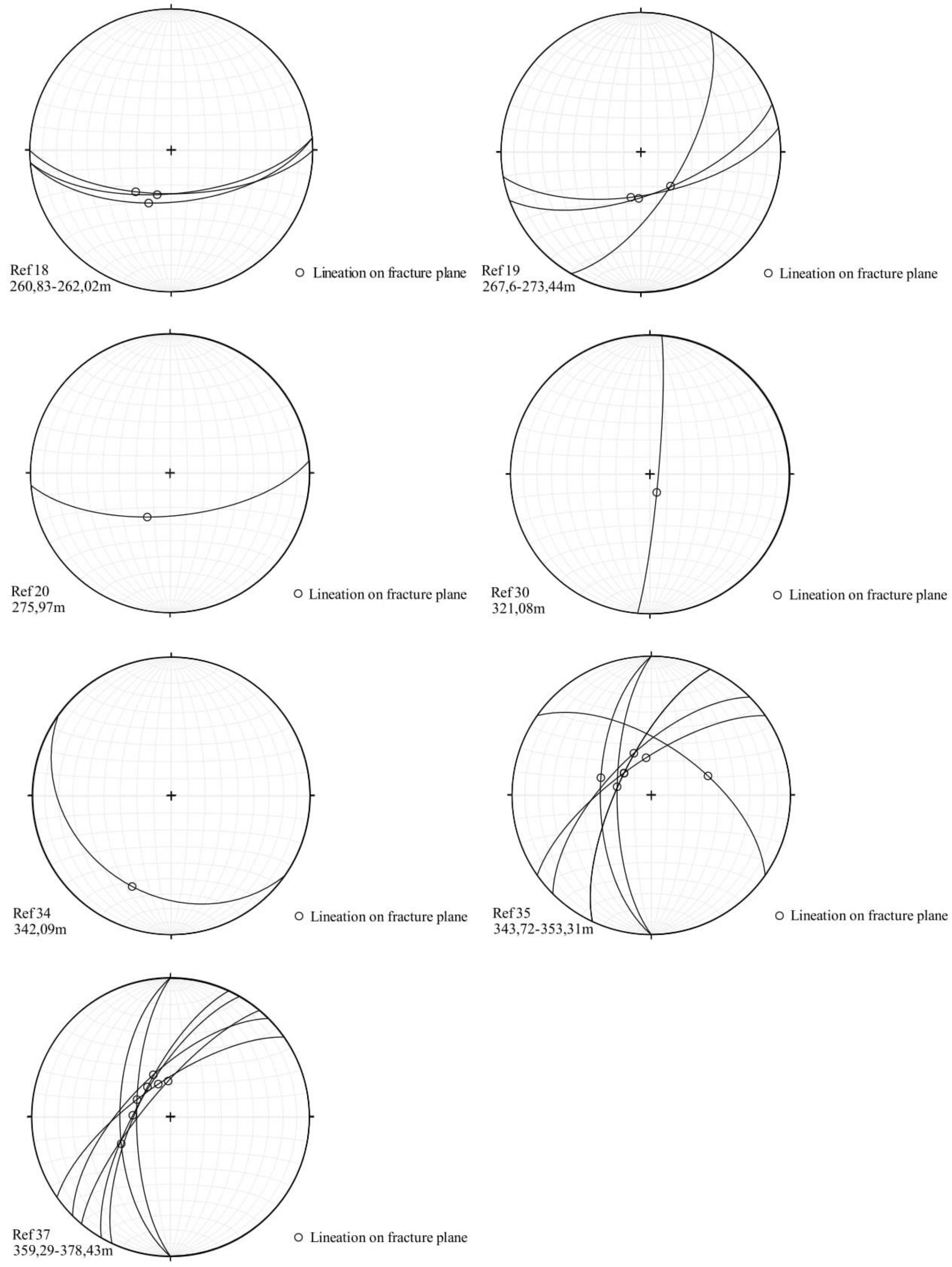

Figure 24. Measured lineations on fracture planes from 260-555m, separated for each reference line. Orientation of reference lines executed as described in section 2.1.

All measured lineations on foliation planes are plunging 10-30°, see *Figure 25*. The lineation trend is mainly in a N-S direction slightly to the NW-SE (reference line 27), a SE-NW orientation (reference lines 39-41) and a N-S direction slightly to the NE-SW (reference lines 58-59).

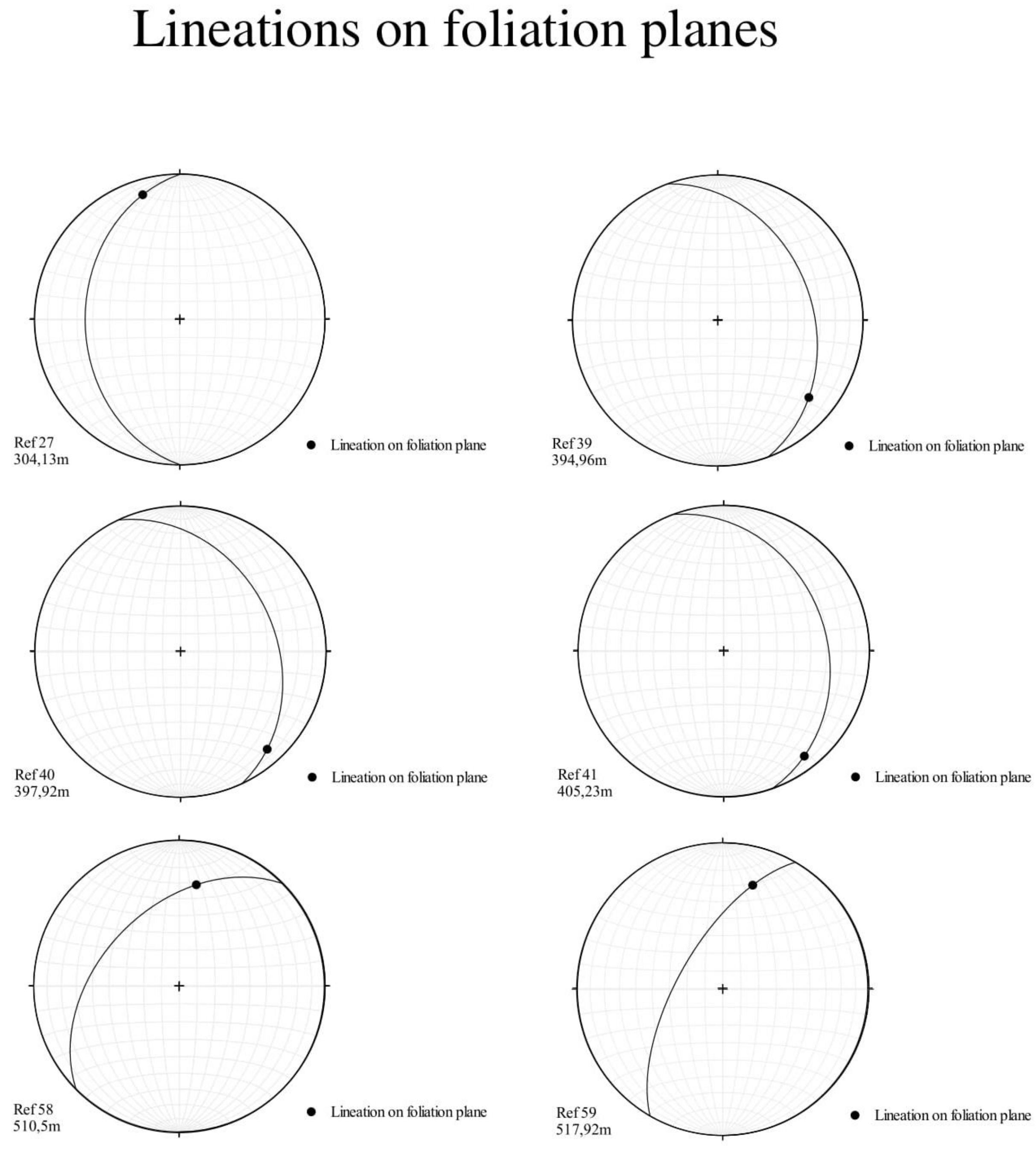

Figure 25. Measured lineations on foliation planes from 260-555m, separated for each reference line. Orientation of reference lines executed as described in section 2.1.

From observed overprinting foliation, see section 3.6, two intersection lineations were detrmined, see *Figure 26*. The intersection lineation at 126,2m has a trend of 145° and a plunge of 38°. The intersection lineation at 518,63m has a trend of 201° and a plunge of 23°. The intersection lineation at 126,2m have NW-SE orientation, similar to the lineations from the foliation planes (reference lines 39-41), see *Figure 25*, however with a slightly steeper plunge. The intersection lineation at 518,63m have a N-S orientation slightly to the NE-SW, similar to the lineations from the foliation planes from reference lines 58-59.

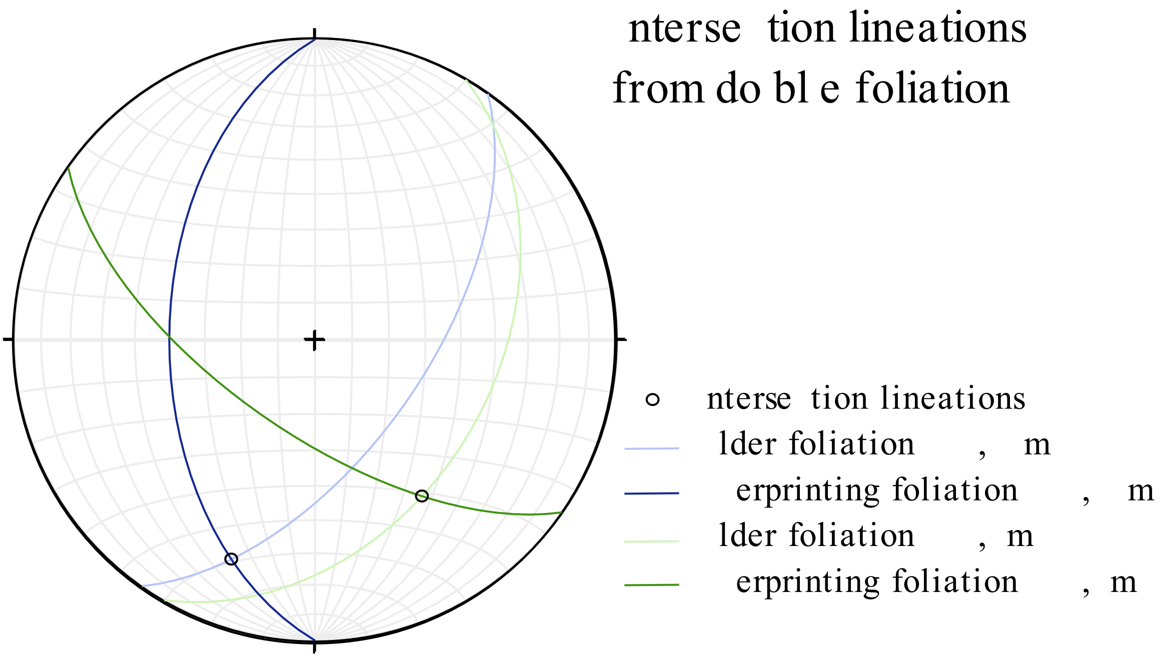

Figure 26. Intersection lineations from observed overprinting foliation intersections at 126,2m and 518,63m. Orientation of reference lines executed as described in section 2.1.

3.8 Mechanical properties

The rebound hardness is quite varied throughout the core, ranging from 39,1-60,2, see *Figure 27*. From 0-100m the rebound number is generally between 53-59. From 100-190m the rebound values are more scattered and generally slightly lower. Between 190-260m the rebound value is quite stable, ranging from 56-60, with an occasional lower measurement. At 260m the rebound hardness drops to 50 and is slowly increasing until reaching 58 at 330m. From 330-403m the rebound values are quite scattered between 51-60, then at 403m the rebound values drop again. From 403-442m and 495-515m the rebound numbers are mainly below 50, and in between 442-495m the rebound hardness is higher, ranging from 51-58.

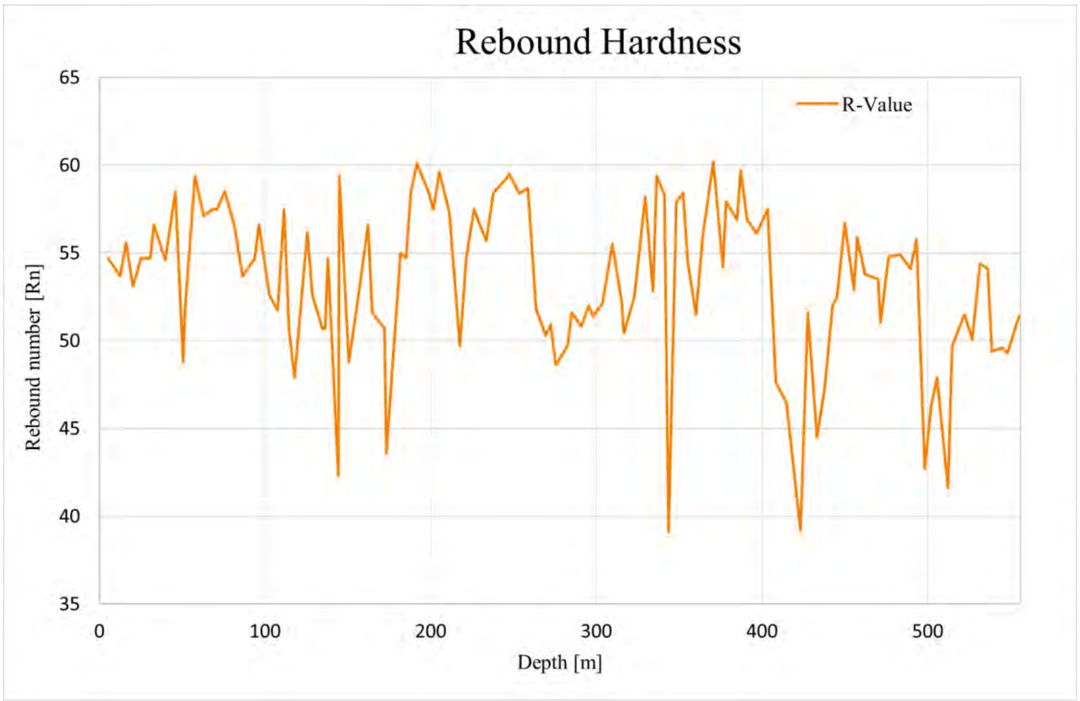

Figure 27. Rebound hardness from 0-555m of the GE1 drill core. Measured with a Schmidt hammer approximately every 5m.

The P-wave propagation time is ranging from 10,25-30,8 µs, see *Figure 28*. From 0-228m there are quite small and abrupt changes ranging from 10,25-14,1 µs. Whereas from 228-490m the changes create a relatively smooth curve with occasional large spikes. The occasional spikes at 290,75m and 433m were both measurements from a granitic gneiss lithology, at 290,75m there was a sealed fracture nearby as well. From 490-555m the scattered measurements continue, however with larger changes than from 0-228m.

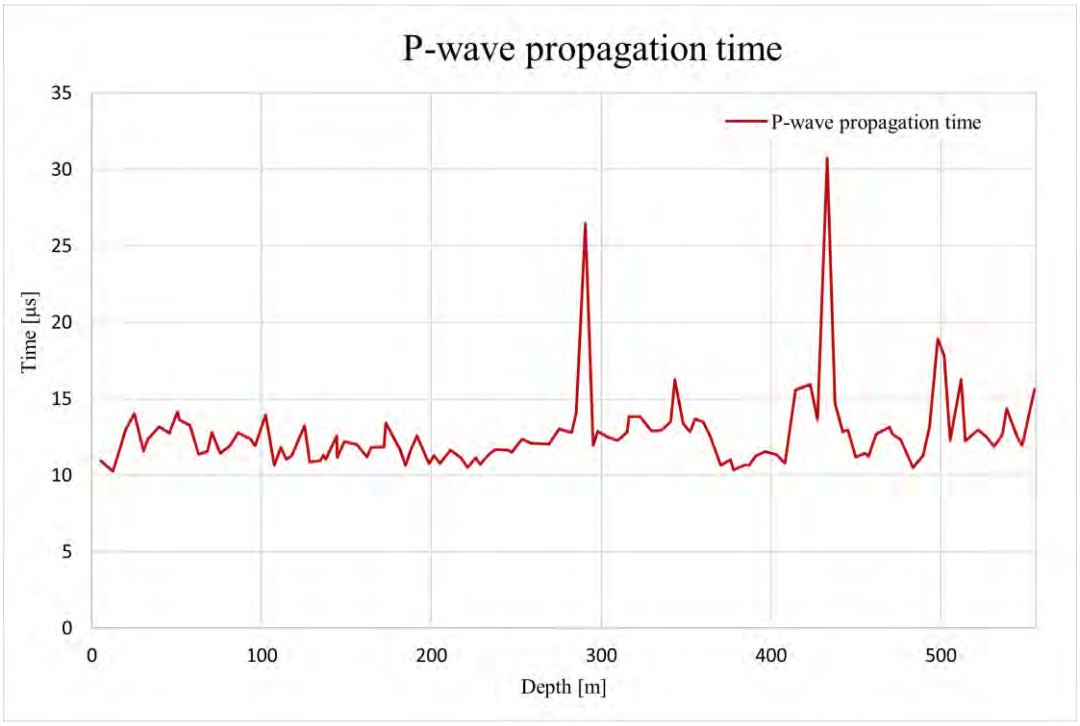

Figure 28. P-wave propagation time from 0-555m of the GE1 drill core. Measured with an ultrasonic pulse velocity instrument approximately every 5m.

4. Discussion

4.1 Foliation

Relative to the orientation of the core segments the dipping direction of the foliation is gradually changing with depth, moving from east, to south, to north, to southwest, to southeast and to northwest, see *Figure 12*. This could partly be the result of the used orientation method, described in section 2.1. Theoretically all positions where a reference line ceases could be located on a fold axis, which could then drastically change the foliation direction of the following reference line. However, this is quite unlikely and thus, if the foliation is changing in accordance with the employed orientation, the foliation orientation is gradually changing. This is further supported by the foliation direction distinctly changing within the same reference line, see *Figure 18*. This would indicate a geologically complex environment where different geological deformation events have formed and folded the bedrock. Additionally, there is no clear tendency for west dipping foliations in the core, which seems to be the most frequently encountered foliation orientation at the surface (SGU, 2006; Persson, 2007; Medan, 2015). This could possibly correspond to similar conditions as along the Göta tunnel (Persson, 2007) where the foliation changed orientation with depth due to folding.

No further analysis of the foliation dip direction will be investigated, as these are not the true foliation orientations.

The dip is independent of the orientation and can therefore be used without assumptions. The measured dip of the core is generally shallow to moderate, ranging from 15-65°, see *Figure 10*. The measured dip from the first 100m of the core is ranging from 20-50°. This is interesting as previous surface investigations (SGU, 2006) suggest the foliation dip is moderate to steep. However, measurements from the West link project and the Göta tunnel (Medan, 2015; Persson, 2007) have documented similar dip of foliation as the GE1 drill core. This would suggest there are areas where the foliation dip is lower than previously thought, additionally the relatively low dip is continuing at greater depths.

4.2 Fractures

Depths with increased number of fractures frequently coincides with general lithologies with an abundance of biotite or biotite zones, see section 3.2 and Appendix A, which might indicate fractures are more easily developed in biotite rich lithologies. This could be due to the structural layering characteristic of biotite, making the minerals particularly weak in certain orientations. However, there are also biotite rich lithologies with few fractures, for instance 67-98m, contradicting previous observation. This indicate there might be a correlation between number of fractures and biotite rich lithologies, but more detailed investigations of the specific lithology for all observed fractures are needed to make any conclusions.

The fracture sets for each 100m interval have a varied dip and dip direction, see *Figure 15*. There is no fracture orientation which is constantly present throughout the core, however generally most fractures are dipping moderately to shallow towards the east and southeast, see *Figure 14*. This is interesting as the orientation deviates from the orientations of the identified fracture groups in the West link project, the Götatunnel and the Nygårdstunnel (Medan, 2015; Persson, 2007). However, similarly to the foliation, no further analysis of the fracture orientations will be investigated as these are not the true orientations.

The angular relation between the orientation of the different fracture sets and foliation sets, see *Table 1*, can tell us something about the formation sequence of the foliation and the fractures.

Fracture set 1.1, 2.1 and 3.1 have similar angles between the changing foliation and the fracture set orientations, indicating the fracture sets are most likely the same fracture set. Their continuous constant angular relation from 0-300m also suggest that the fractures were formed previous to the foliation changing orientation. The sequence of events could be explained by model 1, see *Figure 29*, where a foliated rock was fractured, followed by a folding event changing both orientations of the foliation and the fractures, however keeping their angular relation constant. This explanation could also apply to fracture set 2.3 and 3.3.

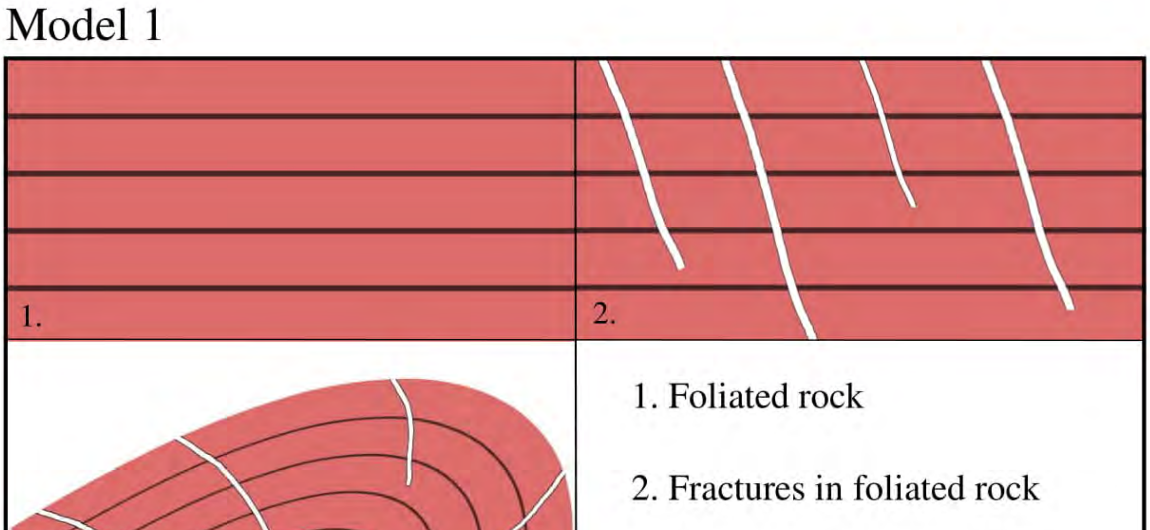

Figure 29. Simplified model of a structural formation sequence. A foliated rock gets fractured, followed by a folding event.

The angular relation between fracture set 1.2, 2.2 and 3.2 and respective foliation are somewhat similar to each other, deviating with 21,2° and model 1 might apply for them as well. However, a more likely explanation might be that the fractures are younger than the event changing the foliation orientation. This could be explained by model 2, see *Figure 30*, where a foliated rock is folded, followed by fracture formations.

From 300-400m the foliation has two separate mean orientations, see *Figure 16*, complicating the interpretation of the different mean fracture sets. If the foliation is gradually changing with depth and if certain mean fracture sets belong to specific depths, the fracture sets might only occur in relation to one of the foliations, therefore making one of the calculated relative angles incorrect because it is non-existent. Therefore 300-400m will not be analysed, however as fracture set 4.3 have quite similar angle relation to both foliation 4.1 and 4.2 (73,9° respectively 78,8°), and the angle relations are relatively similar to fracture set 2.3 (74,6°) and 3.3 (77,3°), they might belong to the same fracture set.

400-500m also have two separate mean foliation orientations, creating similar problems as for 300-400m. However, there are only two mean fracture sets and the angle between fracture set 5.1 and foliation 5.1 (45,8°) are quite close to the angle between fracture set 5.2 and foliation 5.2 (40°), see *Table 1*. The same applies for the angles between fracture set 5.1 and foliation 5.2 (82°) respective fracture set 5.2 and foliation 5.1 (86,8°). This would suggest two plausible explanations; either there have been two younger cross cutting fracture sets formed after a folding of the rock as seen in model 2, see *Figure 30*. Or fracture set 5.1 and 5.2 are not both present throughout 400-500m, which would mean at least one of the calculated angle relations are non-existent. If the second alternative is true, then it is very likely that fracture set 5.1 and 5.2 are the same fracture set and could have been formed in accordance with either model 2 or model 1, see *Figure 29 & 30*.

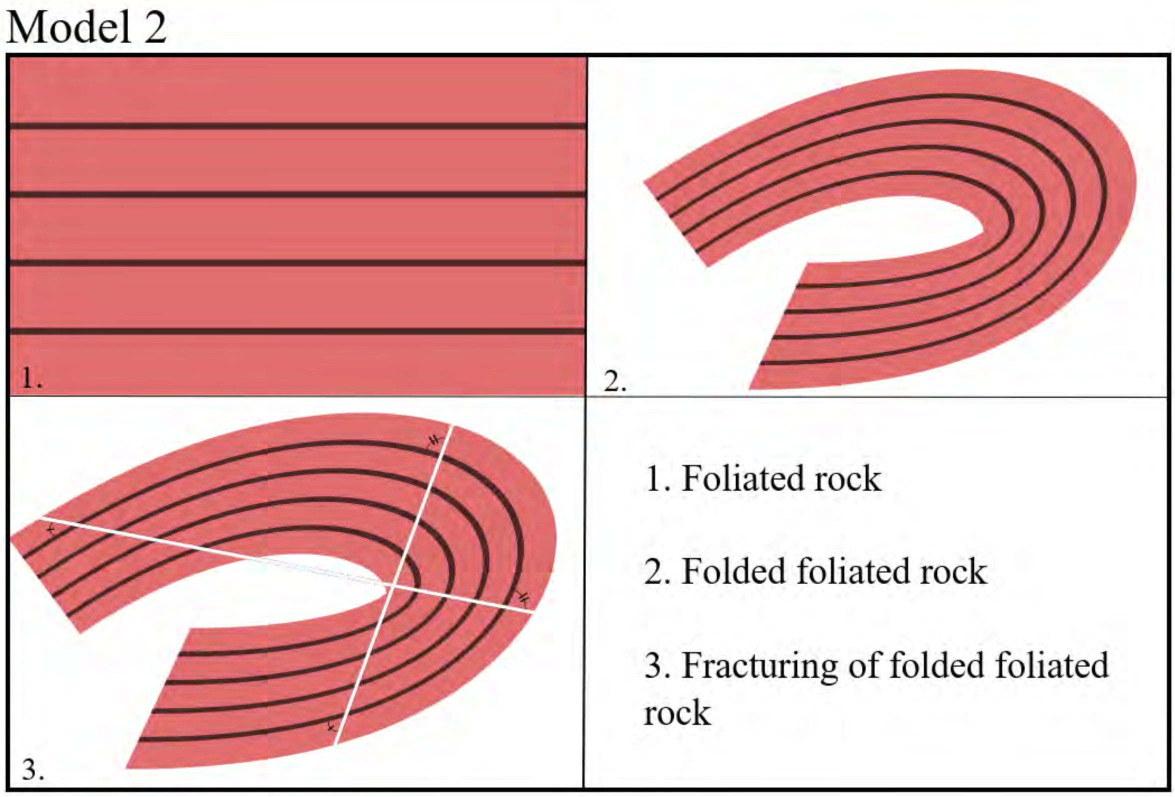

Figure 30. Simplified model of a structural formation sequence. A foliated rock gets folded, followed by a fracturing event.

4.3 Structures indicating different deformation events

The observed overprinting foliations imply there have been at least two different deformation events influencing the stress conditions of the bedrock. Initially one episode where the first foliation was created, followed by another event overprinting the previous foliation. This is further supported by the observed folded folds, see Appendix B, and the two different varieties of observed large scale folds. One fold which according to Fluetys (1964) classification is an upright horizontal fold and another moderately plunging and inclined fold. These folds could not have been created from one single stress condition, therefore there must have been at least two different deformation events which have transformed the bedrock, which is very plausible considering the bedrock has been through two different orogeneses.

I would also argue that the intersecting foliations close to the blue fold axis, see marked area in *Figure 31*, belong to the same foliation and have been folded similarly to the observed fold with the blue fold axis. Likewise, I would argue that the intersecting foliations close to the red fold axis belong to the same foliation and have been folded similarly to the observed fold with the red fold axis. However, the foliations close to the blue and the red fold axes have been formed during different events.

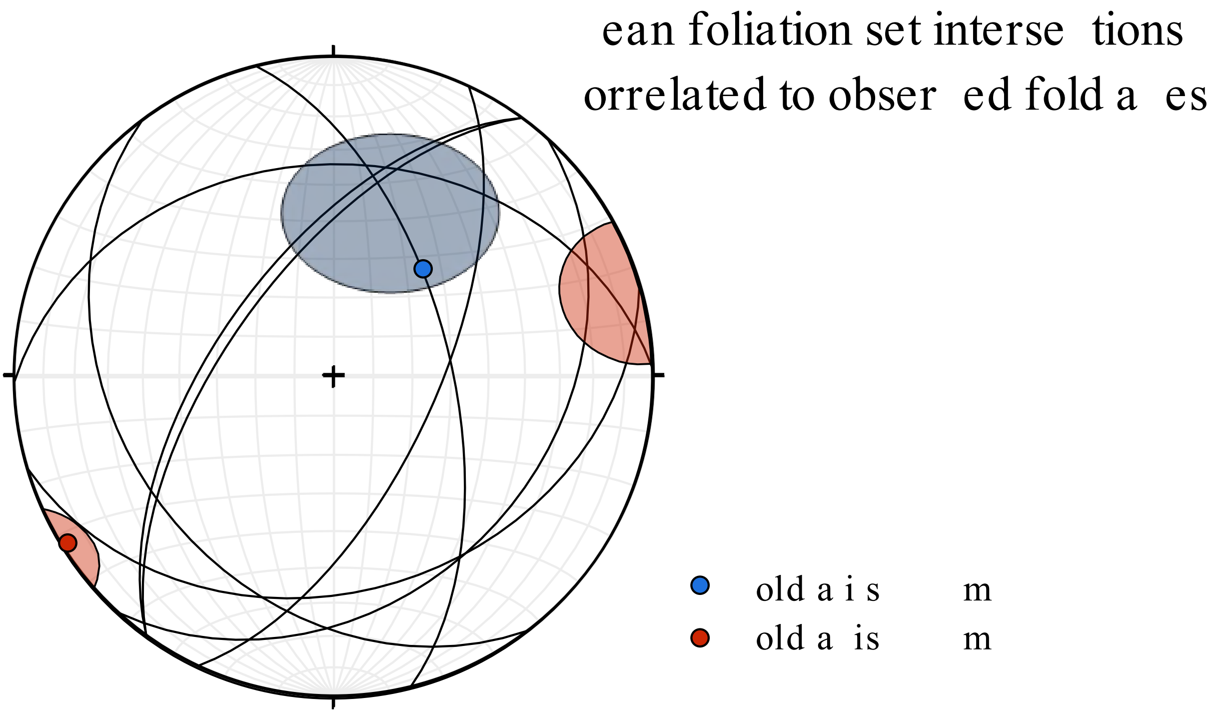

Figure 31. Mean foliation set intersections correlated to observed fold axes. Where the blue area is interpreted as foliation intersections similar to the blue fold axis and the red area is interpreted as foliation intersections similar to the red fold axis. Orientation of reference lines executed as described in section 2.1.

4.4 Lineations

The lineations on the fracture planes are dominantly plunging steeply, see *Figure 24*, implying there have mainly been vertical fault movements. The lineations on the foliation planes on the other hand are gently plunging, see *Figure 25*. Lineations on the foliation planes mainly extends in a SE-NW direction and a N-S direction, slightly to the NW-SE and NE-SW. The calculated intersection lineations from the depths with overprinting foliation, see *Figure 26*, are also trending NW-SE, with a slightly steeper plunge, and N-S slightly to the NE-SW.

The similarity between the lineations on the foliation planes and the intersection lineations indicate that the lineations on the foliation planes might have been formed similarly to the intersection lineations, by an overprinting foliation.

4.5 Mechanical properties

The rebound hardness changes quite irregularly with depth and there is no clear indication of slightly lower or higher values for certain lithologies, see *Figure 27*. However, the P-wave propagation time curve indicates some sort of change at approximately 230m, see *Figure 28*, although it does not correspond to a specific lithologic boundary, the cause of the change therefore remains unknown.

There are some uncertainties in the execution of the measurements with the Schmidt hammer and the Ultrasonic pulse velocity instrument. Measurements with the Schmidt hammer was not taken on securely clamped samples, measurements might therefore have been unevenly influenced by the wooden strips used to create a groove on the steel base. While making measurements with the Ultrasonic pulse velocity instrument, slight differing values was attained depending on the amount of adhesive on the transducers.

The acquired measurements of this thesis are relative and lab-based uniaxial compression tests will be needed to retrieve the absolute values of the measured lithologies, as well as to evaluate the reliability of the data.

4.6 Suitability of a deep geothermal energy plant in Högsbo

For the investigated site to be suitable for deep geothermal energy extraction, from a structural perspective, there needs to be a sufficient number of fractures or zones of weakness at greater depths. Furthermore, the fracture orientations need to be known and relatively connected to be able to predict the flow direction of the liquid. There also needs to be vertical fractures present, which are important to be able to transport liquids to greater depths. Worth noting is that steep dipping fractures are harder to encounter, as they are only present in a limited horizontal area, while horizontal fractures extend through larger horizontal areas. Thus, it is easier to encounter horizontal fractures with a small drill core, than vertical fractures.

There was no indication of increased or decreased number of fractures with depth, see *Figure 13*. Additionally, the preferred fracture orientations are very different for different depths, see *Figure 15*, however generally most of the fractures are dipping moderately to shallowly to the east and southeast, see *Figure 14*, relative to the applied orientation described in section 2.1.

If the fractures continue to dip moderately to shallow with depth one possibility would be to stimulate steep dipping quartz veins and make vertical transportation of liquid possible, provided additional steep dipping veins, as seen in *Figure 23*, are detected at greater depths.

Further investigations of true fracture orientations, fracture numbers- and fracture dips at greater depths are needed to determine if a deep geothermal energy plant would be suitable at the investigated area, from a structural perspective.

5. Conclusion

This thesis has investigated the structural and mechanical properties of the first 555m of the GE1 drill core. From the research the following information can be concluded;

- The true orientations need to be investigated to make definite conclusions from the foliation orientations. However, from the applied orientation, the foliation is generally dipping south, southeast and north, which differs from the general westward foliation orientation at the surface.

- The dip of the foliation is moderate to shallow, which indicate a less steep foliation dip than previous surface mapping suggests. However, the dip is similar to measurements from drill cores from the West link project, the Götatunnel and the Nygårdstunnel.

- Increased number of open fractures quite regularly coincides with lithologies with an abundance of biotite, however not all biotite rich lithologies have an increased number of fractures.

- The true orientations need to be investigated to make definite conclusions from the open fracture orientations. However, from the applied orientation, the fractures are generally dipping moderately to shallowly towards the east and southeast.

- The angular relations between mean fracture sets and mean foliation sets indicate there are both fracture sets formed before folding events and fracture sets formed after folding events.

- There are several indicators for at least two different deformation events altering the bedrock. Both overprinting foliations and folded folds have been observed.

- Lineations along fracture planes are plunging steeply, indicating vertical fault movements. Lineations along foliation planes are similar to calculated intersection lineations from observed overprinting foliations. They could therefore be interpreted as lineations with similar origin.

- Further research is needed to draw any conclusions from the rebound numbers and the P-wave propagation times. Furthermore, to determine the absolute unconfined compressive strength of each lithology, a calibration and further evaluation of the reliability of the measurements are needed.

- Further investigations of the true fracture orientation, fracture numbers at depth and mechanical properties are required to determine if a deep geothermal energy plant would be suitable at the investigated area, from a structural perspective.

In conclusion, the structural documentation of the first 555m of the GE1 drill core has given us new information of the deep bedrock of Gothenburg. However further investigations of the remaining core and other deep drill cores are needed to truly uncover the history of the bedrock beneath our feet.

Acknowledgements

Firstly I would like to thank my supervisor Mark Peternell, for always supporting and showing great interest in my thesis work, but also for showing me how exciting structural geology can get when everything just clicks (and even when it doesn’t).

I would also like to thank Mikael Tillberg for involvement, being able to help at any time and for all the “behind the scenes” core moving.

I thank my opponent Felix Ekström Tormos and my examinator Matthias Schmolke for constructive comments.

I would also like to thank Thomas Eliasson for great explanations and discussions of the regional geology of Gothenburg, Egill Örn and Jacek Krysik for providing both literature tips and interesting fracture discussions, and all others who have dropped by the core logging room, for their curiosity in the project, as well as great discussions.

For giving me an opportunity to work with this core I would like to thank Gothenburg Energy, SGU and Gothenburg university.

Last and most importantly, I would like to thank Anna Hynynen for an exciting, stressful and great time working with the drill core, without you I would still be dragging drill cores in the basement.

References

ASTM D5873-00. (2000). Standard Test Method for Determination of Rock Hardness by Rebound Hammer Method. *ASTM International, West Conshohocken, PA. US.*

Bingen, B., Nordgulen, Ø. & Viola, G. (2008) A four-phase model for the Sveconorwegian orogeny, SW Scandinavia. *Norwegian Journal of Geology, 88*, 43-72. ISSN 029-196X.

Chakraborty, M., & Mukherjee, S. (2020). Structural geological interpretations from unrolled images of drill cores. *Marine and Petroleum Geology, 104241.* doi:10.1016/j.marpetgeo.2020.104241

Fleuty, M. J. (1964). The description of folds. *Proceedings of the Geologists' Association, 75(4), 461–492.* doi:10.1016/s0016-7878(64)80023-7

Fossen, H. (2010). *Structural geology* (2nd ed.). Cambridge university press.

Google. (n.d.). *[Google maps overview of Gothenburg]*. Retrieved 2021-05-24 from https://www.google.com/maps/place/57%C2%B039'20.5%22N+11%C2%B057'05.6%22E/@57.6573714,11.9049827,13.09z/data=!4m5!3m4!1s0x0:0x0!8m2!3d57.655697!4d11.951559

Gorbatschev, R., & Bogdanova, S. (1993). Frontiers in the Baltic Shield. *Precambrian Research, 64(1-4), 3–21.* doi:10.1016/0301-9268(93)90066-b

Gorbatschev, R., & Gaál, G. (1987). The Precambrian history of the baltic shield. *Geodynamics Series, 149–159.* doi:10.1029/gd017p0149

Hegardt, A.E. (2010). *Pressure, temperature and time constraints on tectonic models for southwestern Sweden*. [Doctoral dissertation, University of Gothenburg]. Retrieved from: http://hdl.handle.net/2077/23787.

Hillefors, Å. (2008). Deglaciation models from the Swedish West Coast. *Boreas, 8(2),* 153–169. doi:10.1111/j.1502-3885.1979.tb00796.x

Hynynen, A. (2021). *Lithological investigation and radioisotope concentrations in pilot borehole GE1, Högsbo A first step towards geothermal energy in Gothenburg, Sweden.* [Bachelor thesis, Gothenburg University].

Institute of seismology university of Helsinki. (2020). Report on deep hole drilling in geothermal energy projects, associated environmental perspectives and risk management: Guidelines for permit authorities (S-70). https://doi.org/https://helda.helsinki.fi/handle/10138/313884

ISRM. (1978). Suggested methods for determining hardness and abrasiveness of rocks. *Int. J. Rock Mech. Min. Sci., Geomech.Abstr. 15*, 89–97.

Leary, P., Malin, P., Saarno, T., & Kukkonen, I. (2017). Prospects for Assessing Enhanced Geothermal System (EGS) Basement Rock Flow Stimulation by Wellbore Temperature Data. *Energies, 10(12), 1979.* doi:10.3390/en10121979

Lundqvist, J., Lundqvist, T., Lindström, M., Calner, M., & Sivhed, U. (2011). *Sveriges geologi från urtid till nutid* (3rd ed.). Lund: Studentlitteratur.

Marjoribanks, R. (2010). *Geological Methods in Mineral Exploration and Mining* (2^{nd} ed.). Springer.

Medan, V. (2015). *Mineralogical generations and orientation of fractures, based on drill cores from the West-Link Project, Gothenburg*. [Master thesis, Gothenburg University]. B855.

Park, R., Åhäll, K.-I., & Bland, M. (1991). The Sveconorwegian shear-zone network of SW Sweden in relation to mid-Proterozoic plate movements. *Precambrian Research, 49(3-4), 245–260.* doi:10.1016/0301-9268(91)90036-a

Persson, T. (2007). *Sprickmineralogisk undersökning av borrkärnor från Götatunneln och Nygårdstunneln*. [Project wotk, Gothenburg university] B516.

Rosberg, J., & Erlström, M. (2019). Evaluation of the Lund deep geothermal exploration project in the Romeleåsen Fault Zone, South Sweden: a case study. *Geothermal Energy*, *7*(1). doi: 10.1186/s40517-019-0126-7

SGU (2000). *Regional berggrundsgeologisk undersökning Sammanfattning av pågående undersökningar 1999*. ISBN 91-7158-633- 4

SGU (2006). *Berggrundskartan 7B Göteborg SV*. ISBN 91-7158-770-5

Viola, G., Henderson, I. H. C., Bingen, B., & Hendriks, B. W. H. (2011). The Grenvillian–Sveconorwegian orogeny in Fennoscandia: Back-thrusting and extensional shearing along the “Mylonite Zone.”. *Precambrian Research, 189(3-4), 368–388.* doi:10.1016/j.precamres.2011.06.005

Åhäll, K.-I., & Connelly, J. N. (2008). Long-term convergence along SW fennoscandia: 330m.y. of proterozoic crustal growth. *Precambrian Research, 161(3-4), 452–474.* doi:10.1016/j.precamres.2007.09.007

Åhäll, K. I., & Daly, J. S. (1989). Age, tectonic setting and provenance of Östfold-Marstrand Belt Supracrustals: Westward crustal growth of the Baltic Shield at 1760 Ma. *Precambrian Research, 45(1-3), 45–61.* doi:10.1016/0301-9268(89)90030-2

GE1 pilot drill core, Gothenburg

Deep geothermal energy exploration project

0-100 m

Drill core:	GE1
Drill site:	Högsbo, 57.655697, 11.951559
Date:	26.03.2021 - 26.05.2021
Logged by:	Anna Hynynen and Julia Ladefoged

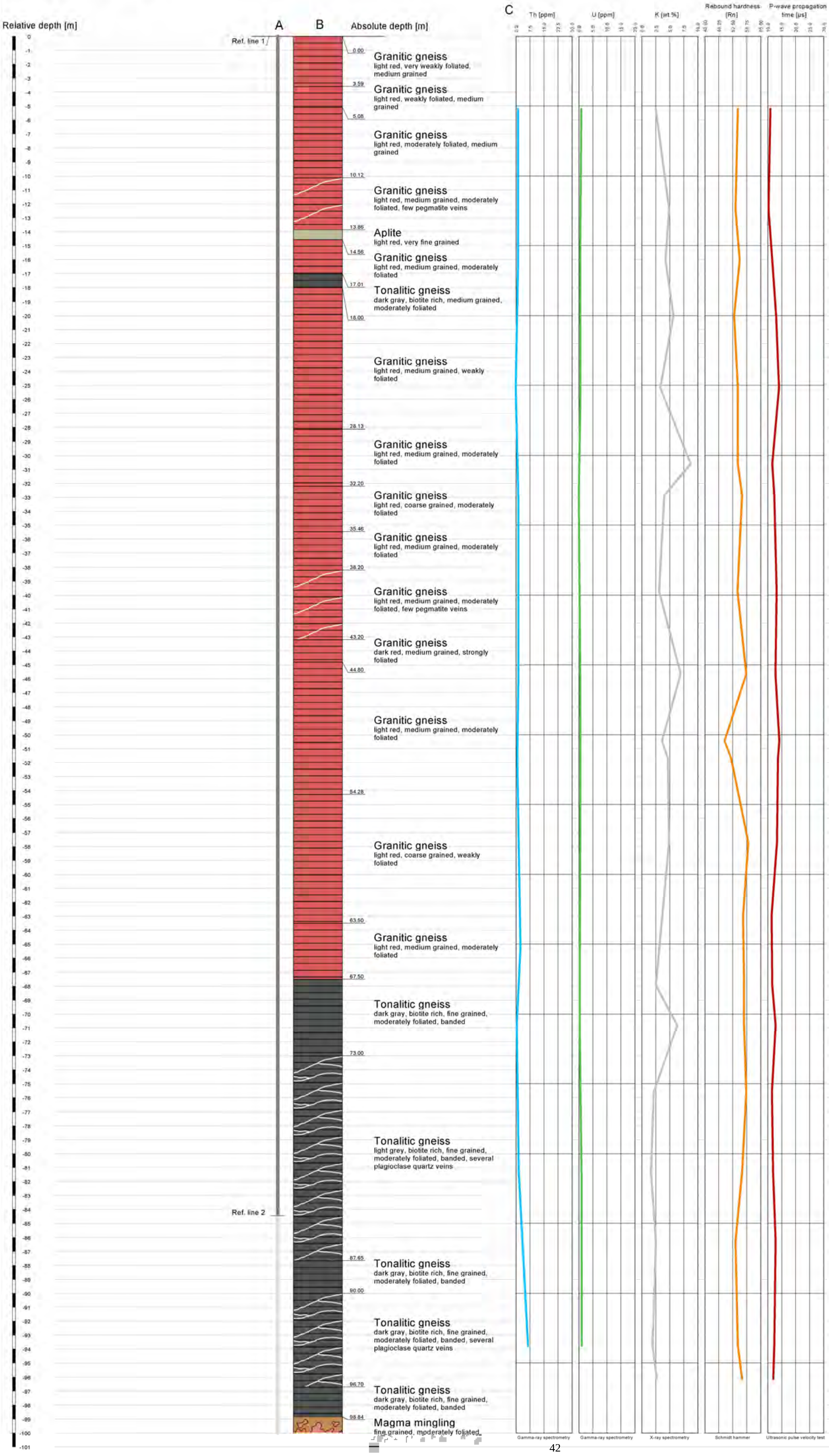

Absolute depth [m]	
0.00	**Granitic gneiss** light red, very weakly foliated, medium grained
3.59	**Granitic gneiss** light red, weakly foliated, medium grained
5.08	**Granitic gneiss** light red, moderately foliated, medium grained
10.12	**Granitic gneiss** light red, medium grained, moderately foliated, few pegmatite veins
13.86	**Aplite** light red, very fine grained
14.56	**Granitic gneiss** light red, medium grained, moderately foliated
17.01	**Tonalitic gneiss** dark gray, biotite rich, medium grained, moderately foliated
18.00	**Granitic gneiss** light red, medium grained, weakly foliated
28.13	**Granitic gneiss** light red, medium grained, moderately foliated
32.20	**Granitic gneiss** light red, coarse grained, moderately foliated
35.46	**Granitic gneiss** light red, medium grained, moderately foliated
38.20	**Granitic gneiss** light red, medium grained, moderately foliated, few pegmatite veins
43.20	**Granitic gneiss** dark red, medium grained, strongly foliated
44.80	**Granitic gneiss** light red, medium grained, moderately foliated
54.28	**Granitic gneiss** light red, coarse grained, weakly foliated
63.50	**Granitic gneiss** light red, medium grained, moderately foliated
67.50	**Tonalitic gneiss** dark gray, biotite rich, fine grained, moderately foliated, banded
73.00	**Tonalitic gneiss** light grey, biotite rich, fine grained, moderately foliated, banded, several plagioclase quartz veins
87.65	**Tonalitic gneiss** dark gray, biotite rich, fine grained, moderately foliated, banded
90.00	**Tonalitic gneiss** dark gray, biotite rich, fine grained, moderately foliated, banded, several plagioclase quartz veins
96.70	**Tonalitic gneiss** dark gray, biotite rich, fine grained, moderately foliated, banded
98.84	**Magma mingling** fine grained, moderately foliated

D

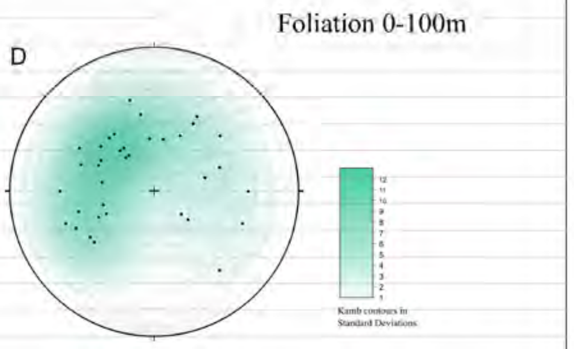

E

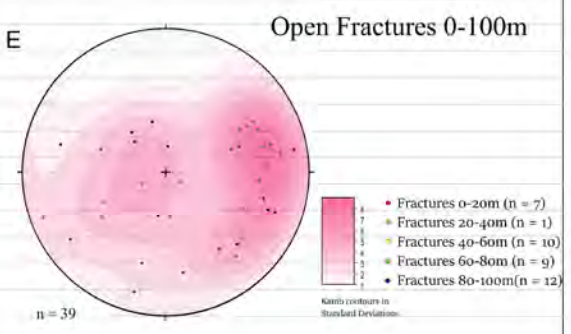

F

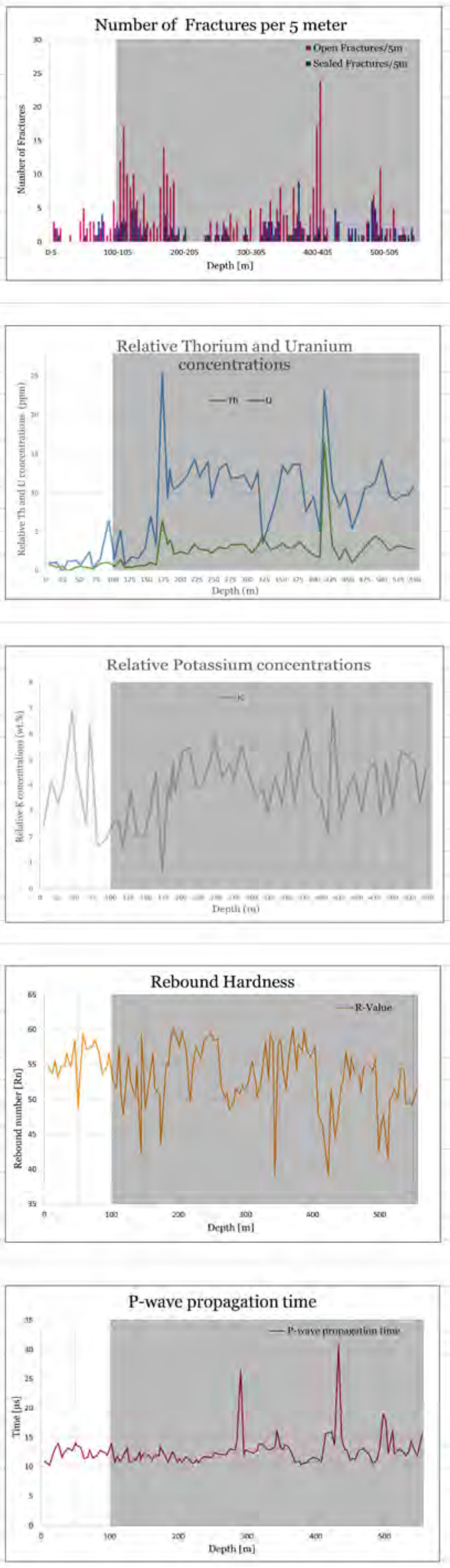

GE1 pilot drill core, Gothenburg

Deep geothermal energy exploration project

100-200 m

Drill core:	GE1
Drill site:	Högsbo, 57.655697, 11.951559
Date:	26.03.2021 - 26.05.2021
Logged by:	Anna Hynynen and Julia Ladefoged

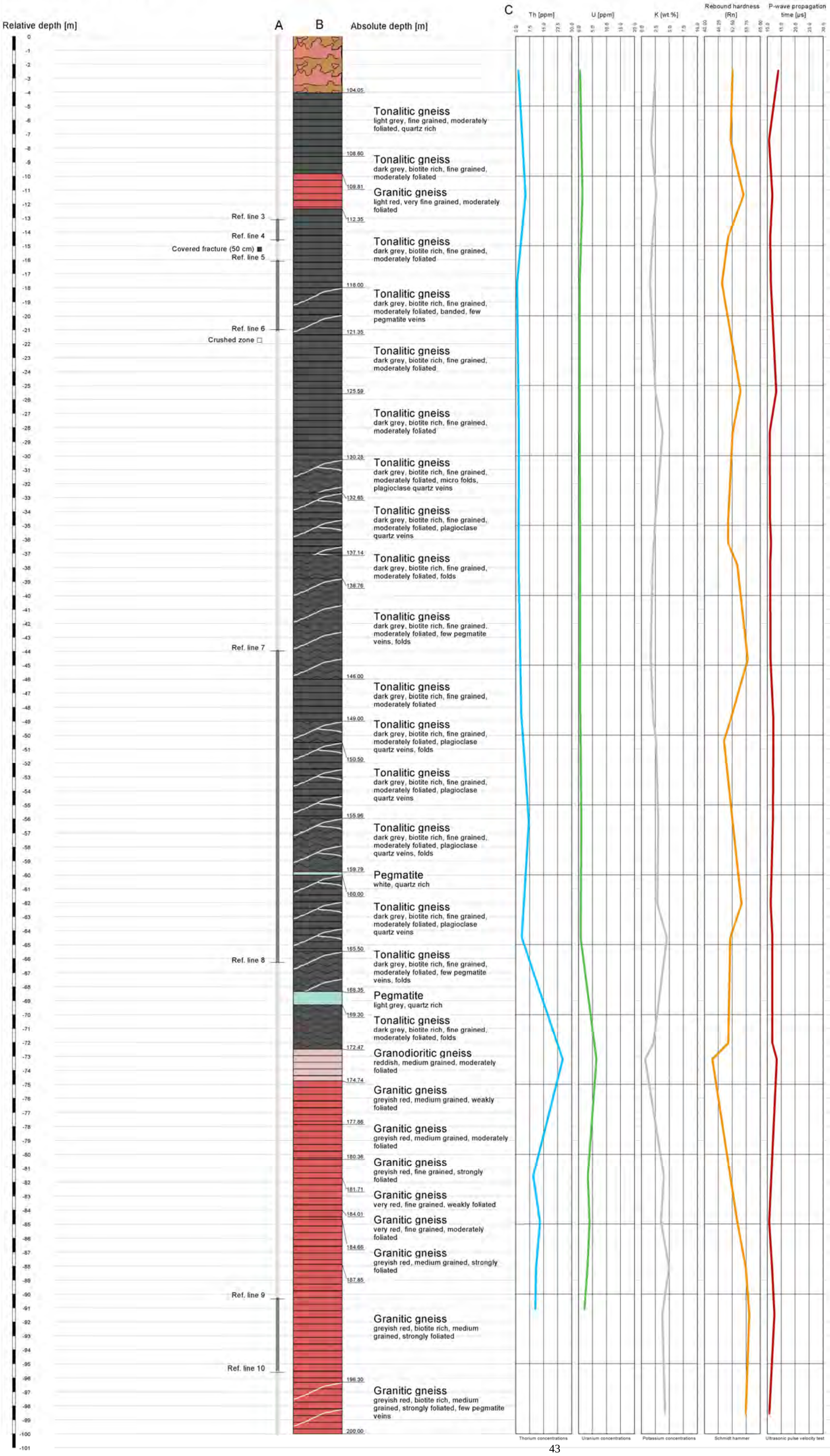

Absolute depth [m]	
104.05	**Tonalitic gneiss** light grey, fine grained, moderately foliated, quartz rich
108.60	**Tonalitic gneiss** dark grey, biotite rich, fine grained, moderately foliated
109.81	**Granitic gneiss** light red, very fine grained, moderately foliated
112.35	**Tonalitic gneiss** dark grey, biotite rich, fine grained, moderately foliated
118.00	**Tonalitic gneiss** dark grey, biotite rich, fine grained, moderately foliated, banded, few pegmatite veins
121.35	**Tonalitic gneiss** dark grey, biotite rich, fine grained, moderately foliated
125.59	**Tonalitic gneiss** dark grey, biotite rich, fine grained, moderately foliated
130.28	**Tonalitic gneiss** dark grey, biotite rich, fine grained, moderately foliated, micro folds, plagioclase quartz veins
132.65	**Tonalitic gneiss** dark grey, biotite rich, fine grained, moderately foliated, plagioclase quartz veins
137.14	**Tonalitic gneiss** dark grey, biotite rich, fine grained, moderately foliated, folds
138.76	**Tonalitic gneiss** dark grey, biotite rich, fine grained, moderately foliated, few pegmatite veins, folds
146.00	**Tonalitic gneiss** dark grey, biotite rich, fine grained, moderately foliated
149.00	**Tonalitic gneiss** dark grey, biotite rich, fine grained, moderately foliated, plagioclase quartz veins, folds
150.50	**Tonalitic gneiss** dark grey, biotite rich, fine grained, moderately foliated, plagioclase quartz veins
155.96	**Tonalitic gneiss** dark grey, biotite rich, fine grained, moderately foliated, plagioclase quartz veins, folds
159.79	**Pegmatite** white, quartz rich
160.00	**Tonalitic gneiss** dark grey, biotite rich, fine grained, moderately foliated, plagioclase quartz veins
165.50	**Tonalitic gneiss** dark grey, biotite rich, fine grained, moderately foliated, few pegmatite veins, folds
168.35	**Pegmatite** light grey, quartz rich
169.30	**Tonalitic gneiss** dark grey, biotite rich, fine grained, moderately foliated, folds
172.47	**Granodioritic gneiss** reddish, medium grained, moderately foliated
174.74	**Granitic gneiss** greyish red, medium grained, weakly foliated
177.86	**Granitic gneiss** greyish red, medium grained, moderately foliated
180.36	**Granitic gneiss** greyish red, fine grained, strongly foliated
181.71	**Granitic gneiss** very red, fine grained, weakly foliated
184.01	**Granitic gneiss** very red, fine grained, moderately foliated
184.66	**Granitic gneiss** greyish red, medium grained, strongly foliated
187.85	**Granitic gneiss** greyish red, biotite rich, medium grained, strongly foliated
196.30	**Granitic gneiss** greyish red, biotite rich, medium grained, strongly foliated, few pegmatite veins
200.00	

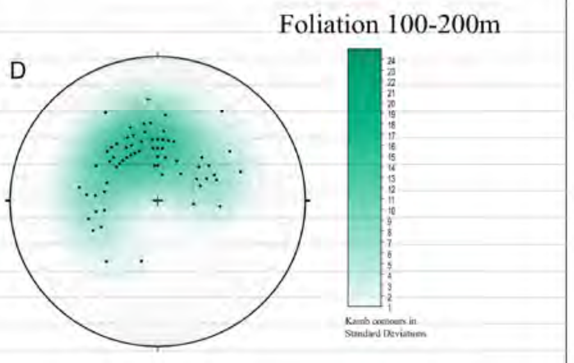

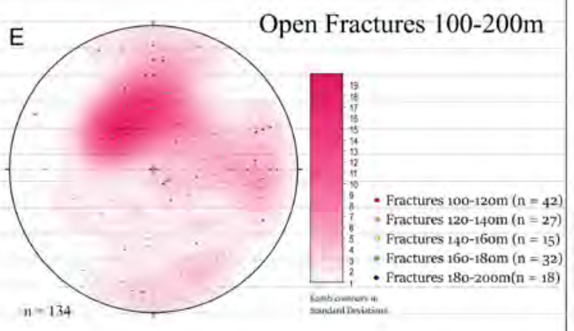

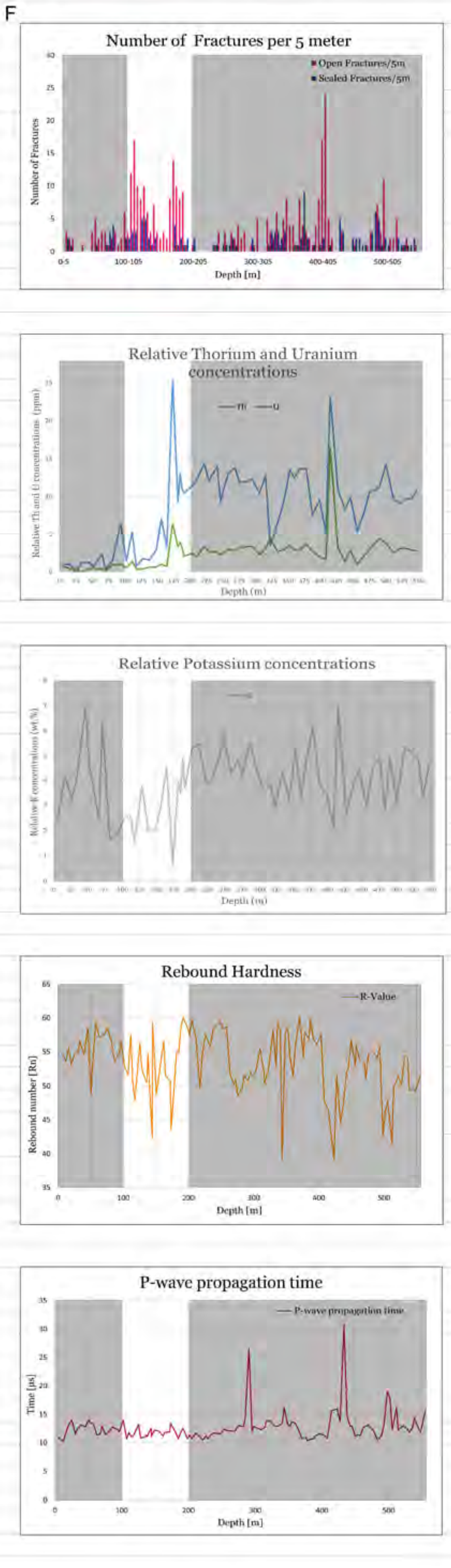

GE1 pilot drill core, Gothenburg

Deep geothermal energy exploration project

200-300 m

Drill core: GE1
Drill site: Högsbo, 57.655697, 11.951559
Date: 26.03.2021 - 26.05.2021
Logged by: Anna Hynynen and Julia Ladefoged

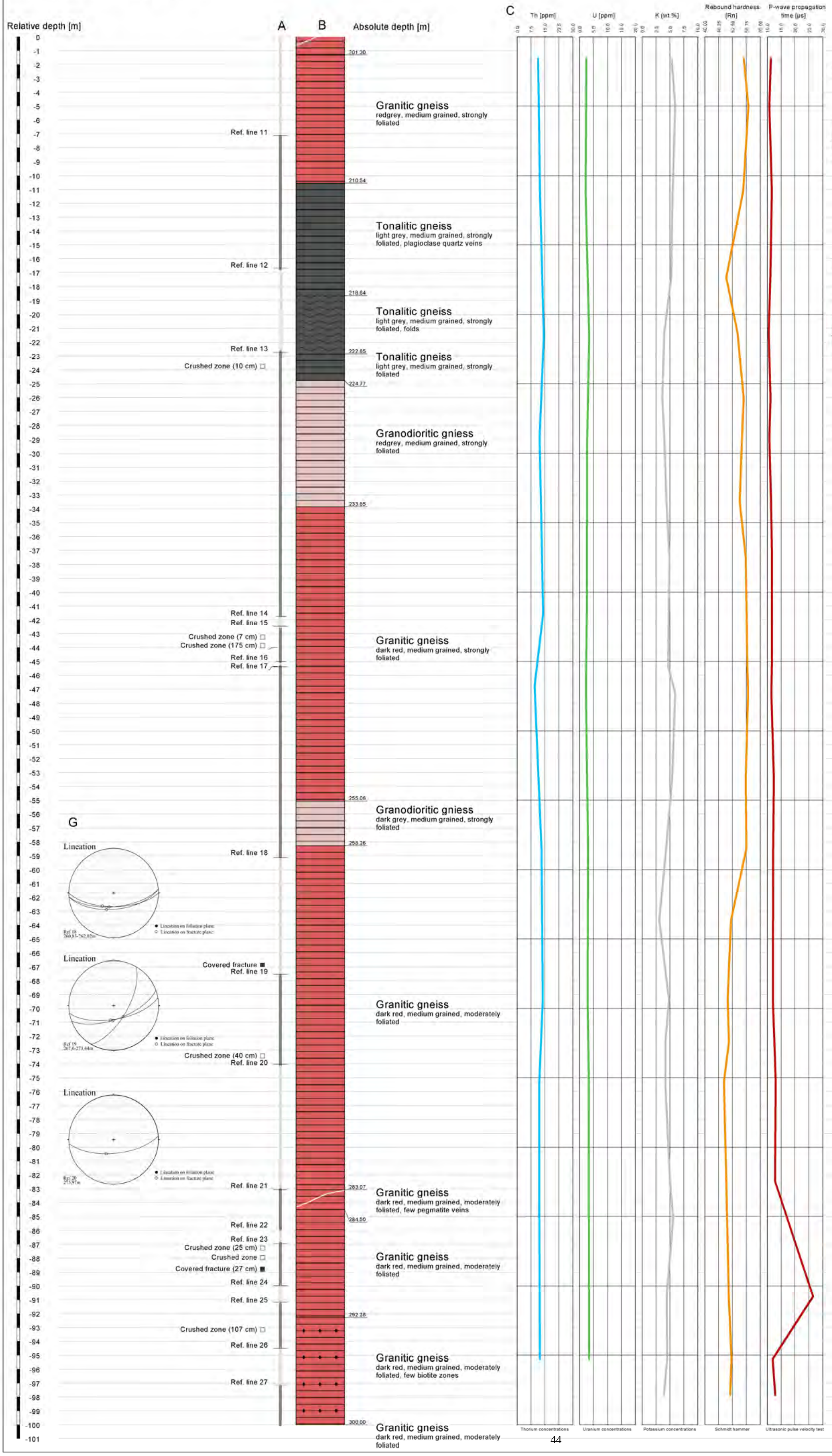

Granitic gneiss
redgrey, medium grained, strongly foliated

Tonalitic gneiss
light grey, medium grained, strongly foliated, plagioclase quartz veins

Tonalitic gneiss
light grey, medium grained, strongly foliated, folds

Tonalitic gneiss
light grey, medium grained, strongly foliated

Granodioritic gneiss
redgrey, medium grained, strongly foliated

Granitic gneiss
dark red, medium grained, strongly foliated

Granodioritic gneiss
dark grey, medium grained, strongly foliated

Granitic gneiss
dark red, medium grained, moderately foliated

Granitic gneiss
dark red, medium grained, moderately foliated, few pegmatite veins

Granitic gneiss
dark red, medium grained, moderately foliated

Granitic gneiss
dark red, medium grained, moderately foliated, few biotite zones

Granitic gneiss
dark red, medium grained, moderately foliated

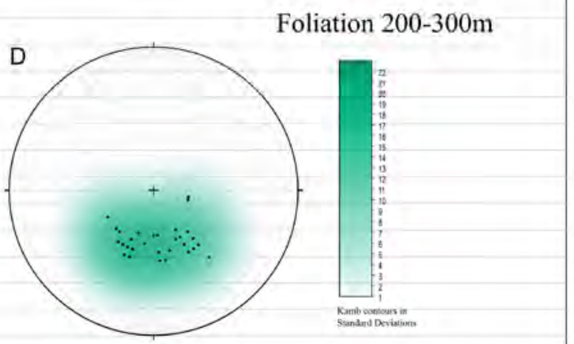

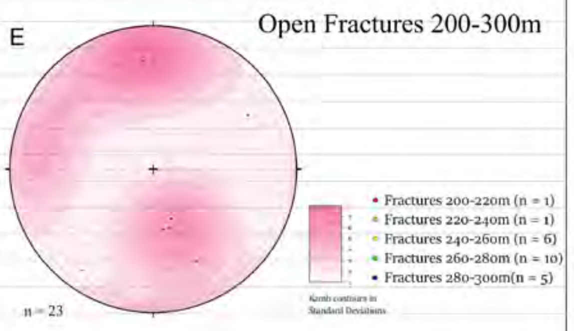

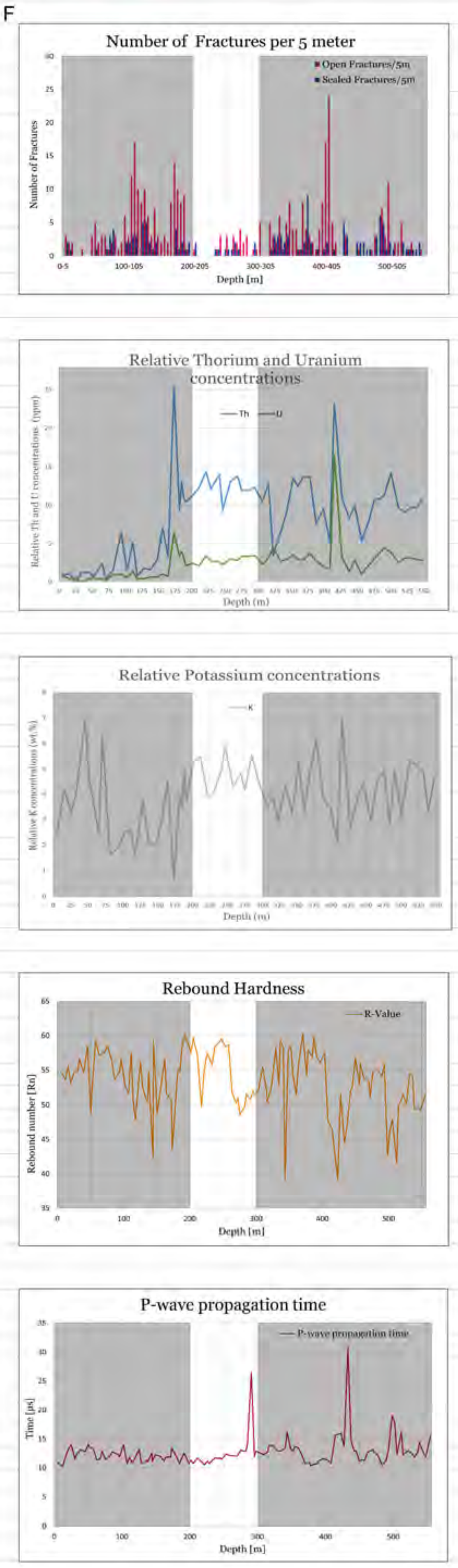

GE1 pilot drill core, Gothenburg

Deep geothermal energy exploration project

300-400 m

Drill core: GE1
Drill site: Högsbo, 57.655697, 11.951559
Date: 26.03.2021 - 26.05.2021
Logged by: Anna Hynynen and Julia Ladefoged

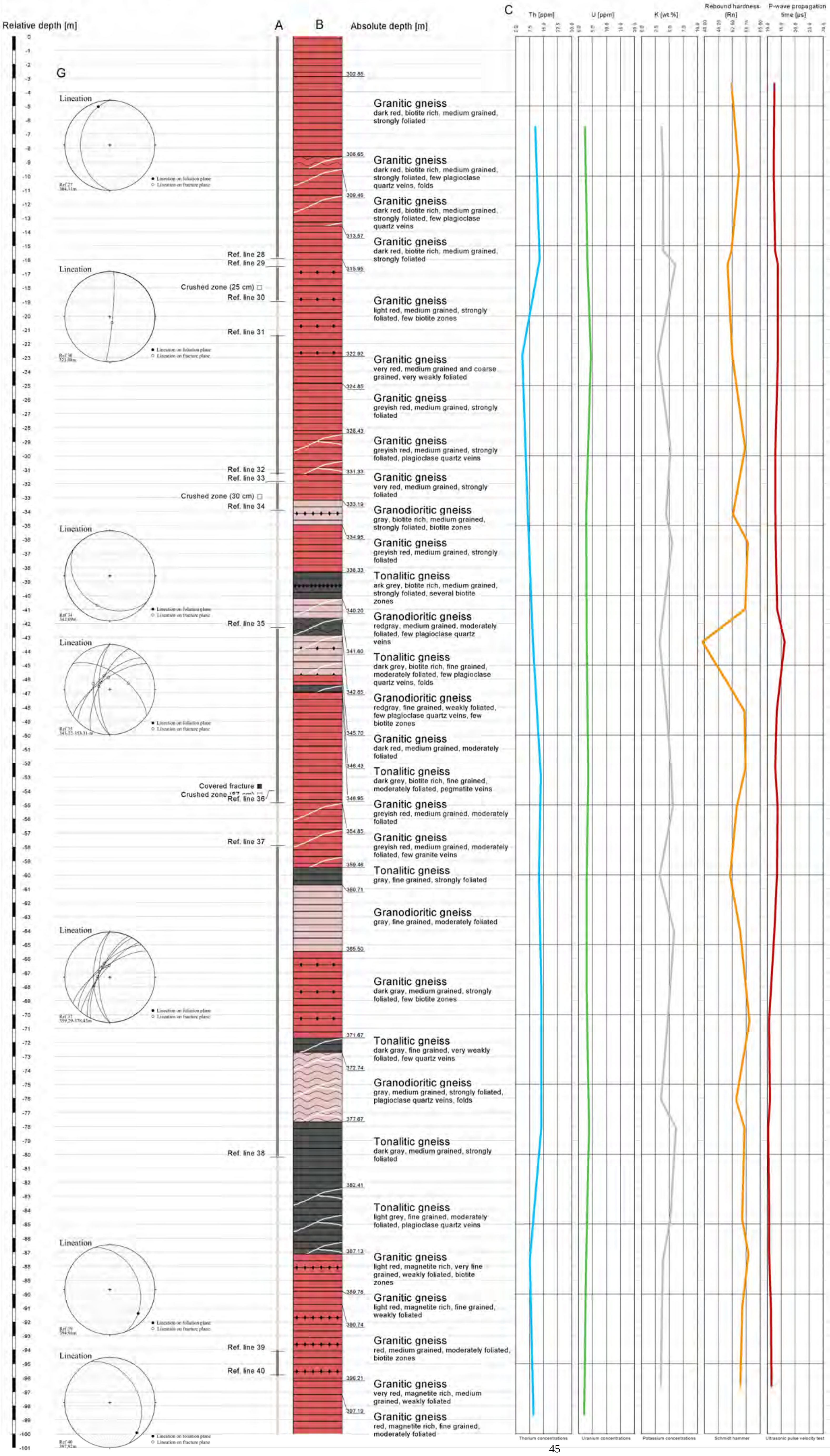

302.86

Granitic gneiss
dark red, biotite rich, medium grained, strongly foliated

308.65

Granitic gneiss
dark red, biotite rich, medium grained, strongly foliated, few plagioclase quartz veins, folds

309.46

Granitic gneiss
dark red, biotite rich, medium grained, strongly foliated, few plagioclase quartz veins

313.57

Granitic gneiss
dark red, biotite rich, medium grained, strongly foliated

315.95

Granitic gneiss
light red, medium grained, strongly foliated, few biotite zones

322.92

Granitic gneiss
very red, medium grained and coarse grained, very weakly foliated

324.85

Granitic gneiss
greyish red, medium grained, strongly foliated

328.43

Granitic gneiss
greyish red, medium grained, strongly foliated, plagioclase quartz veins

331.33

Granitic gneiss
very red, medium grained, strongly foliated

333.19

Granodioritic gneiss
gray, biotite rich, medium grained, strongly foliated, biotite zones

334.95

Granitic gneiss
greyish red, medium grained, strongly foliated

338.33

Tonalitic gneiss
ark grey, biotite rich, medium grained, strongly foliated, several biotite zones

340.20

Granodioritic gneiss
redgray, medium grained, moderately foliated, few plagioclase quartz veins

341.60

Tonalitic gneiss
dark grey, biotite rich, fine grained, moderately foliated, few plagioclase quartz veins, folds

342.85

Granodioritic gneiss
redgray, fine grained, weakly foliated, few plagioclase quartz veins, few biotite zones

345.70

Granitic gneiss
dark red, medium grained, moderately foliated

346.43

Tonalitic gneiss
dark grey, biotite rich, fine grained, moderately foliated, pegmatite veins

348.95

Granitic gneiss
greyish red, medium grained, moderately foliated

354.85

Granitic gneiss
greyish red, medium grained, moderately foliated, few granite veins

359.46

Tonalitic gneiss
gray, fine grained, strongly foliated

360.71

Granodioritic gneiss
gray, fine grained, moderately foliated

365.50

Granitic gneiss
dark gray, medium grained, strongly foliated, few biotite zones

371.67

Tonalitic gneiss
dark gray, fine grained, very weakly foliated, few quartz veins

372.74

Granodioritic gneiss
gray, medium grained, strongly foliated, plagioclase quartz veins, folds

377.67

Tonalitic gneiss
dark gray, medium grained, strongly foliated

382.41

Tonalitic gneiss
light grey, fine grained, moderately foliated, plagioclase quartz veins

387.13

Granitic gneiss
light red, magnetite rich, very fine grained, weakly foliated, biotite zones

389.78

Granitic gneiss
light red, magnetite rich, fine grained, weakly foliated

390.74

Granitic gneiss
red, medium grained, moderately foliated, biotite zones

396.21

Granitic gneiss
very red, magnetite rich, medium grained, weakly foliated

397.19

Granitic gneiss
red, magnetite rich, fine grained, moderately foliated

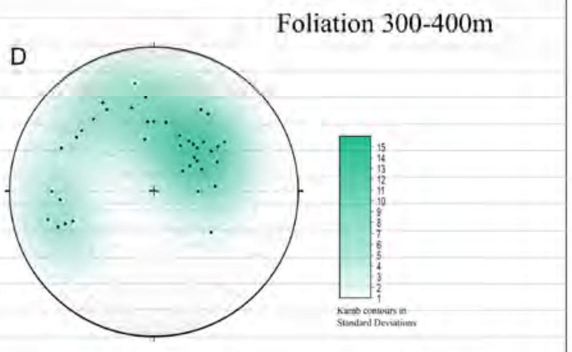

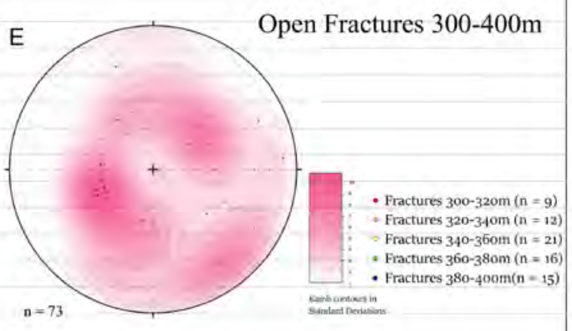

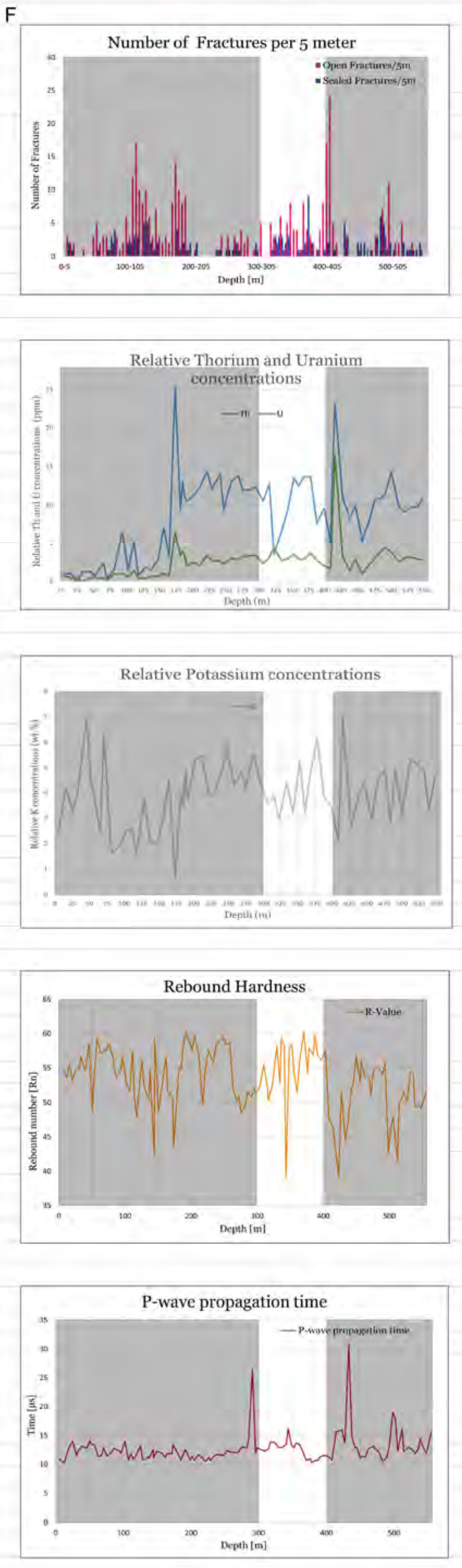

GE1 pilot drill core, Gothenburg

Deep geothermal energy exploration project

400-500 m

Drill core:	GE1
Drill site:	Högsbo, 57.655697, 11.951559
Date:	26.03.2021 - 26.05.2021
Logged by:	Anna Hynynen and Julia Ladefoged

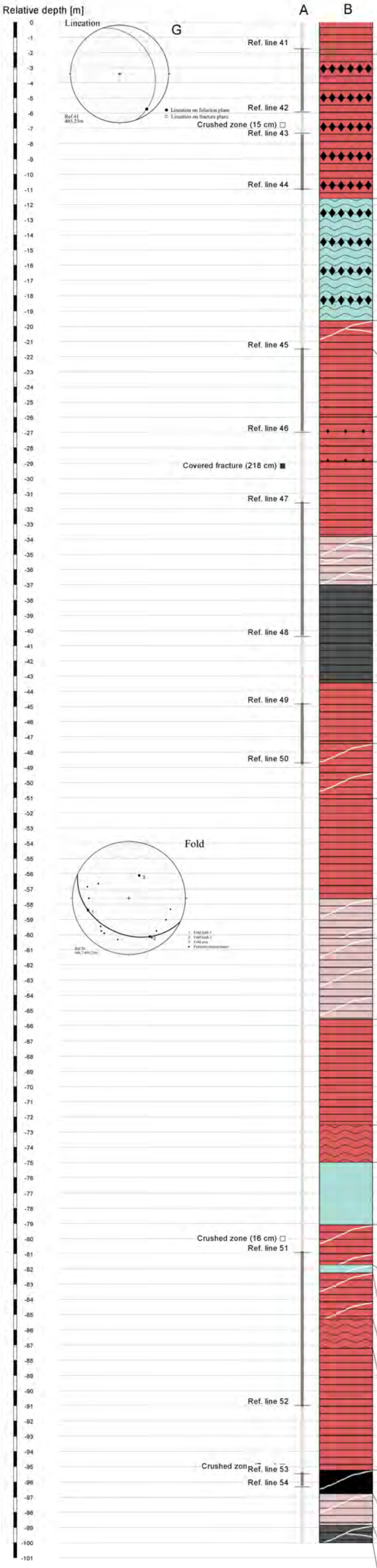

Absolute depth [m]

402.11

Granitic gneiss
redgray, magnetite rich, fine grained, very weakly foliated, several large biotite zones

411.60

Pegmatite
redgray, magnetite rich, fine grained, very weakly foliated, folds, several large biotite zones

419.63

Granitic gneiss
redgray, fine grained, moderately foliated, plagioclase quartz veins

421.51

Granitic gneiss
redgray, fine grained, moderately foliated

425.97

Granitic gneiss
redgray, fine grained, moderately foliated, few biotite zones

428.90

Granitic gneiss
redgray, fine grained, moderately foliated

433.82

Granodioritic gneiss
light gray, magnetite rich, medium grained, weakly foliated, several granite veins

437.00

Tonalitic gneiss
gray, magnetite rich, medium grained, moderately foliated

443.44

Granitic gneiss
greyish red, medium grained, moderately foliated

447.42

Granitic gneiss
greyish red, medium grained, moderately foliated, few quartz veins, few plagioclase quartz veins

451.05

Granitic gneiss
greyish red, magnetite rich, medium grained, weakly foliated

457.63

Granodioritic gneiss
red, magnetite rich, medium grained, weakly foliated, few granite veins

460.25

Granodioritic gneiss
redgray, magnetite rich, medium grained, weakly foliated, few granite veins

465.59

Granitic gneiss
dark red, biotite rich, medium grained, moderately foliated

472.53

Granitic gneiss
dark red, biotite rich, medium grained, moderately foliated, folds

475.00

Pegmatite
very red, amazonite rich, medium grained and coarse grained

479.08

Granitic gneiss
greyish red, biotite rich, medium grained, moderately foliated, few plagioclase quartz veins

481.73

Pegmatite
very red, medium grained and coarse grained, few plagioclase quartz veins

482.26

Granitic gneiss
redgray, medium grained, strongly foliated, few plagioclase quartz veins

485.30

Granitic gneiss
redgray, medium grained, strongly foliated, folds

487.20

Granitic gneiss
redgray, medium grained, strongly foliated

495.23

Biotite zone
dark gray, fine grained, strongly foliated, few quartz veins

496.77

Granodioritic gneiss
light red, medium grained, strongly foliated, few quartz veins

498.85

Tonalitic gneiss
light gray, fine grained, moderately foliated, plagioclase quartz veins

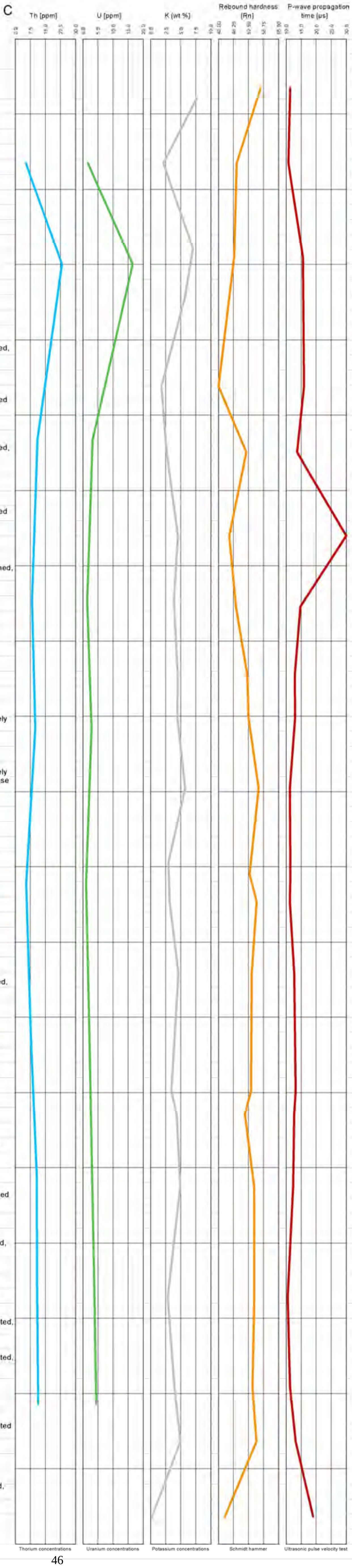

Foliation 400-500m

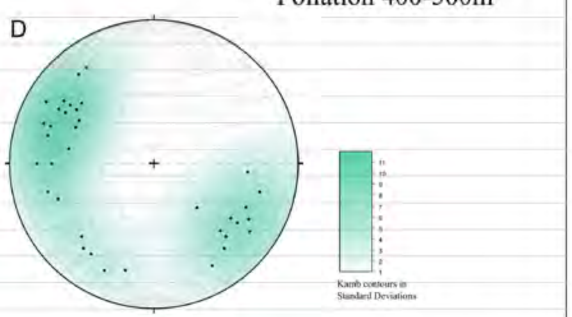

Open Fractures 400-500m

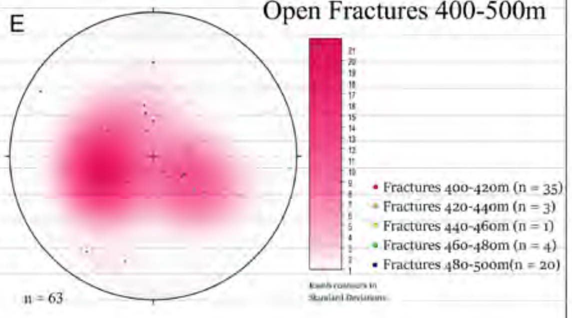

F

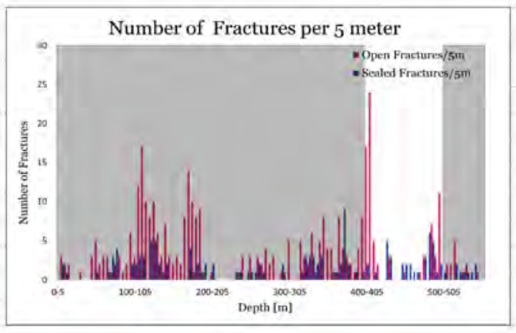

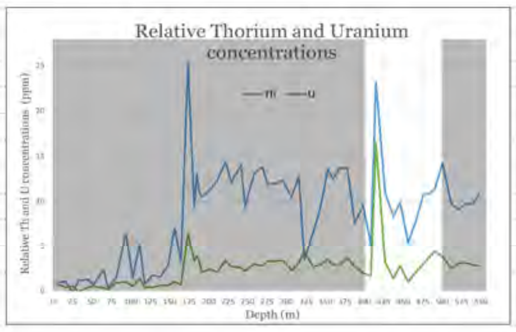

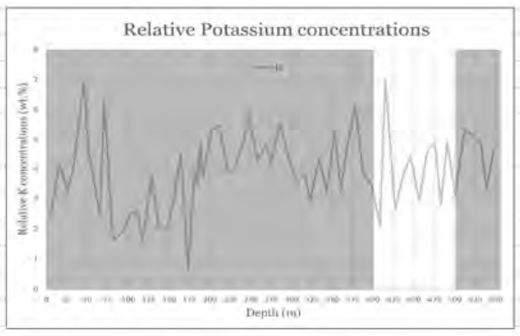

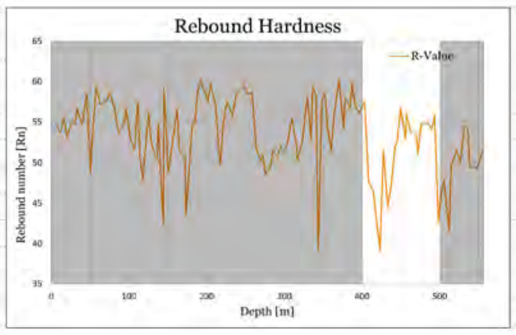

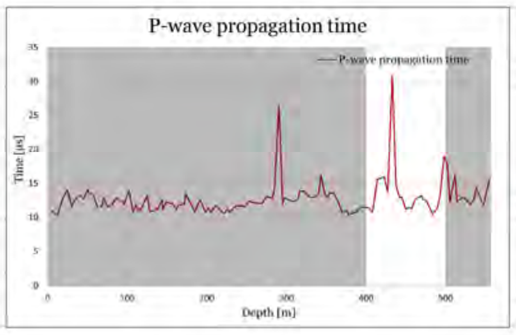

GE1 pilot drill core, Gothenburg

Deep geothermal energy exploration project

500-556 m

Drill core: GE1
Drill site: Högsbo, 57.655697, 11.951559
Date: 26.03.2021 - 26.05.2021
Logged by: Anna Hynynen and Julia Ladefoged

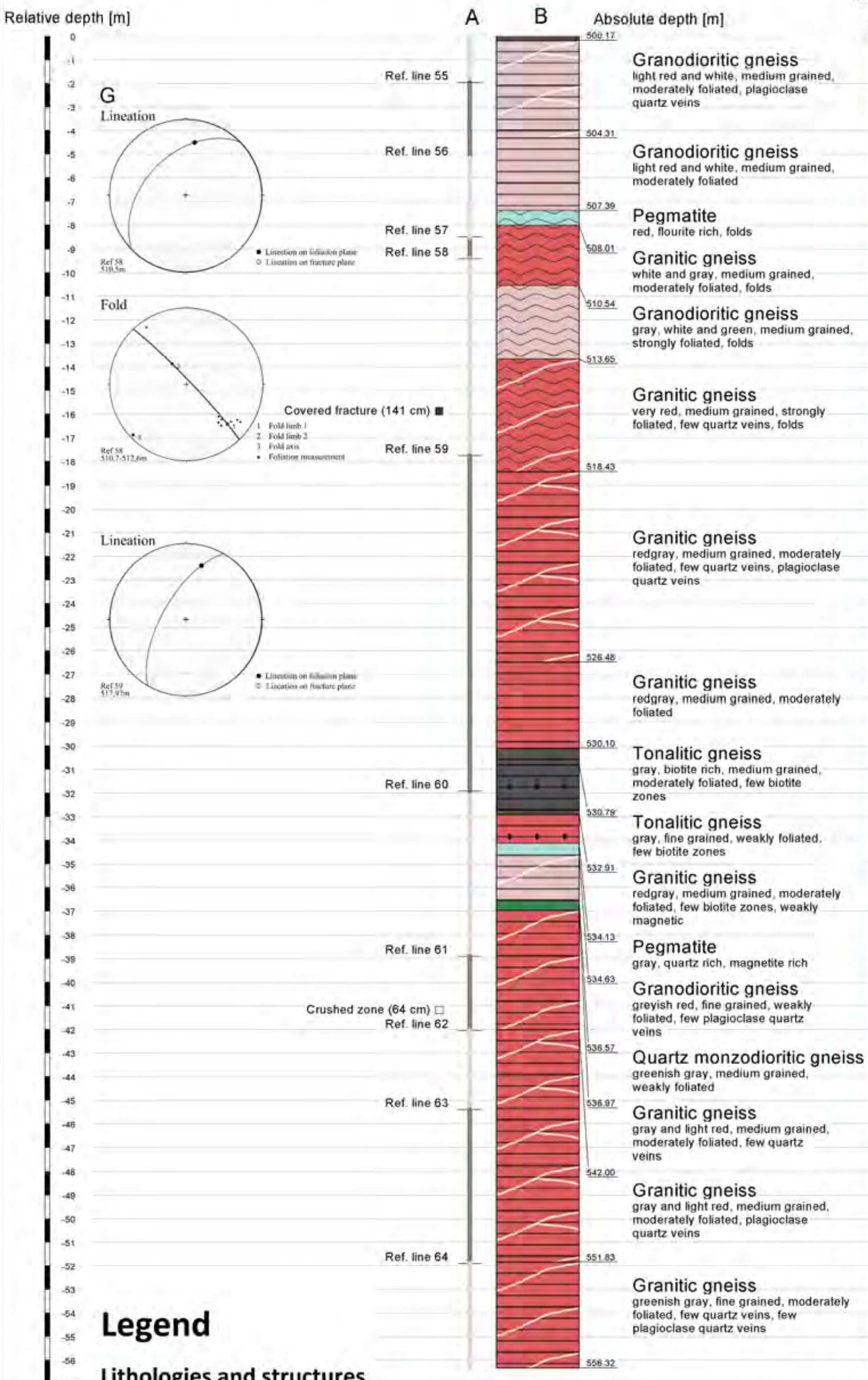

Granodioritic gneiss
light red and white, medium grained, moderately foliated, plagioclase quartz veins

Granodioritic gneiss
light red and white, medium grained, moderately foliated

Pegmatite
red, flourite rich, folds

Granitic gneiss
white and gray, medium grained, moderately foliated, folds

Granodioritic gneiss
gray, white and green, medium grained, strongly foliated, folds

Granitic gneiss
very red, medium grained, strongly foliated, few quartz veins, folds

Granitic gneiss
redgray, medium grained, moderately foliated, few quartz veins, plagioclase quartz veins

Granitic gneiss
redgray, medium grained, moderately foliated

Tonalitic gneiss
gray, biotite rich, medium grained, moderately foliated, few biotite zones

Tonalitic gneiss
gray, fine grained, weakly foliated, few biotite zones

Granitic gneiss
redgray, medium grained, moderately foliated, few biotite zones, weakly magnetic

Pegmatite
gray, quartz rich, magnetite rich

Granodioritic gneiss
greyish red, fine grained, weakly foliated, few plagioclase quartz veins

Quartz monzodioritic gneiss
greenish gray, medium grained, weakly foliated

Granitic gneiss
gray and light red, medium grained, moderately foliated, few quartz veins

Granitic gneiss
gray and light red, medium grained, moderately foliated, plagioclase quartz veins

Granitic gneiss
greenish gray, fine grained, moderately foliated, few quartz veins, few plagioclase quartz veins

Foliation 500-555m

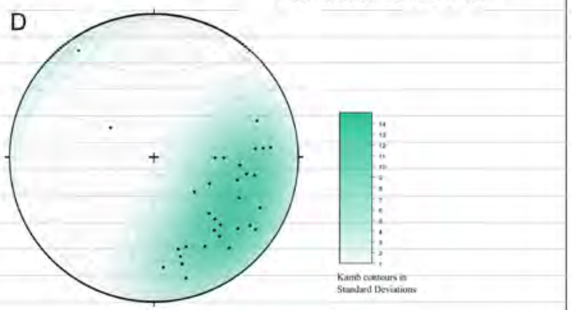

Open Fractures 500-555m

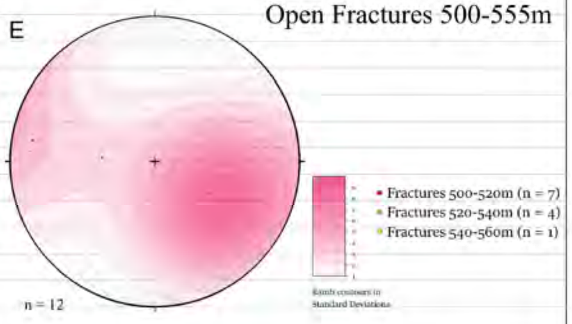

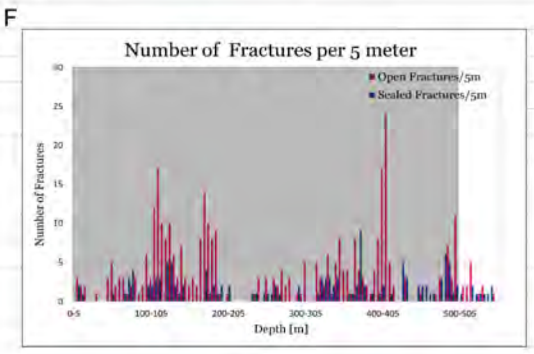

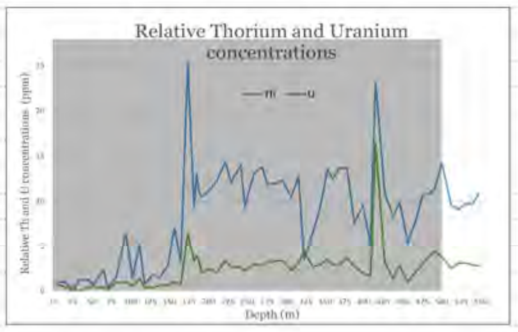

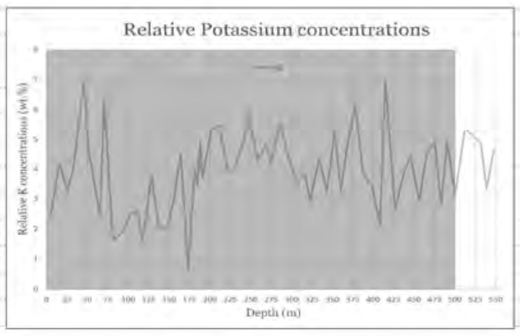

Open Fractures 0-555m

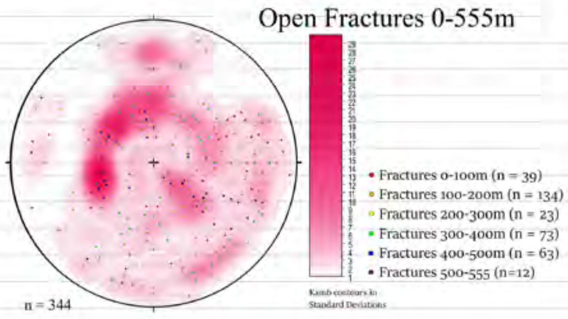

Stereonet contour plot of open fractures from 0-555 m. The drill core was oriented by turning the foliation measurement from the first 15 m approximately to the west. The following reference lines were oriented by turning the first foliation measurement, from each reference line, in the same direction as the last foliation measurement of the previous reference line.

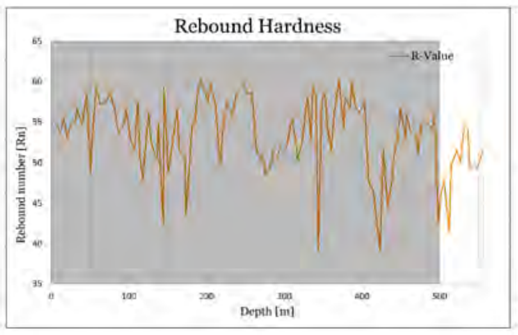

Foliation 0-555m

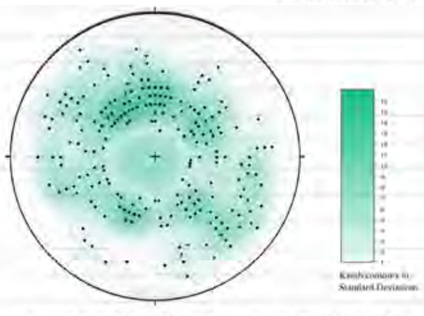

Stereonet contour plot of foliation measurements from 0-555 m. The drill core was oriented by turning the foliation measurement from the first 15 m approximately to the west. The following reference lines were oriented by turning the first foliation measurement, from each reference line, in the same direction as the last foliation measurement of the previous reference line.

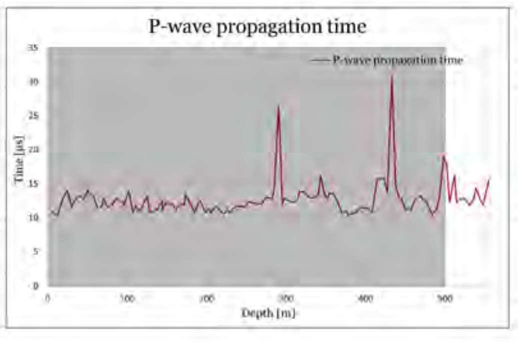

Legend

Lithologies and structures

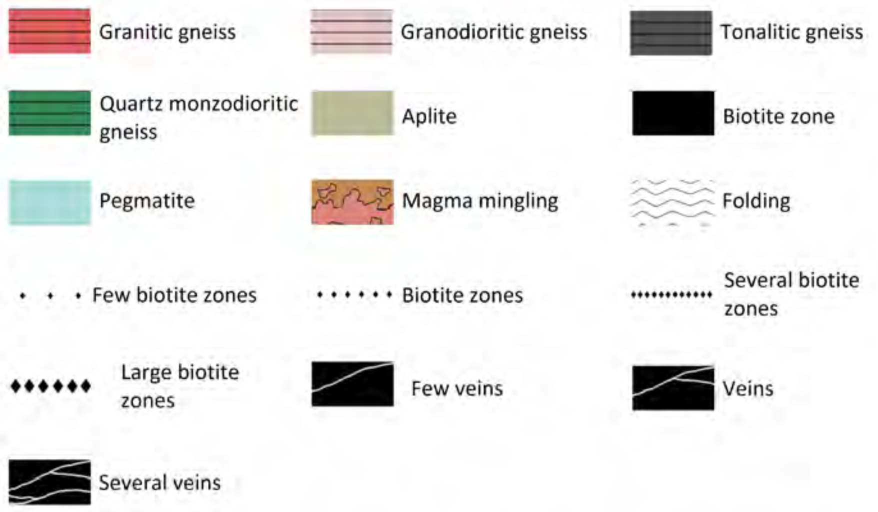

A. **Reference line**
Reference lines for continuous segments of the non-oriented drill core. When core loss or non-continuous segments were encountered, a new reference line was marked.

B. **Stratigraphic log**
100-meter intervals of the core log showing absolute depths of lithological and structural changes. 0-100 m on the first page, 100-200 m on the second page etc. See text on the right side of the log for detailed information.

C. **Measured diagrams**
Diagrams showing measurements made on the representative depth for each page. Diagrams from left to right are: Thorium concentration [ppm], Uranium concentration [ppm], Potassium concentration [wt. %], Rebound hardness [Rn] and P-wave propagation time [µs].

D. **Stereonet: Foliation**
Stereonet contour plots of Foliation measurements for each 100-meter interval. The drill core was oriented by turning the foliation measurement from the first 15 m approximately to the west. The following reference lines were oriented by turning the first foliation measurement, from each reference line, in the same direction as the last foliation measurement of the previous reference line.

E. **Stereonet: Open fractures**
Stereonet contour plot of Open fracture measurements for each 100-meter interval. The drill core was oriented by turning the foliation measurement from the first 15 m approximately to the west. The following reference lines were oriented by turning the first foliation measurement, from each reference line, in the same direction as the last foliation measurement of the previous reference line.

F. **Diagram, 0-550 meters depth.**
Diagrams showing measurements from 0-556 meters. The white box represents the shown depth interval for each page. Diagrams from top to bottom are:

Number of Fractures per 5 meters
Histogram showing fracture density for every 5 meters. Blue represents the number of sealed fractures and pink represents the number of open fractures.

Relative Thorium and Uranium concentration
Thorium and Uranium concentrations ranging from 0-30 ppm on the y-axes. Blue line represents Th values and the green line represents U values.

Relative Potassium concentrations
Potassium concentrations (grey line) ranging from 0-8 wt.% on the y-axes.

Rebound hardness
Diagram showing the rebound number. The measurements were made with a Schmidt hammer.

P-wave propagation time
Diagram showing measurements of the P-wave propagation time through the core. The measurements were made with an Ultrasonic pulse velocity instrument.

G. **Stereonets: Lineation and Fold**
Stereonet plots of observed lineations and folds, separated for each reference line. The drill core was oriented by turning the foliation measurement from the first 15 m approximately to the west. The following reference lines were oriented by turning the first foliation measurement, from each reference line, in the same direction as the last foliation measurement of the previous reference line.

Appendix B

Used Definitions
Open fractures – Separated fractures in the core exhibiting fracture minerals or weathering

Sealed fractures – Visible fractures which were still intact

Documented Structures

Depth (m)	Structures	Comments	Mineral	Thickness[cm]	Lineations[Clockwise/Anticlockwise]	Referenceline	Dip direction(Beta)	Alpha	Dip
5,08	Foliation					1	320	30	60
6,5	Foliation					1	290	35	55
7,6	Sealed Fracture					1	110	30	60
9,02	Fracture					1	325	35	55
9,24	Sealed Fracture					1	350	45	45
9,45	Fracture					1	105	25	65
9,95	Fracture					1	260	10	80
10	Fracture					1	350	30	60
10,13	Vein		Kalifeldspar	1		1	50	70	20
10,14	Vein		Pegmatite	11		1	50	70	20
10,2	Fracture					1	70	10	80
10,24	Foliation					1	270	35	55
10,34	Vein		Pegmatite	17		1	50	60	30
10,75	Vein		Pegmatite	39		1	45	80	10
12,1	Foliation					1	255	60	30
12,5	Foliation					1	310	65	25
12,6	Vein		Pegmatite	40		1	140	45	45
13,7	Foliation					1	210	45	45
13,9	Contact					1	195	40	50
14,07	Vein		Kalifeldspar	0,5		1	270	65	25
14,12	Vein		Biotite	0,5		1	135	35	55
14,15	Sealed Fracture					1	155	15	75
14,58	Contact					1	280	70	20
14,72	Foliation					1	210	40	50
15,02	Fracture					1	55	20	70
15,5	Foliation					1	230	40	50
15,85	Foliation					1	250	50	40
17,13	Contact					1	260	55	35
17,65	Fracture					1	250	45	45
18,32	Vein		Pegmatite	8		1	45	70	20
19,5	Foliation					1	120	55	35
22,3	Foliation					1	115	55	35
25,16	Vein		Pegmatite	6		1	160	55	35
27,3	Foliation					1	170	45	45
32,72	Fracture					1	355	65	25
36,5	Foliation					1	145	50	40
38	Foliation					1	130	50	40
38,79	Vein		Pegmatite	2		1	330	60	30
40,4	Foliation					1	110	45	45
42,5	Foliation					1	90	35	55
42,84	Vein		Pegmatite	2		1	230	80	10
42,94	Vein		Pegmatite	13		1	100	50	40
43,5	Foliation					1	130	50	40
45	Fracture					1	310	30	60
46	Foliation					1	120	40	50
47,14	Fracture					1	295	40	50
47,42	Vein		Pegmatite	8		1		90	0
47,75	Fracture					1	265	30	60
47,89	Foliation					1	100	60	30
48,5	Foliation					1	75	60	30
50,28	Fracture					1	240	35	55
51	Foliation					1	55	45	45
51,5	Foliation					1	55	45	45
51,8	Fracture					1	55	45	45
53,4	Fracture					1	65	50	40
53,59	Fracture					1	65	50	40
53,89	Sealed Fracture					1	140	10	80
54,6	Fracture					1	240	30	60
54,6	No Foliation	Weak foliation				1			
55,12	Fracture					1	260	20	70
56,7	Foliation					1	65	40	50
57,5	Foliation					1	75	45	45
57,87	Fracture					1	300	80	10
59,3	Foliation					1	50	45	45
60,06	Fracture					1	65	75	15
60,94	Foliation					1	70	35	55
63,25	Fracture					1	275	35	55
63,9	Fracture					1	245	30	60
64	Foliation					1	65	60	30
65,09	Fracture					1	255	30	60
66,3	Foliation					1	50	45	45
66,4	Sealed Fracture					1	255	30	60
67,54	Contact					1	65	55	35
67,6	Foliation					1	65	55	35
67,79	Fracture					1	250	50	40
69,06	Fracture					1	240	40	50
69,1	Unreadable foliation					1			
69,43	/Vein/Foliation					1	260	65	25
69,59	Vein		Bigger crystals Tonalite/quartz	14		1		90	0
69,8	Foliation					1	310	70	20
70	Sealed Fracture					1	5	25	65
70,94	Vein		Quartz/plagioclase	1		1	340	60	30
71,55	Sealed Fracture					1	230	10	80
71,55	Vein		Quartz/plagioclase	0,5		1	210	55	35
71,55	Unreadable foliation					1			
73,01	Vein		Quartz/plagioclase	1		1	65	55	35
73,33	Vein		Quartz/plagioclase	0,5		1	255	25	65
73,45	Vein		Quartz/plagioclase	13		1	155	65	25
74,25	Fracture					1	255	25	65
74,28	Vein		Quartz/plagioclase	0,3		1	70	65	25
74,81	Sealed Fracture					1	225	15	75
75,13	Fracture					1	110	50	40
75,45	Vein		Quartz/plagioclase	0,3		1	75	55	35
75,98	Vein		Quartz/plagioclase	0,3		1	155	30	60
76,2	Fracture					1	320	25	65
76,82	Foliation					1	165	35	55
77,19	Vein		Quartz/plagioclase	2		1	160	55	35
77,22	Vein		Quartz/plagioclase	2,5		1	150	60	30
72,26	Vein		Quartz/plagioclase	6,5		1	165	55	35
77,37	Vein		Quartz/plagioclase	3		1	10	60	30
77,49	Sealed Fracture					1	190	10	80
77,79	Vein		Quartz/plagioclase	2		1	160	70	20
78,1	Sealed Fracture					1	300	20	70
78,35	Foliation					1	205	55	35
79,03	Sealed Fracture					1	65	20	70
79,28	Vein		Quartz/plagioclase	0,5		1	275	60	30
79,38	Sealed Fracture					1	315	20	70
80,72	Foliation					1	190	60	30
80,85	Fracture					1	-	-	
80,87	Vein		Quartz/plagioclase	16,5		1	170	55	35

81,17	Vein		Quartz/plagioclase	12		1	165	55	35
81,44	Vein		Quartz/plagioclase	6		1	105	45	45
82,02	Vein		Quartz/plagioclase	1,5		1	190	55	35
82,04	Vein		Quartz/plagioclase	1,5		1	190	55	35
82,13	Vein		Quartz/plagioclase	0,5		1	190	45	45
82,41	Vein		Quartz/plagioclase	0,5		1	190	55	35
82,42	Fracture					1	15	15	75
82,71	Vein		Quartz/plagioclase	1		1	220	55	35
82,77	Vein		Quartz/plagioclase	1		1	220	60	30
82,91	Vein		Quartz/plagioclase	1		1	220	55	35
83	Foliation					1	175	60	30
83,27	Fracture					1	185	75	15
83,27	Vein		Quartz/plagioclase	5		1	185	75	15
84	Foliation					1	145	60	30
84,2	Vein		Quartz/plagioclase	0,5		1	135	65	25
84,5	Foliation					1	140	60	30
84,9	Foliation					2	125	65	25
85,45	Vein		Quartz/plagioclase	1		2	165	65	25
85,51	Vein		Quartz/plagioclase	0,5		2	185	60	30
85,62	Vein		Quartz/plagioclase	0,5-3		2	170	65	25
86,42	Vein		Quartz/plagioclase	1,5		2	120	65	25
86,45	Vein		Quartz/plagioclase	1,5		2	120	65	25
86,48	Vein		Quartz/plagioclase	2,0-4		2	130	70	20
86,64	Vein		Quartz/plagioclase	0,5		2	130	70	20
86,8	Vein		Quartz/plagioclase	0,5		2	150	65	25
87,13	Fault	Displacement 0,5 cm				2	260	10	80
87,27	Foliation					2	130	60	30
87,38	Vein		Quartz/plagioclase	0,5		2	145	60	30
87,54	Vein		Quartz/plagioclase	0,5		2	140	55	35
87,64	Vein		Quartz/plagioclase	0,5		2	140	55	35
87,65	Vein		Quartz/plagioclase	0,5		2	140	55	35
88,91	Fracture					2	0	35	55
89,25	Foliation					2	125	60	30
89,95	Foliation					2	125	50	40
90,02	Vein		Pegmatite			2	130	70	20
90,38	Vein		Quartz/plagioclase	0,5		2	130	60	30
90,42	Vein		Quartz/plagioclase	0,5		2	140	60	30
90,45	Vein		Quartz/plagioclase	0,5		2	140	60	30
90,64	Vein		Quartz/plagioclase	0,5		2	145	60	30
90,76	Vein		Quartz/plagioclase	0,5		2	145	60	30
91,28	Vein		Quartz/plagioclase	0,5		2	110	60	30
91,36	Vein		Quartz/plagioclase	0,5		2	110	60	30
91,39	Vein		Quartz/plagioclase	1		2	110	60	30
91,51	Vein		Quartz/plagioclase	3		2	110	60	30
91,67	Vein		Quartz/plagioclase	0,7		2	110	60	30
91,91	Vein		Quartz/plagioclase	2		2	110	60	30
91,95	Vein		Quartz/plagioclase	1,5		2	110	60	30
92,02	Vein		Quartz/plagioclase	1,5		2	110	60	30
91,97	Fracture					2	120	65	25
92,35	Vein		Quartz/plagioclase	1,0-3		2	120	50	40
92,48	Vein		Quartz/plagioclase	2		2	120	50	40
92,68	Vein		Granite	7		2	120	50	40
93,39	Vein		Quartz/plagioclase	2		2	115	60	30
93,45	Vein		Quartz/plagioclase	2		2	115	60	30
93,71	Vein		Quartz/plagioclase	1		2	115	60	30
93,71-96,7	Veins	Gradually more veins deeper	Quartz/plagioclase	0,5-4		2			
94,45	Fracture					2	125	60	30
94,45	Foliation					2	125	60	30
95,5	Foliation					2	130	65	25
96,5	Sealed Fracture					2	-	-	
96,77	Fracture					2	275	25	65
97,32	Fracture					2	275	20	70
97,75	Fracture					2	270	30	60
97,83	Sealed Fracture					2	260	25	65
98,28	Vein		Quartz/plagioclase	0,5		2	20	60	30
98,84-104,05	Magma mingling	unregular shapes		5,0-30		2			
99,01	Unreadable foliation					2			
99,09	Fracture					2	355	65	25
99,19	Vein		Quartz/plagioclase	0,5		2	355	65	25
99,24	Fracture					2	300	30	60
99,32	Vein		Quartz/plagioclase	2		2	0	65	25
99,74	Fracture					2	150	60	30
100,14	Fracture					2	205	70	20
101,25	Fracture					2	350	45	45
101,87	Fracture					2	170	55	35
103,78	Vein		Quartz/plagioclase	1		2	150	55	35
104,24	Sealed Fracture					2	285	10	80
104,25	Foliation					2	175	65	25
104,45	Sealed Fracture					2	295	20	70
105,5	Sealed Fracture					2	275	20	70
106,2	Vein		Quartz/plagioclase	1,5		2	10	50	40
106,37	Fracture					2	280	17	73
106,7	Sealed Fracture					2	285	10	80
107,49	Foliation					2	165	55	35
108,13	Fracture					2	260	25	65
108,15	Fault	Displacement 0,5 cm				2			
108,23	Fault	Displacement 0,5 cm				2	250	15	75
108,25	Fold					2			
108,5	Fracture					2	125	60	30
108,5	Foliation					2	125	60	30
108,6	Fracture					2	125	60	30
108,64	Fracture					2	125	60	30
108,69	Fracture					2	125	60	30
108,97	Fracture	A nonmeasurable fracture as well				2	115	45	45
109,04	Fracture					2	115	60	30
109,09	Fracture					2	115	60	30
109,13	Fracture					2	90	60	30
109,18	Fracture					2	5	40	50
109,23	Fracture					2	105	55	35
109,3	Foliation					2	115	60	30
109,53	Sealed Fracture					2	165	10	80
110,41	Sealed Fracture					2	285	15	75
110,36	Fracture					2	120	60	30
110,52	Fracture					2	255	20	70
111,1	Fold					2			
111,61	Vein		Pegmatite	11		2	100	70	20
111,98	Fracture					2	115	65	25
112,21	Foliation					2	95	60	30
112,38	Fracture					2	90	55	35
112,59	Fracture					2	110	60	30
112,61	Sealed Fracture					2	270	15	75
112,73	Fracture					2	125	65	25
112,76	Fracture					2	100	10	80
112,96	Fracture					2	130	65	25
113	Foliation					2	125	60	30
113,02	Fracture					2	350	15	75
113,11	Fracture					2	115	60	30
113,18	Fracture					3	110	60	30
113,21	Foliation					3	110	60	30
113,55	Fracture					3	240	15	75
113,55	Fracture					3	240	35	55
114,19	Fracture					3	300	40	50
114,19	Fracture					3	250	65	25
114,34	Sealed Fracture					3	325	25	65
114,49	Foliation					3	150	65	25

114,5-114,6	Crushed					3			
114,57	Fracture					4	165	60	30
114,57	Fracture					4	290	20	70
114,6	Foliation					4	135	60	30
114,77	Sealed Fracture					4	285	20	70
114,94	Vein		Pegmatite	16		4			
115,15	Fracture					4	350	15	75
115,15	Fracture					4	110	10	80
115,5	Protected Fracture					4			
116	Protected Fracture					4			
116,11	Fracture					5	185	15	75
116,2	Foliation					5	115	60	30
116,35	Fracture					5	125	60	30
116,47	Fracture					5	115	60	30
116,68	Fracture					5	145	60	30
117,56	Fracture					5	175	50	40
117,8	Fracture					5	90	55	35
118	Foliation					5	125	75	15
118-119,8	Veins	1/m	Pegmatite	10,0-15		5			
118-121,5	Veins	2/m	Pegmatite/quartz	1,0-2		5	90/120	55	35
118,29	Fracture					5	100	70	20
119,79	Fracture					5	95	65	25
119,93	Shear?					5			
120,2	Foliation					5	120	55	35
120,26	Fracture					5	115	65	25
120,4	Shear?					5			
120,5	Wavy vein		Quartz/plagioclase			5			
120,54	Sealed Fracture					5	270	15	75
120,7	Foliation					5	120	60	30
121-121,15	Crushed					5			
121,19	Fracture					6	110	50	40
121,23	Foliation					6	115	55	35
121,26	Fracture					6	110	50	40
121,3	Sealed Fracture					6	110	55	35
121,34	Sealed Fracture					6	100	55	35
121,37	Fracture					6	110	55	35
121,44	Foliation					6	115	40	50
122	Foliation					6	105	45	45
123,2	Foliation	changing and hard to meassure				6	130	35	55
123,8	Fracture					6	135	15	75
123,98	Sealed Fracture					6	135	35	55
124,08	Fracture					6	210	35	55
124,22	Fracture					6	125	30	60
124,3	Sealed Fracture					6	265	15	75
124,58	Fracture					6	130	10	80
125,02	Fracture					6	350	35	55
125,89	Fracture					6	45	45	45
126,2	Foliation	Older				6	145	25	65
126,2	Foliation	Overprinting				6	50	50	40
126,31	Fault	Displacement 0,5 cm				6	235	20	70
126,37	Fracture					6	60	55	35
126,5	Foliation					6	70	50	40
127,06	Fracture					6	110	55	35
127,18-127,46	Magma mingling					6			
127,4	Fault	Displacement 0,5 cm				6	300	5	85
127,75	Foliation					6	115	50	40
127,77	Fault	Displacement 0,5 cm				6	230	25	65
127,84	Foliation	OBS! Foliation changing				6	30	60	30
128	Sealed Fracture					6	225	25	65
128,03	Fracture					6	65	55	35
128,03	Vein		Pegmatite	3		6			
128,45	Sealed Fracture					6	270	20	70
128,55	Foliation					6	75	50	40
128,8	Fracture					6	220	35	55
128,82	Sealed Fracture					6	300	20	70
128,93	Fracture					6	215	25	65
128,95	Sealed Fracture					6	220	35	55
129,1	Fracture					6	305	20	70
129,38	Fracture					6	120	60	30
129,6	Foliation					6	115	60	30
129,83	Fracture					6	250	25	65
129,9	Sealed Fracture					6	265	35	55
129,96	Pegmatite rests					6			
130,2	Fracture					6	125	55	35
130,22	Foliation					6	125	55	35
130,28-130,55	Folds					6			
130,78	Sealed Fracture					6	250	30	60
130,98	Fracture					6	215	25	65
131,2	Fracture					6	255	25	65
131,34	Fault	Displacement 1 cm				6	255	35	55
131,52	Foliation					6	120	55	35
131,36-132,35	Veins	2-3/m	quartz/plagioclase/pegmatite	2,0-5		6	100	50	40
131,8-132,35	Folds		quartz/plagioclase			6			
132,48	Fracture					6	130	60	30
132,65	Foliation					6	115	55	35
132,65	Folds					6			
132,84	Fracture					6	275	30	60
133,67	Sealed Fracture					6	255	40	50
133,79	Foliation					6	135	65	25
134,59	Foliation					6	180	65	25
134,71	Fracture					6	160	60	30
135,1	Sealed Fracture					6	295	20	70
135,2	Foliation					6	160	60	30
135,6	Foliation					6	165	55	35
135,8	Folding		quartz/plagioclase/pegmatite			6			
137	Shear ?		quartz/plagioclase/pegmatite			6			
137,14	Folds		quartz/plagioclase/pegmatite			6			
137,33	Foliation					6	180	55	35
137,72	Fracture					6	205	55	35
137,95	Fracture					6	175	50	40
138,76-139,1	Folds		Pegmatite			6			
139,45	Foliation					6	205	70	20
139,6-140,32	Folds		Quartz	0,5		6			
139,88	Fracture					6	130	40	50
140,03	Fracture					6	205	55	35
140,05	Foliation					6	205	55	35
140,4-140,85	Folds		Quartz	0,5		6			
140,86	Foliation					6	170	65	25
140,99	Fracture					6	150	55	35
140,99	Vein		Pegmatite	12		6			
141,3-146	Folds					6			
142,43	Sealed Fracture					6	75	75	15
142,5	Foliation					6	175	55	35
142,72	Fracture					6	90	70	20
143,23	Vein		Pegmatite	20		6			
143,63	Vein		Pegmatite	37		6			
144,02	Fracture					7	130	60	30
144,14	Fracture					7	60	55	35
144,25	Sealed Fracture					7	100	30	60
144,28	Fracture					7	120	65	25
144,43	Foliation					7	195	60	30
144,74	Fracture					7	175	60	30
144,78	Foliation					7	175	55	35
145,12	Foliation					7	200	40	50

145,25	Foliation					7	125	70	20
145,66	Fracture					7	285	20	70
146	Foliation					7	185	40	50
146,09	Vein		Kalifeldspar/plagioclase	1		7	130	75	15
146,17	Vein		Kalifeldspar/plagioclase	1		7	130	75	15
146,25	Foliation					7	130	65	25
146,58	Fracture					7	125	55	35
146,66	Foliation					7	125	55	35
147,05	Fracture					7	115	55	35
147,1	Foliation					7	115	55	35
147,4	Foliation					7	125	60	30
149-149,25	Folds		quartz/plagioclase	0,5		7			
149,85	Foliation					7	105	60	30
149,98	Folds					7			
150,1	Fracture					7	295	5	85
150,5	Folds					7			
151,25-154,13	Veins	~2/m	quartz/plagioclase	0,5-3		7	100	55	35
152,05	Foliation					7	105	50	40
152,45	Fracture					7	100	45	45
152,48	Vein		Pegmatite	10		7	100	45	45
152,86	Vein		Pegmatite	5		7	110	60	30
153,2	Foliation					7	105	55	35
154,13-156,5	Veins	1-2/m	quartz/plagioclase	0,5-2		7	95/105	55	35
155,21	Fracture					7	100	60	30
155,74	Shear					7	100	55	35
155,96	Fracture					7	100	50	40
155,96	Fold					7			
156,5-158,9	Veins	1/m	quartz/plagioclase	0,5-2		7	80	55	35
157,81	Foliation					7	70	50	40
158,6-158,9	Folds					7			
158,9-164,5	Veins	1/m	quartz/plagioclase	0,5-2		7	75/85	55	35
159	Foliation					7	85	55	35
159,79	Vein		Pegmatite	21		7			
159,88	Fracture					7	100	55	35
161,04	Fracture					7	105	60	30
161,42	Foliation					7	100	60	30
162	Fracture					7	80	60	30
162,4	Foliation					7	80	60	30
162,6	Foliation					7	95	60	30
165,4	Foliation					7	110	60	30
165,5	Folds		Pegmatite/Biotite/quartz	15		7	140	45	45
165,7	Foliation					7	110	50	40
166	Fracture					7	255	65	25
166,15	Fracture					7	140	45	45
166,24	Fracture					7	140	45	45
166,26	Fracture					7	65	70	20
166,4	Folds		Pegmatite	33		8			
166,8	Foliation					8	100	60	30
166,72	Fracture					8	70	65	25
166,72	Foliation					8	80	60	30
167,66	Folds		Pegmatite/biotite	9		8			
167,71	Fracture					8	70	55	35
168	Foliation					8	85	60	30
168,2	Foliation					8	75	60	30
168,32	Vein		Pegmatite	86		8			
168,4	Fracture					8	10	40	50
169,06	Fracture					8		90	0
169,28	Foliation					8	90	55	35
169,33	Vein		Pegmatite	10		8			
169,33	Folds		Quartz			8			
170,14	Fracture					8	355	60	30
170,23	Fracture					8	350	50	40
170,32	Sealed fracture					8	320	45	45
170,39	Folds		Biotite/quartz	25		8			
170,62	Fracture					8	95	50	40
170,69	Foliation					8	100	45	45
170,79	Fracture					8	240	80	10
170,85	Vein		Pegmatite	1		8	80	40	50
171	Fracture					8	135	30	60
171,18	Foliation					8	110	45	45
171,4	Foliation					8	125	50	40
171,5	Fracture					8	100	50	40
171,6	Foliation					8	110	50	40
171,73	Fracture					8	305	50	40
171,99	Fold					8			
172,13	Fracture					8	120	55	35
172,33	Fracture					8	140	20	70
172,4	Fracture					8	160	45	45
172,73	Foliation	Weak foliation				8	115	30	60
173,1	Foliation					8	15	50	40
173,63	Fracture					8	210	45	45
173,65	Sealed fracture					8	205	10	80
173,85	Fracture					8	210	45	45
173,88	Sealed fracture					8	220	10	80
174,2	Fracture					8	~200	~40	
174,26	Sealed fracture					8	200	30	60
174,27	Fracture					8	30	25	65
174,5	Foliation					8	70	55	35
174,7	Foliation					8	120	70	20
175,07	Fracture					8	220	25	65
175,1	Sealed fracture					8	345	5	85
175,17	Vein		Pegmatite	2		8			
175,29	Fracture					8	105	15	75
175,39	Fracture					8	190	40	50
175,59	Foliation					8	160	70	20
175,69	Fracture					8	285	25	65
176,09	Fracture					8	270	70	20
176,57	Fracture					8	200	50	40
176,61	Fracture					8	310	15	75
176,65	Fracture					8	200	60	30
176,87	Fracture					8	300	15	75
177,6	Foliation					8	90	30	60
178	Fracture					8	205	30	60
179,4	Foliation					8	75	50	40
180,4	Foliation					8	20	60	30
180,53	Sealed fracture					8	200	35	55
181,2	Foliation					8	40	45	45
182,11	Fracture					8	125	45	45
182,18	Fracture					8	250	80	10
182,2	Sealed fracture					8	125	55	35
182,84	Fracture	Unmeassurable				8			
182,92	Fracture					8	110	50	40
183,42	Fracture					8	190	20	70
183,64	Fracture					8	190	20	70
183,92	Fracture					8	105	45	45
184,34	Fracture					8	190	25	65
185,18	Fracture					8	105	45	45
185,25	Fracture					8	100	40	50
185,84	Fracture					8	265	80	10
186,05	Fracture					8	115	35	55
186,5	Foliation					8	35	55	35
186,95	Fracture					8	120	25	65
187,01	Fracture					8	125	25	65
187,14	Fracture					8	120	35	55
187,68	Fracture					8	165	75	15

187,96	Fracture					8	120	25	65
189,79	Sealed fracture					8	140	20	70
189,94	Foliation					8	35	50	40
190,35	Fracture					9	90	15	75
190,63	Sealed fracture					9	35	15	75
190,87	Foliation					9	5	55	35
190,97	Foliation	Moderate				9	350	55	35
191,17	Vein		Quartz/kalifeldspar			9	340	50	40
192,28	Sealed fracture					9	55	40	50
192,78	Foliation	Moderate				9	335	50	40
195,6	Foliation					10	345	55	35
196,3	Vein		Pegmatite	17		10			
198,03	Foliation					10	320	45	45
198,36	Vein		Quartz	3		10	315	40	50
198,73	Vein		Quartz/pegmatite	7		10	280	75	15
199,25	Vein		Pegmatite	18		10	35	25	65
198,93	Foliation					10	295	55	35
200	Foliation					10	310	55	35
200,33	Foliation					10	305	50	40
200,85	Vein		Quartz/pegmatite	2		10	280	40	50
201,6	Vein		Quartz/kalifeldspar	0,5		10	155	50	40
201,74	Sealed fracture					10	165	30	60
203,34	Fracture					10	160	25	65
203,5	Foliation					10	310	55	35
204,49	S-structure					10			
204,86	Sealed fracture					10	15	15	75
205,34	Vein		Kalifeldspar	2		10	295	65	25
205,39	Fold					10			
205,59	Foliation					10	300	50	40
207,15	Vein		Pegmatite	14		10			
207,17	Foliation					11	305	65	25
208,85	Foliation					11	330	60	30
209,79	Foliation					11	310	50	40
210,45	Foliation	Strong				11	210	70	20
210,5-213,7	Veins	2/m	Quartz /plagioclase	1,0-3		11	260	60	30
211,25	Foliation					11	260	60	30
212,25	Foliation					11	250	50	40
214,11	Vein		Pegmatite	18		11			
213,7-214,11	Foliation	Strong				11	205	70	20
214,29-216,75	Foliation	Weak				11	255	60	30
216,75-218,64	Vein	1/meter	Quartz /plagioclase	1		12	210	55	35
218,82-219,5	Foliation	Moderate				12	235	65	25
219,5-220,82	Foliation	Weak				12	225	60	30
220,72	Vein		Quartz /plagioclase	2		12			
220,82-222,85	Folds	A few ones				12			
222,75-222,85	Crushed					13			
222,95	Foliation	Moderate				13	215	50	40
226	Foliation					13	250	55	35
225,24	Vein		Quartz	6		13	260	70	20
228,7	Foliation					13	245	50	40
230,7	Foliation					13	265	60	30
234,87	Sealed fracture					13	0	25	65
234,95	Foliation					13	280	55	35
237,27	Fracture					13	355	25	65
237,98	Sealed fracture					13	195	5	85
238,98	Foliation					13	290	55	35
238,78	Vein		Pegmatite	2		13	260	75	15
240,3	Fracture					13	340	15	75
240,45	Fracture					13	345	20	70
240,53	Fracture					13	350	25	65
240,75	Foliation					13	275	55	35
241,8	Foliation					14	250	55	35
242,07	Crushed	7cm				14			
242,5	Foliation					15	245	50	40
242,73-244,48	Crushed					15			
245	Foliation					16	270	55	35
245,37	Foliation					17	235	50	40
245,79	Sealed fracture					17	220	30	60
246	Vein		Quartz	1		17	245	70	20
248,85	Foliation					17	250	55	35
250,29	Fracture					17	40	25	65
250,4	Fracture					17	40	20	70
252	Foliation					17	240	55	35
252,56	Fracture					17	335	25	65
253,15	Sealed fracture					17	340	5	85
254,48	Vein		Quartz	1		17	250	50	40
254,56	Vein		Quartz	1		17	250	50	40
255,8	Foliation					17	255	60	30
257,68	S-structure					17			
258,13	Vein		Pegmatite	2		17	245	70	20
258,85	Sealed fracture					17	50	20	70
259,05	Vein		Pegmatite	14		18	205	60	30
259,75	Foliation	weak				18	240	60	30
260,83	Fracture				Frp 70C	18	20	25	65
260,92	Sealed fracture					18	15	20	70
261,28	Foliation	Moderate				18	260	60	30
261,91	Fracture				Frp 75C	18	15	30	60
262,02	Fracture				Frp 80C	18	15	25	65
262,33	Foliation	Weak				18	260	60	30
263,92	Sealed fracture					18	320	30	60
264,19	Foliation	Weak				18	200	65	25
265,59	Sealed fracture					18	10	20	70
266	Foliation	Weak				18	225	60	30
267,13	Plastic fracture					18			
267,6	Fracture				Frp 80C	19	10	25	65
267,75	Foliation					19	225	55	35
268,53	Fracture				Frp 80C	19	0	25	65
270	Foliation	Moderate				19	185	55	35
271,83	Vein	Mylonite	Biotite	9		19			
271,93	Fracture					19	170	55	35
272,27	Vein		Pegmatite	6		19			
273,44	Fracture				Frp 82C	19	320	25	65
273,61	Fracture					19	165	60	30
273,65	Foliation					19	170	50	40
273,68-274,08	Crushed					19			
274,2	Foliation					20	160	55	35
274,61	Vein		Biotite	0,5		20	175	60	30
274,72	Fracture	Unmeasurable				20			
275	Foliation	Weak				20	175	55	35
275,57	Fracture					20	165	30	60
275,97	Fracture				Frp 75C	20	5	25	65
276,3	Vein		Pegmatite	11		20	165	75	15
277,18	Foliation					20	210	55	35
279,3	Foliation	Weak				20	185	65	25
283,07	Vein		Pegmatite	2		21			
283,58	Vein		Pegmatite	23		21	180	55	35
283,58	Fracture					21	190	55	35
283,88	Fracture					21	185	60	30
283,92	Fracture					21	185	60	30
283,98	Vein		Pegmatite	8		21	190	75	15
284,5	Foliation	Moderate				21	200	50	40
285,8	Foliation					21	165	40	50
285,9	Foliation					22	175	50	40
286,57-286,82	Crushed					22			
286,9	Foliation					23	170	50	40

287,59	Crushed					23			
289,03-289,3	Plastic fracture					23			
290	Foliation	Moderate				24	170	60	30
290,54	Sealed fracture					24	220	5	85
291,3	Foliation					25	190	55	35
291,72	Fracture					25	265	15	75
292,58	Vein	Mylonite	Biotite	10,5		25	170	65	25
293,41-294,48	Crushed					25			
294,56	Vein	Mylonite	Biotite	14		26	160	65	25
294,81	Vein		Quartz	3		26	160	70	20
294,81	Sealed fracture	Parallell fracture 20-30cm				26			
294,9	Vein		Quartz	4		26	150	65	25
294,94	Vein	Mylonite	Biotite	7		26	160	60	30
294,2	Foliation					26	150	60	30
295,73	Vein	Mylonite	Biotite	9		26	170	55	35
296,28	Vein	Mylonite	Biotite	6		26	180	50	40
296,33	Fracture					26	180	55	35
297,2	Foliation					27	190	55	35
299,9	Vein		Aplit/Granite	14		27			
300,13	Vein		Biotite	12		27	170	55	35
300,07	Fracture					27	180	50	40
300,25	Fracture					27	165	45	45
300,25-302,1	Fracture					27	135	10	80
300	Foliation					27	175	50	40
301,98	Fracture					27			
304,13	Fracture				Fol 20C	27	140	55	35
304,13	Vein	Mylonite	Biotite	1		27	125	60	30
304,25	Vein					27	150	55	35
305	Foliation					27	135	55	35
307	Foliation					27	115	60	30
306,85	Vein		Biotite	0,5		27	115	60	30
307,5	Vein		Quartz/pegmatite	3		27	110	50	40
308,65	Vein		Aplit/Granite	2,5		27	140	55	35
309,06	Vein		Aplit/Granite	4		27	95	55	35
309,19-309,46	Fold					27			
310,46	Vein		Pegmatite/biotite	2		27	135	50	40
310,62	Foliation					27	140	65	25
312,03	Vein		Pegmatite	2,5		27	135	50	40
312,05	Vein		Aplit/Granite	7,5		27	135	50	40
312,2	Foliation					27	115	50	40
313,47	Vein		Aplit/Granite	10		27	110	75	15
315,5	Foliation	Moderate				27	105	60	30
315,9	Foliation	Moderate				28	160	65	25
316,77	Foliation					28	160	60	30
316,48	Vein		Pegmatite/quartz			29	155	65	25
316,99	Vein	Mylonite	Biotite	2		29	125	60	30
317,01	Fracture					29	320	60	30
317,05	Fracture					29	125	20	70
317,7	Vein	Mylonite	Biotite	7		29	125	60	30
317,78	Fracture					29	125	60	30
317,93	Foliation					29	115	70	20
318,12	Vein		Pegmatite	5		29	145	60	30
318,24-318,49	Crushed					29			
318,96	Fracture					30	130	45	45
318,96	Vein	Mylonite	Biotite	5		30	130	60	30
319,65	Vein	Mylonite	Biotite	9		30	120	55	35
319,73	Fracture					30	140	65	25
319,85	Sealed fracture					30	320	20	70
319,99	Foliation					30	140	50	40
320,03	Sealed fracture					30	35	20	70
320,96	Sealed fracture					30	180	5	85
321,08	Sealed fracture				Frp 80C	30	0	5	85
321,44	Fracture					31	145	55	35
321,44	Vein	Mylonite	Biotite	3		31	145	55	35
321,49	Fracture					31	145	55	35
321,95	Foliation					31	135	45	45
323,28	Fracture					31	325	55	35
324,9	Foliation	Weak				31	115	55	35
325,15	Sealed fracture					31	220	10	80
326,22	Foliation	Moderate				31	120	55	35
328	Sealed fracture					31	310	50	40
328,43	Vein		Aplit/Granite	2,5		31	90	60	30
328,5	Vein		Aplit/Granite	3		31	10	5	85
328,84	Vein		Aplit/Granite	0,5		31	110	50	40
328,96	Vein		Aplit/Granite	7		31	85	85	5
329-329,2	Foliation	Stron/moderate				31	105	55	35
329,26	Vein	Mylonite	Biotite	6		31	105	60	30
329,42	Vein		Aplit/Granite	1		31	90	60	30
329,34	Sealed fracture					31	0	15	75
329,78	Fracture					31	280	50	40
329,85	Fracture					31	295	55	35
329,91	Shear	0,1m				31			
330,15-330,5	Folding					31			
330,9	Foliation	Moderate				31	130	60	30
331,2	Fracture					31	125	55	35
331,2	Vein	Mylonite	Biotite	3		31	110	55	35
331,26	Fracture					32	110	55	35
331,39	Sealed fracture					32	290	15	75
331,5	Fracture					32	275	55	35
331,65	Sealed fracture					32	320	20	70
331,65	Foliation					32	120	60	30
331,85	Fracture					33	110	60	30
332	Foliation	Moderate				33	85	60	30
332,04	Fracture					33	90	45	45
332,18	Fracture					33	240	45	45
332,24	Sealed fracture					33	245	35	55
332,56	Foliation					33	90	50	40
332,94	Vein		Pegmatite	3		33			
333,17-333,47	Crushed					33			
333,63	Vein		Biotite	6		33			
333,91	Vein	mylonite	Biotite	5		34	90	45	45
334	Foliation					34	90	55	35
334,39	Vein	Deformed Mylonite	Biotite	23		34	90	40	50
334,4	Foliation					34	90	40	50
335,19	Sealed fracture					34	265	15	75
335,31	Vein		Pegmatite	1		34	95	65	25
335,52	Foliation					34	90	65	25
335,93	Sealed fracture	Unmeassurable				34			
336,27-336,7	Foliation	Stronger				34			
336,38	Fracture					34	95	60	30
336,38	Vein	Mylonite	Biotite	4		34	95	60	30
336,47	Vein	Mylonite	Biotite	14		34	90	60	30
338,4	Vein	Mylonite	Biotite	2		34	65	55	35
338,52		Mylonite	Biotite	7		34	65	55	35
338,74		Mylonite	Biotite	13		34	65	55	35
339,3		Mylonite	Biotite	92		34	65	55	35
338,31-339,6	Veins/banding	3-5/m	Biotite	1-40		34	65	55	35
339,5	Foliation	Moderate				34	65	60	30
340,76	Vein		Aplit/Granite	4		34	65	40	50
341,02	Vein		Aplit/Granite	0,5		34	65	40	50
341,19	Vein		Aplit/Granite	1		34	65	40	50
341,97	Sealed fracture	Unmeassurable				34			
342,09	Fracture				Frp 80AC	34	70	60	30
342,16	Fracture					34	50	50	40
342,29-342,85	Vein?	Microfolds. Shear? Mylonite	Biotite			35			

342,95	Sealed fracture					35	235	10	80
343,13	Sealed fracture	Unmeassurable				35			
343,18	Vein		Aplit/Granite	1		35	45	50	40
343,68	Fracture					35	240	25	65
343,72	Fracture				Frp 70C	35	245	30	60
343,9	Foliation	Weak				35	60	35	55
344,1	Foliation	Moderate				35	65	35	55
344,8	Fracture				Frp 85C	35	230	15	75
345,17	Fracture					35	220	30	60
345,31	Vein		Biotite	3		35	55	60	30
345,36	Vein		Biotite	1		35	55	60	30
345,4	Vein		Biotite	1		35	55	60	30
345,41	Fracture					35	55	60	30
345,66	Fracture				Frp 80C	35	230	15	75
346,71	Vein	Deformed	Pegmatite	15		35	340	60	30
346,93	Vein		Pegmatite	1		35	30	60	30
347,41	Fracture				Frp 80C	35	45	30	60
347,46	Fracture					35	40	30	60
347,54	Fracture					35	260	50	40
347,86	Fracture					35	210	10	80
348	Foliation					35	40	50	40
348,62	Vein		Aplit/Granite	15		35			
348,85	Foliation	Moderate				35	30	50	40
349,7	Fracture				Frp 85C	35	190	20	70
349,75	Foliation	Weak				35	20	60	30
350,15	Vein		Aplit/Granite	5		35	30	55	35
350,47	Fracture					35	180	20	70
351,4	Foliation	Moderate/strong				35	40	50	40
351,55	Fracture				Frp 85C	35	175	20	70
352,47	Fracture					35	165	20	70
353,31	Fracture				Frp 80C	35	170	20	70
353,93-98	Plastic					35			
353,98-354,85	Crushed					35			
354,85	Foliation	Weak				36	60	50	40
355,68	Vein		Plagioclase/kalifeldspar	1		36	45	55	35
355,8	Fracture					36	210	20	70
356,03	Fracture					36	210	15	75
356,36	Foliation	Moderate				36	45	50	40
356,91	Sealed fracture	Unmeassurable				36			
357	Fracture					36	185	20	70
357,06	Vein		Plagioclase/kalifeldspar	3		36	20	40	50
357,39	Vein		Plagioclase/kalifeldspar	1		36	20	40	50
357,51	Vein		Plagioclase/kalifeldspar	1		36	20	40	50
357,9	Foliation	Moderate/strong				37	15	55	35
357,95	Vein		Plagioclase/kalifeldspar	2		37	25	55	35
359,29	Fracture				Frp 75C	37	150	15	75
359,78	Vein		Quartz/Pegmatite	8		37	335	50	40
360,7	Foliation	Strong				37	350	60	30
361,89	Sealed fracture					37	125	15	75
362,4	Foliation					37	285	55	35
362,9	Vein		Quartz	1		37	265	55	35
363,03	Vein		Quartz	1		37	265	55	35
363,16	Vein		Pegmatite	12		37	265	55	35
363,67	Vein		Biotite	20		37	285	70	20
363,8	Fracture				Frp 80C	37	110	20	70
364,68	Vein		Aplit			37	285	70	20
365,22	Sealed fracture					37	100	10	80
365,61	Foliation					37	330	55	35
365,74	Vein	Mylonite	Biotite			37			
365,92	Vein		Plagioclase/kalifeldspar	2		37	350	45	45
366,09	Vein		Plagioclase/kalifeldspar	2		37	350	45	45
366,57	Foliation					37	340	55	35
366,72	Vein		Aplit/Granite	4		37			
366,94	Fracture					37	355	60	30
366,96	Vein		Pegmatite	3		37	5	55	35
367,22	Foliation					37	5	50	40
367,3	Fracture					37	190	70	20
367,15	Micro s structur					37			
367,32	Vein	Mylonite	Biotite	1		37			
367,59	Fracture					37	190	45	45
367,81	Vein	Mylonite	Biotite	3		37	0	55	35
367,94	Fracture					37	0	55	35
367,96	Fracture					37	0	55	35
368,2	Fracture					37	200	40	50
368,68	Sealed fracture					37	170	40	50
368,72	Vein		Quartz/pegmatite	1		37	0	65	25
368,77	Vein		Quartz/pegmatite	2		37	0	65	25
368,91	Fracture				80C	37	155	25	65
369,01	Vein		Biotite	1		37	0	50	40
369,37	Fracture				85C	37	165	20	70
369,56	Micro s structur					37			
370	Vein		Quartz	1		37	15	50	40
370,09	Vein		Quartz	2		37	15	50	40
370,2	Vein		Biotite	4		37	15	50	40
370,21	Sealed fracture					37	155	15	75
370,3	Fracture					37	15	50	40
370,41	Vein		pegmatite	1		37	5	50	40
370,65	Foliation	Strong				37	10	65	25
371,02	S-structure					37			
371,6	S-structure					37			
371,96	Fracture				80AC	37	140	20	70
372,26	Sealed fracture					37	170	40	50
372,23	Vein		Quartz	0,5		37	0	60	30
372,32	Vein		Quartz	1		37	5	65	25
372,4	Sealed fracture					37	160	20	70
372,48	Sealed fracture					37	190	65	25
372,5	Sealed fracture					37	190	70	20
372,53	Sealed fracture					37	190	50	40
372,61	Fracture					37	200	60	30
372,51	Vein		Quartz	1		37	355	65	25
372,62	Sealed fracture					37	195	60	30
372,71	Sealed fracture					37	210	60	30
372,67	Vein		Quartz/pegmatite	6		37	10	65	25
372,68	Foliation	Strong				37	5	50	40
372,89	Vein		Aplit/Granite	3		37	10	55	35
373,34	S-structure					37			
374,64	Fracture					37	195	55	35
374,86	Sealed fracture					37	180	55	35
374,99	Vein		Quartz/aplit	2		37	350	60	30
375,11	Sealed fracture					37	190	60	30
375,26	Vein		Quartz/aplit	2		37	345	50	40
375,31	S-structure					37			
375,43	Fracture				80C	37	135	20	70
375,62-375,85	Folded					37			
376,29	Vein		Quartz/aplit	1		37	310	60	30
376,34	Vein		Quartz/aplit	1		37	310	60	30
376,66	Foliation	Strong				37	315	60	30
376,97	Vein		Quartz/aplit	2		37			
377	Vein		Quartz/aplit	1		37			
377,17	Vein		Quartz/aplit	2		37			
376,97-377,17	Folds					37			
377,56	Vein		Aplit/pegmatite	4		37			
378	Foliation	Strong				37	350	55	35

378,43	Fracture				75AC	37	110	30	60
378,57-378,77	Folds					37			
379,03	Vein	Mylonite	Biotite	36		37	320	55	35
379,23	Sealed fracture					37	125	5	85
379,86	Fracture					37	320	55	35
380,2	Fracture					38	320	55	35
380,23	Fracture					38	320	55	35
381,1	Vein		Aplit	2		38	270	70	20
381,2	Foliation	Moderate				38	325	60	30
382,18	Vein		Quartz/plagioclase	5		38	280	55	35
382,41	S-vein		Quartz/plagioclase	5,0-10		38			
384,05	Vein		Quartz			38	240	65	25
385,92	Vein		Quartz	2		38			
381,29-386,09	Veins	smaller veins in foliation direction 1-3/m	Quartz/plagioclase	0,5		38			
386	Foliation	Moderate				38	265	60	30
382	Foliation	Moderate				38	300	55	35
386,36	Vein		Kalifeldspar	0,5		38	260	50	40
386,86	Sealed fracture					38	60	20	70
387,33	Vein		Biotite/pegmatite	12		38	275	60	30
387,78	Vein		Biotite	4		38	270	60	30
387,79	Fracture					38	270	60	30
388,65	Vein		Biotite	16		38	260	60	30
389,63	Vein	Less foliated after this vein	Biotite	10		38	260	60	30
389,73	Foliation	Weak				38	250	65	25
391	Foliation	Weak/Moderate				38	245	60	30
392,41	Vein		Biotite	27		38	255	50	40
393,95	Vein		Biotite	6		38	185	60	30
393,97	Fracture					38	185	60	30
394,1	Foliation	Strong				39	190	55	35
394,21	Vein		Biotite	15		39	185	60	30
394,26	Fracture					39	185	60	30
394,84	Vein		Biotite	11		39	190	55	35
394,86	Fracture					39	190	55	35
394,87	Foliation	Moderate				39	190	55	35
394,96	Fracture					39	190	55	35
394,96	Foliation				35C	39	190	55	35
395,11	Sealed fracture					39	10	20	70
395,32	Fracture					39	190	55	35
395,5	Vein		Biotite	17		39	185	60	30
395,65	Vein		Biotite	10		39			
395,76	Fracture					39	185	60	30
395,77	Fracture					39	185	60	30
395,78	Foliation	Weak				40	170	50	40
396,97	Fracture					40	260	25	65
397,41	Fracture	Mirror				40	170	60	30
397,3-398	Veins	3/m	Biotite	1,0-3		40			
397,92	Vein		Biotite	25	20C	40	165	55	35
398,06	Fracture					40	165	55	35
398,65	Vein		Biotite	12		40	165	55	35
398,91	Vein		Biotite	25		40	165	55	35
399,15	Fracture					40	165	55	35
399,18	Fracture					40	165	55	35
400,49	Fracture					40	165	55	35
400,55	Fracture					40	165	55	35
400,75	Fracture					40	165	55	35
401,13	Fracture					40	165	55	35
401,46	Fracture					40	165	55	35
401,63	Fracture					41	60	20	70
401,93	Sealed fracture					41			
401,98	Fracture					41	90	60	30
402	Fracture					41	80	55	35
402,28	Fracture					41	95	60	30
402,69	Fracture					41	95	60	30
402,73	Fracture					41	95	60	30
403,34	Sealed fracture					41	75	70	20
403,56	Fracture					41	320	35	55
403,94	Fracture					41	320	45	45
404,7	Fracture					41	95	60	30
404,75	Fracture					41	95	60	30
404,9	Fracture					41	95	60	30
404,97	Fracture					41	95	60	30
405,05	Fracture					41	95	60	30
405,23	Foliation				20C	41	95	60	30
405,92	Fracture					42	180	35	55
406,1	Fracture					42	95	65	25
406,35	Fracture					42	95	65	25
406,35	Vein	Deformed	Quartz	0,5-2		42	80	70	20
406,45	Fracture					42	90	65	25
406,5	Fracture					42	100	65	25
406,56	Fracture					42	95	65	25
406,58	Fracture					42	100	65	25
406,7	Fracture					42	110	65	25
406,73	Fracture					42	90	65	25
406,76	Fracture					42	95	65	25
406,77	Fracture					42	90	65	25
406,92	Fracture					42	105	65	25
406,94	Fracture					42	90	65	25
407,03-407,18	Crushed					42			
407,32	Vein		Pegmatite	6		43	100	60	30
407,46	Fracture					43	75	70	20
408,43	Fracture					43	110	60	30
408,53	Fracture					43	110	60	30
408,9	Fracture					43	110	60	30
408,91	Fracture					43	110	60	30
409,13	Fracture					43	110	60	30
409,14	Fracture					43	110	60	30
409,15	Fracture					43	110	60	30
409,91	Fracture					43	45	25	65
409,96	Fracture					43	100	60	30
410	Fracture					43	100	60	30
410,14	Foliation	Moderate				43	100	60	30
410,29-416,18	Folded	Moderate				43			
410,3	Fracture					43	100	60	30
410,39	Fracture					43	100	60	30
410,6	Foliation	Moderate				43	150	50	40
410,7	Fracture					43	100	60	30
410,97	Sealed fracture					44	300	15	75
411	Vein		Pegmatite	16		44		90	0
411,44	Vein		Pegmatite	18		44	320	75	15
411,79	Vein	Folded	Plagioclase/quartz/kalifeldspar	0,5		44	320	75	15
411,86	Vein	Folded	Plagioclase/quartz/kalifeldspar	1		44			
412,3	Vein	Folded	Plagioclase/quartz/kalifeldspar	2		44			
412,48	Vein		Plagioclase/quartz/kalifeldspar	2		44			
412,57	Fracture					44	70	60	30
412,72	Vein		Quartz/pegmatite	30		44	290	55	35
413,27	Vein	some biotite	Quartz/pegmatite	153		44			
415,11	Fracture					44	70	60	30

415,21-418,55	Veins	Folded veins,~ 3/m	Quartz/pegmatite	2,0-15		44			
416,18-418,55	Folded	Strongly				44			
416,18	Fracture					44	70	60	30
418,97	Foliation	Very weak				44	70	60	30
419,7	Foliation	Weak/Moderate				44	80	55	35
420,26	Vein		Quartz/plagioclase	1,5		44	55	60	30
420,7	Vein		Quartz/plagioclase	1		44	80	60	30
420,86	Vein		Quartz/plagioclase	7		44	70	50	40
421,2	Vein	With magnetite	Quartz/plagioclase	1		44	70	50	40
421,51	Vein		Quartz/plagioclase	1		45	60	55	35
421,8	Foliation	Moderate				45	65	55	35
422,48	Vein		Kalifeldspar/Quartz	0,5		45	180	45	45
423,58	Vein		Plagioclase	4		45			
419,5-423,58	Foliation	Moderate/strong				45	60	55	35
424,52	Vein		Pegmatite	7		45	50	80	10
425,97	Vein		Biotite	11		45			
426,4	Foliation	Moderate				45	60	60	30
427	Foliation	Moderate				46	55	65	25
427,1	Vein		Kalifeldspar	1		46	70	80	10
428,03	Vein		Kalifeldspar	1		46	80	80	10
428,42	Sealed fracture					46	180	5	85
428,55	Sealed fracture	Unmeasurable				46			
428,56	Vein		Biotite	11		46	70	75	15
428,78	Sealed fracture					46	95	10	80
428,8	Foliation					46	70	70	20
428,9	Vein		Biotite	9		46	55	70	20
428,95	Sealed fracture					46	230	50	40
429,21	Sealed fracture					46	95	60	30
429,13	Foliation					46	50	75	15
429,43-431,61	Protected fractures					46			
431,61	Fracture					47	240	70	20
431,73	Sealed fracture					47	95	55	35
431,8	Foliation					47	100	65	25
431,82	Fracture					47	100	65	25
431,94	Fracture					47	100	55	35
432,08	Sealed fracture					47	210	15	75
433	Sealed fracture	Unmeasurable				47			
433,84	Vein		Kalifeldspar/Quartz	1,0-4		47			
434,02	Vein		Kalifeldspar/Quartz	12		47			
433,33	Vein		Kalifeldspar/Quartz	2		47	95	60	30
434,53	Vein		Kalifeldspar/Quartz	3		47	330	70	20
434,86	Vein		Kalifeldspar/Quartz	4		47	75	70	20
434,96	Foliation	Weak				47	80	50	40
435,88	Vein		Kalifeldspar/Quartz	3		47	300	80	10
436,2	Vein		Kalifeldspar/Quartz	4		47	70	55	35
436,26	Vein		Kalifeldspar/Quartz	5		47	40	60	30
436,34	Vein		Kalifeldspar/Quartz	3		47	40	70	20
436,69	Vein		Kalifeldspar/Quartz	17		47	10	85	5
437	Foliation	Moderate				47	5	70	20
438,75	Foliation	Weak/Moderate				47	70	70	20
440,39	Vein		Quartz/plagioclase/kalifeldspar	5		48	10	70	20
442	Foliation	Weak				48	30	60	30
442,7	Foliation	Moderate				48	50	70	20
444,48	Vein		Biotite	0,5		48	155	60	30
444,85	Foliation	Moderate				49	50	65	25
445,39	Vein		Kalifeldspar/Quartz	1		49	35	60	30
447,42	Vein		Quartz	3		49	175	15	75
447,97	Sealed fracture					49	175	15	75
448	Foliation	Weak/moderate				49	30	60	30
448,7	Foliation	Moderate				50	350	60	30
448,75	Sealed fracture					50	145	20	70
448,37	Vein		Quartz	1		50	135	20	70
448,59	Vein		Quartz	1		50	145	15	75
448,89	Vein		Quartz	1		50	140	10	80
449,01	Vein	Cutting the previous one	Plaigoclase/kalifeldspar/quartz	2		50	310	70	20
449,07	Vein		Plaigoclase/kalifeldspar/quartz	2		50	315	75	15
449,3	Foliation	Moderate				50	5	65	25
450,48	Vein		Quartz/plagioclase	2,5		50	0	70	20
450,65	Vein		Quartz/plagioclase	5		50	330	75	15
450,86	Fracture					50	15	60	30
450,97	Sealed fracture					50	350	40	50
451,5	Vein		Aplit/Granite	10		50	310	45	45
451,81	Vein		Aplit/Granite	15		50	310	55	35
453,25	Foliation	Weak				50	15	50	40
453,85	Sealed fracture	Unmeasurable ~1m				50			
455,01	Vein		Quartz	22		50	15	40	50
455,23	sealed fracture					50			
457	Foliation	Weak				50	335	65	25
457,95	Vein		Plagioclase/quartz/kalifeldspar	8		50	310	80	10
458,36	Vein		Plagioclase/quartz/kalifeldspar	20		50	280	80	10
458,37	Sealed fracture					50	70	5	85
459,44	Vein		Plagioclase/quartz/feldspar	8		50	280	55	35
459,7	Foliation	Weak/moderate				50	305	60	30
459,77	Vein		Plagioclase/quartz/kalifeldspar			50	315	50	40
460,14	Sealed fracture					50	55	5	85
460,49	Foliation	Moderate				50	295	65	25
461,04	Vein		Plagioclase/quartz	2		50	280	65	25
461,61	Vein		Plagioclase/quartz	2		50	280	65	25
464,59	Vein		Plagioclase/kalifeldspar/quartz	34		50			
465	Foliation	Weak				50	300	65	25
465,5	Vein		Quartz	2		50	280	45	45
465,6	Sealed fracture					50	45	5	85
466,32	Vein		Quartz	3		50	280	65	25
467,12	Foliation	Moderate				50	275	65	25
467,16	Vein		Plagioclase/quartz	2		50	290	70	20
468,67	Vein		Plagioclase/quartz	1		50	235	70	20
471,61	Vein		Plagioclase/kalifeldspar/quartz	2		50	270	35	55
471,85	Foliation	Moderate				50	230	70	20
472,53-473,31	S-structures					50			
474,65	Fracture					50	175	5	85
475,02	Sealed fracture					50	30	20	70
475,15	Vein		Quartz/kalifeldspar	1		50			
475,73	Vein		Quartz/kalifeldspar	2		50	210	65	25
475,84	Vein		Kalifeldspar/plagioclase	10		50			
476,01	Vein		Kalifeldspar/plagioclase	2		50	235	80	10
476,1	Foliation	Moderate				50	220	65	25
476,46	Vein		Pegmatite	55		50			
477,29	Vein		Pegmatite	95		50			
478,74	Vein		Pegmatite	28		50			
479,06	Fracture					50	210	60	30
479,07	Fracture					50	210	60	30
479,13	Sealed fracture					50	45	10	80
479,17	Vein		Biotite	34		50	210	60	30

479,38	Fracture					50	210	60	30
479,57	Foliation					50	200	65	25
479,63	Sealed fracture	With quartz in it				50	290	5	85
479,65	Vein		Kalifeldspar/quartz	1		50	220	65	25
479,96	Vein		Kalifeldspar/quartz	1		50	170	65	25
480	Foliation					50	185	65	25
480,25-480,41	Crushed					50			
480,9	Foliation	Strong				51	210	65	25
481,77	Vein		Pegmatite	55		51	240	50	40
482,42	Sealed fracture	Unmeasurable				51			
482,57	Vein		Kalifeldspar/plagioclase/quartz	1		51	180	70	20
482,72	Sealed fracture					51	285	55	35
483,4	Sealed fracture					51	340	15	75
483,74	Vein		Kalifeldspar/quartz	2		51	185	40	50
483,95	Foliation	Härifrån och frammåt har 220 grader adderats på betavinkeln, då referenslinjen blivit felutmärkt				51	240	35	55
484,01	Vein		Kalifeldspar/quartz	2		51	60	55	35
484,33	Sealed fracture					51	325	15	75
484,38	Sealed fracture					51	0	25	65
484,48	Vein		Kalifeldspar/plagioclase	2		51	250	75	15
484,93	Vein		Kalifeldspar/plagioclase	1		51	250	75	15
484,93	Sealed fracture/fault	Displacement ~1 cm				51	175	15	75
485,14	Vein		Quartz/kalifeldspar	0,5		51	220	90	0
483,95	Foliation					51	240	35	55
485,3	Sealed fracture					51	305	5	85
485,3-485,5	S-structures					51	220		90
485,74	Fracture					51	95	60	30
486,11	Foliation	Moderate				51	70	70	20
486,35	Sealed fracture					51			
486,55	Sealed fracture	Unmeasurable, ~1,5 m				51			
486,54-487,2	S-structures					51			
487,34	Foliation	Moderate/strong				51	220	60	30
487,43	Fracture					51	230	70	20
487,53	Fracture					51	225	70	20
487,61	Vein		Quartz/plagioclase	1		51	225	85	5
488,07	Sealed fracture					51	225	10	80
488,09	Fracture					51	90	75	15
488,15	Foliation	Moderate/strong				51	240	55	35
488,12	Sealed fracture					51	80	80	10
488,47	Fracture					51	95	65	25
488,5	Fracture					51	105	70	20
488,56	Fracture					51	105	35	55
488,67	Vein		Plagioclase/quartz/kalifeldspar	1		51	160	75	15
489,85	Vein		Plagioclase/quartz/kalifeldspar	1		51	200	75	15
490,18	Vein		Quartz/kalifeldspar	1,5		51	210	70	20
490,53	Sealed fracture					51	195	65	25
490,84	Fracture					51	180	70	20
490,98	Foliation	Strong				52	190	60	30
491,06	Fracture	Unmeasurable				52			
491,13	Fracture					52	195	75	15
491,48	Vein		Quartz/kalifeldspar	5		52	190	75	15
493,23	Vein		Kalifeldspar/plagioclase	1		52	170	80	10
493,55	Foliation	Strong				52	180	60	30
495,23	Vein		Quartz	3		52			
495,26-495,33	Crushed					52			
495,46-495,66	Folded					53			
495,73	Foliation	Strong				53	140	70	20
495,78	Vein		Quartz/pegmatite	15		53			
495,93	Vein		Biotite	39		53			
495,96	Fracture					53	140	70	20
495,98	Fracture					53	140	70	20
496,01	Fracture					53	140	70	20
496,03	Fracture					53	140	70	20
496,13	Fracture					53	140	70	20
496,32	Vein		Quartz	15		54	130	70	20
496,49	Fracture					54	160	80	10
496,47	Vein		Biotite	45		54			
496,67	Fracture					54	140	55	35
496,72	Fracture					54	140	55	35
496,73	Fracture					54	140	55	35
496,83	Fracture					54	315	10	80
496,93	Foliation					54	140	55	35
497,09	Fracture					54	140	55	35
497,42	Sealed fracture					54	210	25	65
497,93	Vein		Plagioclase	1,0-5		54			
498,02	Sealed fracture					54	115	70	20
498,42		Strong foliation or mylonite				54			
499	Foliation					54	110	55	35
499,6	Vein		Quartz	3		54	95	60	30
500,47	Vein		Plagioclase	1,0-3		54	130	60	30
500,93	Foliation					54	115	60	30
501,96	Sealed fracture					55	210	20	70
501,96	Foliation	Strong				55	125	55	35
502,35	Foliation	Weak/moderate				55	120	50	40
503,3-504,31	Veins	Small veins 2-4/m	Plagioclase	0,5-1		55	80	65	25
505,16	Vein		Kalifeldspar/plagioclase	3,0-4		56	40	65	25
505,26	Foliation	Moderate				56	40	50	40
505,71	Vein		Quartz	1,0-4		56	70	65	25
505,81	Fracture					56	65	55	35
505,82	Vein		Biotite/quartz	8		56	65	55	35
505,95	Foliation					56	60	55	35
507,37	Vein		Pegmatite	30		56	60	65	25
507,75	Vein		Pegmatite	25		56	100	70	20
508,19	Vein		Pegmatite	18		56			
508,5-509,3	Folded veins		Kalifeldspar/plagioclase/quartz	1		57			
508,61	Fracture					57	270	70	20
509,41	Foliation					58	370	70	20
509,86	Vein		Kalifeldspar/plagioclase	5		58	50	70	20
510,29	S-folded pegmatite		pegmatite	20		58			
510,5	Foliation				45C	58	30	45	45
510,52	Fracture					58	30	40	50
510,72	Foliation	Strong				58	30	50	40
510,75	Foliation EXTRA measured					58	30	35	55
510,95	Foliation EXTRA measured					58	30	35	55
511	Foliation EXTRA measured					58	30	40	50
511,51	Foliation EXTRA measured					58	220	10	80
511,65	Foliation EXTRA measured					58	35	30	60
511,75	Foliation EXTRA measured					58	35	35	55
512	Foliation EXTRA measured					58	20	20	70
512,3	Foliation EXTRA measured					58	25	25	65
512,6	Foliation EXTRA measured					58	20	15	75
510,65		Micro shear zone		20		58			
511,17	Fracture					58	30	50	40
511,59	Fold					58			
511,44	Vein		Kalifeldspar/quartz	0,5		58	145	55	35

512,4	Vein		Plagioclase/quartz	3		58	220	90	0
512,5	Vein		Quartz	0,5		58	20	20	70
512,8	Foliation	Strong				58	25	30	60
512,83-513,75	Folds	Micro				58			
513,38	Vein		Quartz	1		58	30	40	50
513,74-518,2	Strongly folded	Folded folds				58			
514,5	Foliation					58	10	55	35
514,46	Veins	Veins fused together	Quartz	2		58	10	55	35
514,65	Vein		Pegmatite	23		58			
514,89-516,13	Folded veins					58			
515,7	Fracture	Unmeasurable				58			
516,13-517,54	Protected with plastic					58			
517,76	Fracture					59	0	25	65
517,92	Fracture	In foliation plane			30C	59	10	25	65
518,08	Veins		Quartz veins merged together			59			
518,2	Foliation	Strong				59	5	35	55
518,33	Sealed fracture					59	190	15	75
518,63	Foliation 1	Moderate				59	340	40	50
518,63	Foliation 2	Weaker than above foliation				59	195	30	60
518,64	Sealed fracture					59	85	5	85
518,69	Fracture					59	165	60	30
518,95	Fracture					59	170	15	75
518,97	Vein	with magnetite	Quartz	5		59	310	55	35
519,14	Vein		Quartz/plagioclase	0,5		59	335	65	25
519,4	Foliation	Weak				59	355	50	40
519,79	Vein		Quartz	1,0-4		59			
520,01	Vein		Quartz/kalifeldspar	1		59	340	50	40
520,69	Foliation	Very weak, unmeassurable				59			
521,55	Vein		Pegmatite	4		59	335	60	30
521,9	Vein		Quartz	1		59	330	60	30
521,95	Foliation	Very weak				59	340	35	55
522,45	Sealed fracture					59	155	35	55
522,52	Vein	Red	Kalifeldspar/quartz	8		59	250	70	20
522,85	Foliation	Weak/moderate				59	355	50	40
522,98	Vein	Red	Kalifeldspar/quartz	1		59	330	65	25
523,08	Vein	Red	Kalifeldspar/quartz	2		59	320	70	20
523,29	Vein	Red	Kalifeldspar/quartz/plagioclase	1		59	250	65	25
523,44	Vein	Red	Kalifeldspar/quartz/plagioclase	1		59	250	65	25
523,75	Vein	Red	Kalifeldspar/quartz/plagioclase	4		59	250	65	25
523,81	Vein	Red	Kalifeldspar/quartz/plagioclase	2		59	250	65	25
524,42	Vein	Red	Kalifeldspar/quartz/plagioclase	0,5		59	345	60	30
524,57	Vein	Red	Kalifeldspar/quartz/plagioclase	1		59	345	60	30
524,62	Vein	Red	Kalifeldspar/quartz/plagioclase	6		59	345	60	30
524,87	Vein	Red	Kalifeldspar/quartz/plagioclase	3		59	345	60	30
525,15	Vein		Pegmatite	6		59	250	70	20
525,59	Foliation	Moderate/strong				59	335	60	30
525,63	Fracture					59	335	60	30
525,66	Sealed fracture					59	70	10	80
525,69	Vein	With sigma clasts	Biotite	21		59	350	65	25
526,71	Vein		Kalifeldspar/plagioclase	0,5		59	310	65	25
526,71	Foliation	Moderate				59	350	60	30
527,42	Vein		Kalifeldspar/plagioclase	2		59	350	60	30
529,07	Vein		Pegmatite/kalifeldspar	8		59	305	70	20
528,85	Foliation	Moderate				59	320	65	25
530	Vein		Quartz/kalifeldspar	3		59	315	65	25
530,25	Vein		Biotite	20		59	315	65	25
530,78	Foliation	Weak				59	335	70	20
530,68	Vein		Quartz/plagioclase	2		59	220	90	0
531,91	Fracture					60	180	15	75
532,08	Foliation	Weak/moderate				60	350	65	25
532,5	Vein		Quartz/plagioclase	5		60	15	60	30
532,55	Sealed fracture					60	15	60	30
532,62	Vein		Biotite	29		60	15	60	30
532,91	Fracture					60	15	60	30
534,04	Vein	with magnetite	Quartz/pegmatite	13		60	25	70	20
534,31	Vein	with magnetite	Quartz/pegmatite	16		60	25	70	20
534,47	Vein		Biotite	7		60			
534,62	Vein		Aplit	10		60	20	25	65
534,78	Vein		Aplit	3		60	20	25	65
535,12	Vein		Aplit	3		60	20	25	65
535,56	Sealed fracture	with some quartz				60	125	10	80
535,81	Fracture					60	20	40	50
536,06	Foliation	Weak/moderate				60	55	60	30
537,19	Vein		Quartz/kalifeldspar	1		60	75	50	40
537,5	Foliation	Weak				60	70	60	30
538,9	Foliation	Weak				61	125	65	25
539,2	Vein	redish	Quartz	5		61	125	50	40
541,35	Vein		Quartz	1		61	350	60	30
541,38	Vein		Quartz	1		61	350	60	30
541,43-542,07	Crushed	A bit crushed quartz and some natural fractures				61			
542,05	Foliation	Weak/moderate				62	0	55	35
542,67	Sealed fracture					62	65	25	65
542,72	Sealed fracture					62	65	25	65
543,13	Vein		Quartz/kalifeldspar	1		62	285	80	10
544	Foliation	Moderate				62	5	65	25
545,4	Foliation	Weak/moderate				63	10	75	15
547,14	Vein		Biotite	34		63	335	55	35
547,49	Fracture					63	335	55	35
547,62	Vein		Quartz/plagioclase	7		63	300	70	20
548,21	Vein	red	Quartz/plagioclase	2		63	290	70	20
548,36	Vein		Quartz/plagioclase	1		63	350	60	30
548,4	Foliation					63	0	55	35
548,9	Vein		Quartz/plagioclase	9		63	250	70	20
549,34	Vein		Quartz/plagioclase	6		63	320	80	10
550,11	Vein		Quartz/plagioclase	2		63	260	80	10
550,3	Vein		Quartz/plagioclase	13		63	260	80	10
550,54	Vein		Quartz/plagioclase	2		63	270	85	5
551,07	Vein		Quartz/plagioclase	5		63	270	85	5
551,6	Foliation	Moderate				63	340	70	20
551,9	Foliation	Moderate				64	315	60	30
552,25	Vein		Quartz	1		64	310	60	30
552,72	Vein	red	Quartz/kalifeldspar	1		64	335	65	25
552,79	Vein	red	Quartz/kalifeldspar	1		64	335	70	20
552,86	Vein	red	Quartz/kalifeldspar	1		64	290	80	10
553,57	Vein	red	Quartz/kalifeldspar	5		64	300	60	30
555,55	Vein		Quartz	6		64	270	70	20
555,72	Vein		Quartz	8		64	270	70	20

Appendix C

Orientation correction

Orientation correction where the first foliation measurement is oriented in the same direction as the last foliation measurement of the previous reference line

Reference line	Orientation correction [ ]
1	0
2	15
3	30
4	45
5	65
6	70
7	50
8	60
9	-270
10	-280
11	-285
12	95
13	105
14	-230
15	-225
16	-250
17	-215
18	-200
19	-200
20	170
21	155
22	145
23	150
24	150
25	130
26	170
27	130
28	75
29	120
30	95
31	100
32	110
33	145
34	145
35	150
36	130
37	160
38	-175
39	-120
40	-100
41	-25
42	
43	-30
44	50
45	65
46	70
47	20
48	60
49	60
50	-260
51	75
52	125
53	165
54	165
55	155
56	235
57	
58	285
59	290
60	-85
61	220
62	-15
63	-20
64	5

Appendix D

Mechanical properties

Depth [m]	P-wave propagation time [s]	Average [R]	Rebound hardness [Hr]	Comments	Date
5,2	10,943	54,1	54,7		12.04.21
12,39	10,25	53,1	53,7		12.04.21
16,05	11,591	55	55,6		12.04.21
19,99	12,993	52,6	53,1		12.04.21
25,19	14,016	54,1	54,7		12.04.21
30,6	11,575	54,1	54,7		12.04.21
32,85	12,33	56	56,6		12.04.21
39,7	13,17	54	54,6		12.04.21
45,65	12,742	57,9	58,5		12.04.21
50,43	14,133	48,3	48,8		12.04.21
51,67	13,613	51,2	51,7		12.04.21
57,7	13,282	58,8	59,4		12.04.21
62,96	11,363	56,9	57,1		13.04.21
67,94	11,569	56,9	57,5		12.04.21
70,8	12,8	56,9	57,5		12.04.21
75,6	11,446	57,9	58,5		12.04.21
81,35	11,909	56	56,6		12.04.21
86,26	12,773	53,1	53,7		12.04.21
93,77	12,331	54,1	54,7		12.04.21
96,12	11,923	56	56,6		12.04.21
102,46	13,971	52,1	52,6		12.04.21
107,45	10,642	51,2	51,7		12.04.21
111,35	11,838	56,9	57,5		12.04.21
114,4	11,042	50,1	50,6		12.04.21
117,68	11,293	47,4	47,9		12.04.21
125,43	13,235	56	56,2		13.04.21
128,32	10,864	52,1	52,6		12.04.21
134,53	10,961	50,2	50,7		12.04.21
136,29	11,32	50,2	50,7		12.04.21
137,81	11,059	54,1	54,7		12.04.21
144,29	12,567	41,9	42,3	Fractured while testing	12.04.21
144,6	11,164	58,8	59,4		12.04.21
148,87	12,207	51,2	51,7		12.04.21
150,39	12,167	48,3	48,8		12.04.21
156,2	12,009	52,1	52,6		12.04.21
162,09	11,205	56	56,6		12.04.21
164,5	11,84	51,1	51,6		12.04.21
172,04	11,86	50,2	50,7		12.04.21
173,2	13,427	43,2	43,6		12.04.21
181,54	11,672	54,4	55	Fractured while testing	12.04.21
184,85	10,659	54,1	54,7		12.04.21
188,07	11,707	57,9	58,5		12.04.21
191,45	12,577	60,3	60,1		20.04.21
198,53	10,773	58,7	58,5		20.04.21
201,55	11,275	57,7	57,5		20.04.21
205	10,775	59,8	59,6		20.04.21
211,1	11,658	57,5	57,3		20.04.21
217,35	11,129	49,9	49,7		20.04.21
221,32	10,5	54,9	54,7		20.04.21
226,04	11,147	57,7	57,5		20.04.21
228,82	10,72	57	56,8		20.04.21
233,47	11,322	55,9	55,7		20.04.21
237,49	11,681	58,6	58,4		20.04.21
245,38	11,635	59,4	59,2		20.04.21
247,27	11,496	59,7	59,5		20.04.21
253,45	12,375	58,6	58,4		20.04.21
258,47	12,107	58,9	58,7		20.04.21
263,65	12,071	52	51,8		20.04.21
269,37	12,032	50,5	50,3		20.04.21
272,42	12,533	51,1	50,9		20.04.21
275,28	13,036	48,8	48,6		20.04.21
282,46	12,8	49,9	49,7		20.04.21
285,13	14,063	51,8	51,6	Fractured while testing	20.04.21
290,75	26,493	51	50,8	Sealed fractures	20.04.21
295,27	11,942	52,2	52		20.04.21
297,85	12,88	51,6	51,4		20.04.21
303,4	12,529	52,3	52,1		20.04.21
309,66	12,286	55,7	55,5		20.04.21
315,37	12,807	52,3	52,1		20.04.21
316,35	13,838	50,6	50,4		20.04.21
322,84	13,841	52,7	52,5		20.04.21
329,45	12,913	58,4	58,2		20.04.21
334,2	12,9	53	52,8		20.04.21
336,2	13,04	59,6	59,4		20.04.21

Anvil standard for Schmidt hammer	Verifying test	Date	Correction factor Schmidt hammer
58	57,4	12.04.21	1,010452962
58	57,8	13.04.21	1,003460208
58	58,2	20.04.21	0,996563574
58	58,1	26.04.21	0,99827883

340,97	13,5	58,5	58,3		20.04.21
343,33	16,24	39,3	39,1		20.04.21
348,26	13,38	58,1	57,9		20.04.21
352,3	12,836	58,6	58,4		20.04.21
355,13	13,679	54,7	54,5		20.04.21
360,02	13,463	51,7	51,5		20.04.21
364,05	12,546	56,2	56		20.04.21
370,49	10,65	60,3	60,2		26.04.21
376,12	11,007	54,3	54,2		26.04.21
378,06	10,35	58	57,9		26.04.21
384,67	10,69	57	56,9		26.04.21
387,13	10,665	59,8	59,7		26.04.21
390,95	11,26	57	56,9		26.04.21
396,56	11,54	56,2	56,1		26.04.21
403,26	11,35	57,6	57,5		26.04.21
408,27	10,775	47,7	47,6		26.04.21
414,5	15,582	46,6	46,5		26.04.21
423,09	15,929	39,3	39,2		26.04.21
427,46	13,63	51,7	51,6		26.04.21
433	30,758	44,6	44,5		26.04.21
437,72	14,71	47,4	47,3		26.04.21
442,28	12,85	52,1	52		26.04.21
445,08	12,97	52,6	52,5		26.04.21
449,77	11,2	56,8	56,7		26.04.21
455,5	11,433	53	52,9		26.04.21
457,3	11,236	56	55,9		26.04.21
462,06	12,682	53,9	53,8		26.04.21
469,91	13,15	53,6	53,5		26.04.21
471,42	12,682	51,1	51		26.04.21
476,24	12,33	54,9	54,8		26.04.21
483,6	10,518	55	54,9		26.04.21
489,59	11,282	54,2	54,1		26.04.21
493,2	13,145	55,9	55,8		26.04.21
498,15	18,92	42,75	42,7		26.04.21
501,95	17,84	46,38	46,3		26.04.21
505,56	12,27	48	47,9		26.04.21
512,05	16,28	41,7	41,6		26.04.21
514,5	12,256	49,8	49,7		26.04.21
522	12,964	51,6	51,5		26.04.21
526,66	12,55	50,2	50,1		26.04.21
531,33	11,89	54,5	54,4		26.04.21
536,16	12,68	54,2	54,1		26.04.21
538,6	14,36	49,5	49,4		26.04.21
545,08	12,47	49,7	49,6		26.04.21
547,88	11,936	49	49,3		26.04.21
555,06	15,582	52	51,4		26.04.21

Appendix E


GE1.
Start 1.65– 4,40
Box1
GE1.
4,40– 9,12
Box2
5,08
6,50
GE01.
9,12 - 13,72
Box3
9,50
12,50


GE1
13,72 - 18,50
B
15,50
18,50
GE1
18,50 - 23,22
Box5
21,50
GE1
23.22-27,91
Box6
24,50
27,50


GE1
27,91-32,62
BOX 7
30,50


GE1
32,62 -37,35
BOX 8
33.50
36.50


GE1
37,35-42,01
BOX 9
39,50


GE 1
42,01 - 46,69
Box 10
42,50
45,50
GE1
46,69 - 51,50
Box 11
48,50
51,50
GE 1
51,50 - 56,09
Box 12
52,45
54,50


GE1
56,09 - 60.84
Box 13
57,50
60,50
60,50
GE1
60,84 — 65,65
Box 14
63,50
GE1
65,65 - 70,35
Box 15
66,50
69,50


GE1
70,35 – 75,14
Box 16
72,50
GE1
75,14 - 79,92
Box 17
GE1
79,92- -84,50
Box 18
81,50
84,50

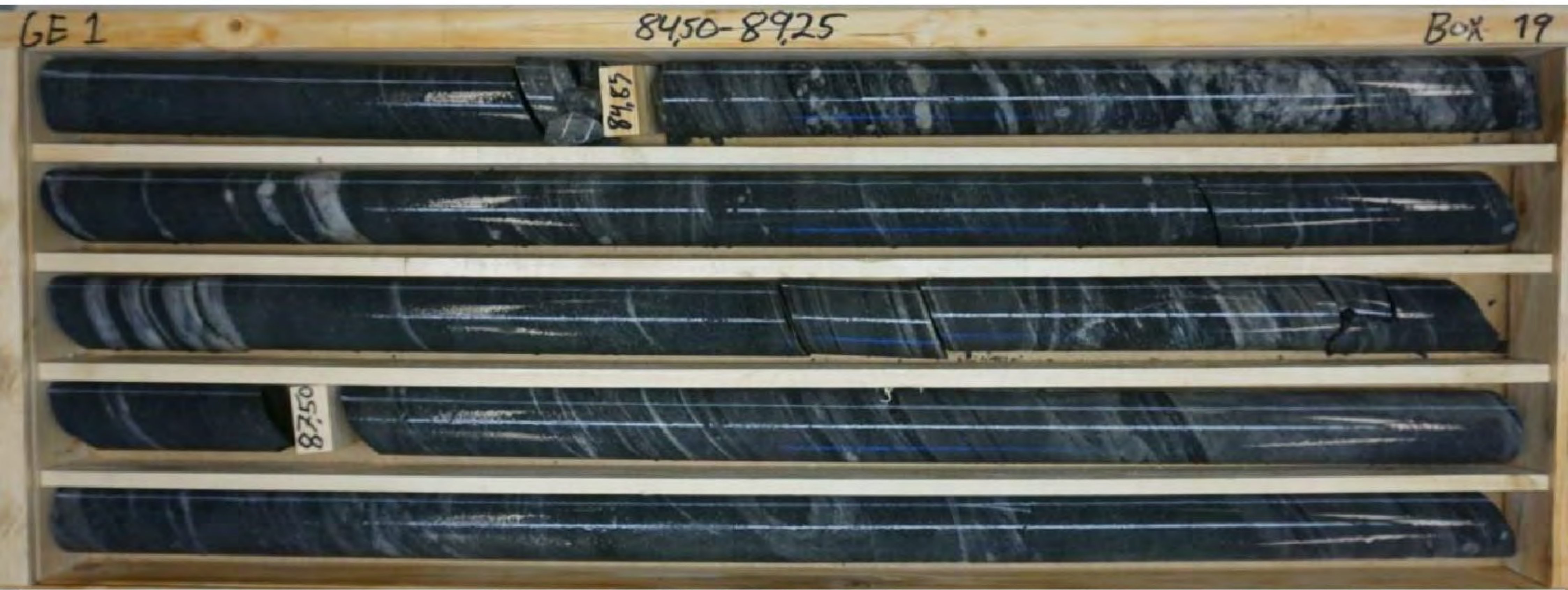
GE 1
84,50-89,25
Box 19
84,57
87,50

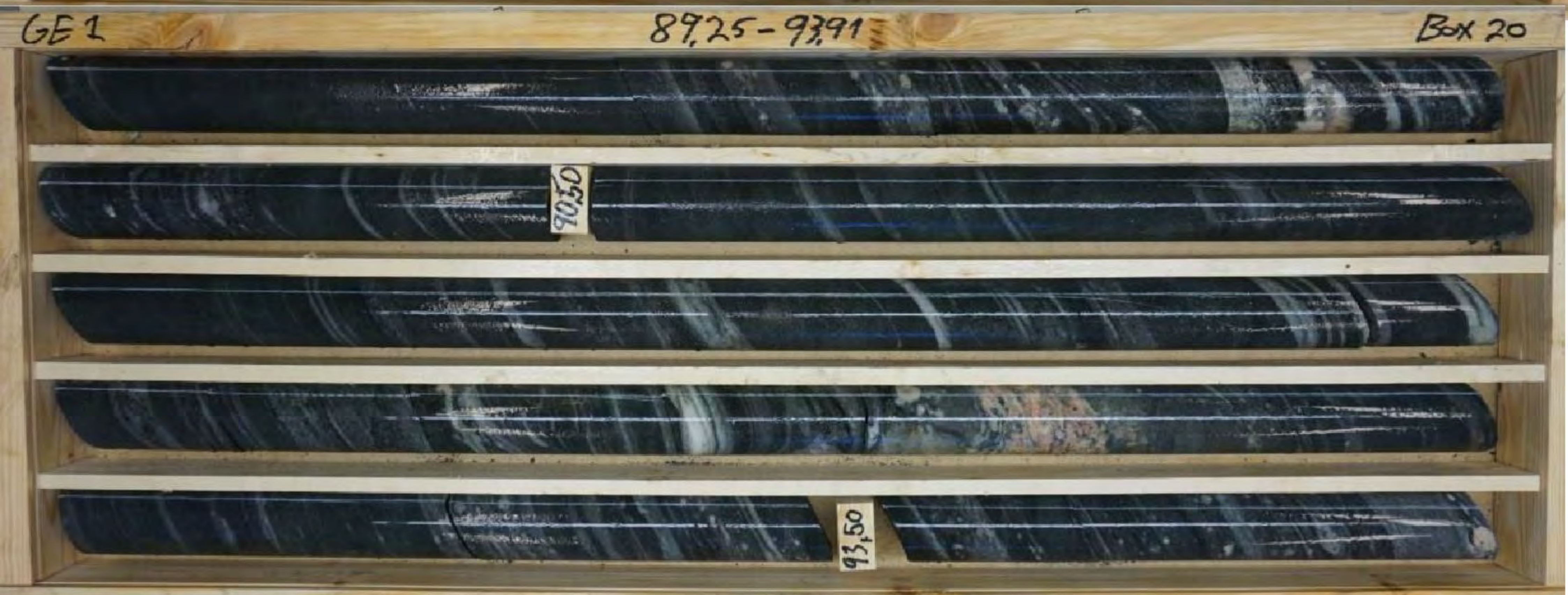
GE 1
89,25-93,91
Box 20
90,50
93,50


GE 1
93.91- 98.62
Box 21
96.50


GE 1
98,62 –103,50
Box 22
99,50
102,50
GE1
103,50—108,10
Box 23
105,50
GE1
108,10– 112,65
Box 24
108,50
111,50


GE1
112,65 - 117,28
Box25
114,50
115,25m
CC+Py
GE 1
117,28 - 121,91
Box 26
117,50
120,50
GE1
121,91-126,50
Box 27
123,50
126,50


GE1
126.50– 131, 10
Box 28
129,50
GE1
131,10 - 135,69
Box 29
132,50
135,50
GE1
135,69– 140,32
Box 3
138,50


GE1
140,32 – 144,89
Box 3
141,50
144,50
GE1
144,89 – 149,60
Box 32
147,50
GE1
149,60 – 154,13
Box33
150,50
153,50


GE1
154,13 – 158,90
Box34
156,50
GE1
158,90 – 163,48
Box35
159,50
162,50
GE1
163,48 – 168,10
Box36
165,50


GE1
168,10 – 172.63
Box 37
168,50
171,50
GE1
172,63 – 177,11
Box 38
173,00
174,40
GE1
177,11 – 181,71
Box 39
177,50
180,50


GE1.
181,71-186,30
BOX 40
182,53
185,65


GE1
186,30 - 190.97
BOX 41
188.30


GE1
190,97 - 195,50
BOX 42
191,35
193.98
195,50


GE1
195,50 - 200,23
BOX 43
GE1
200,23 - 204,85
BOX 44
201,85
GE1
204,85 - 209,57
BOX 45
207,85


GE1
209,58-214,29
Box 46
213,85
GE1
214,29-218,94
Box 47
215,90
216,75
GE1
218,94-223,80
Box 48
222,85

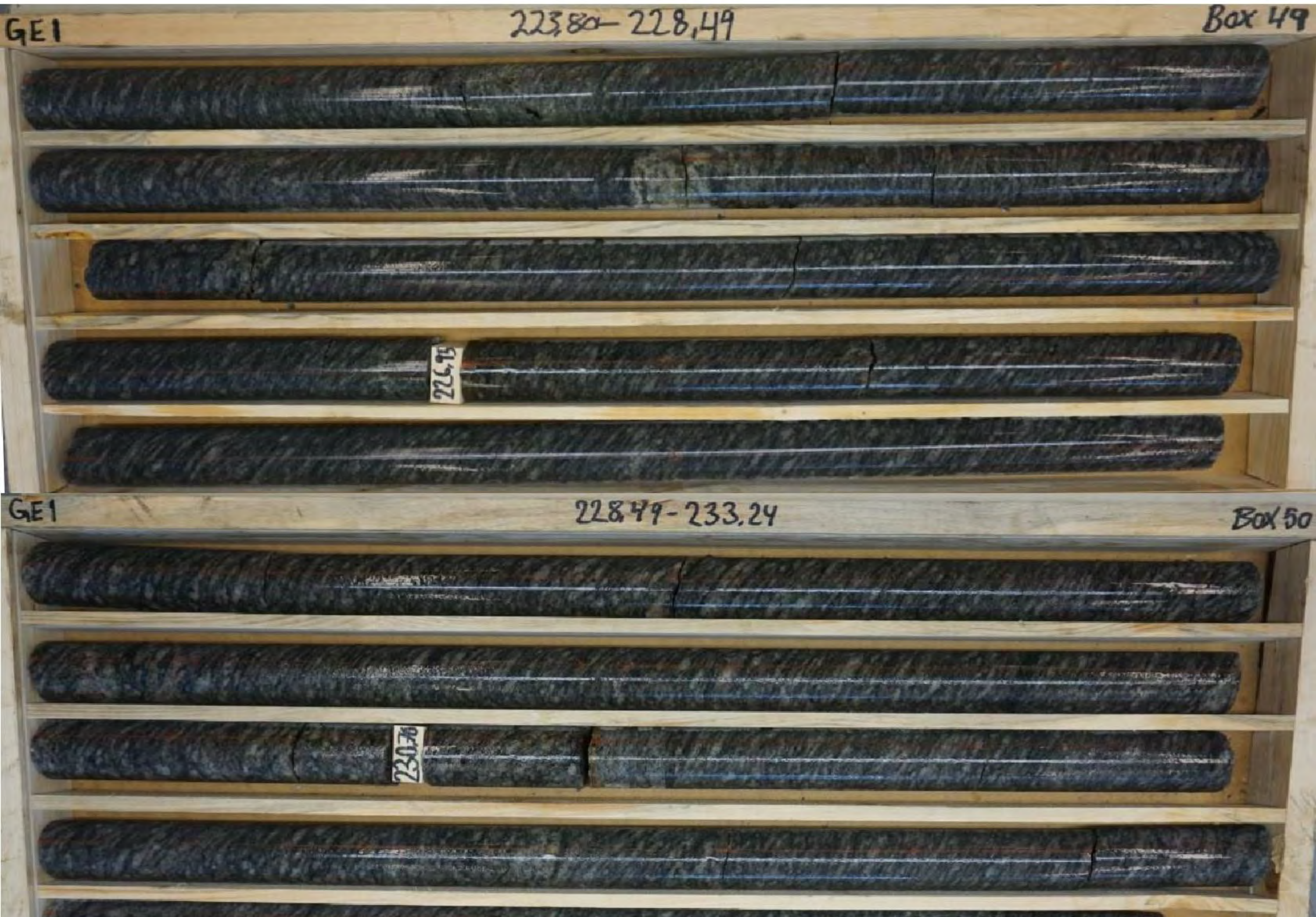
GE1
223,80–228,49
Box 49
226,95
GE1
228,49-233,24
Box 50
230,76
GE1
233,24–237,98
Box5
234,85


GE1
237,98 – 242,73
Box 52
240,85
GE1
242,73 – 246,57
Box
GE1
246,57 - 251,27
Box 5
246,85

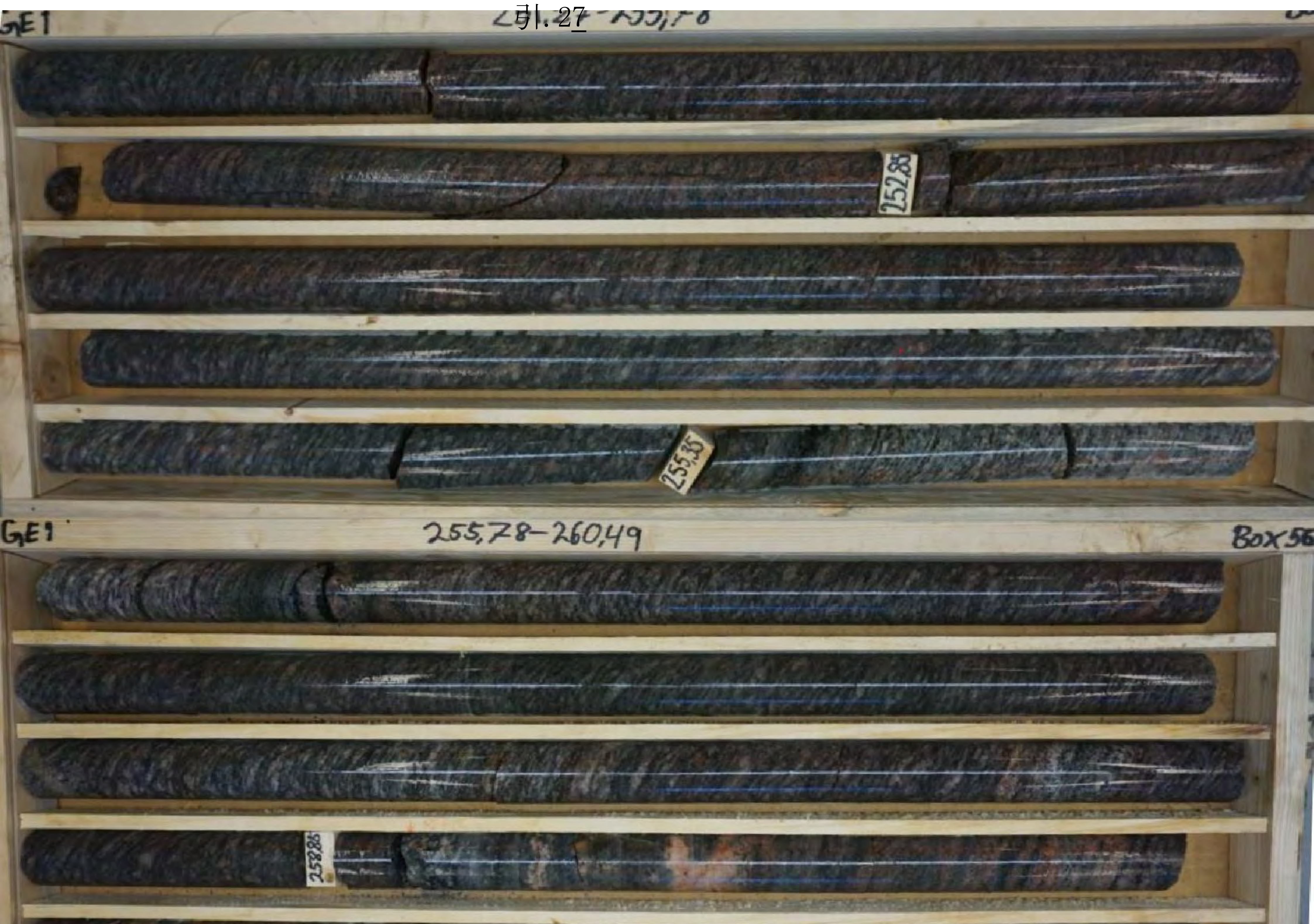
GE1
GE1
255,78-260,49
Box 56
GE1
260,49-265,25
Box 57
252,85
255,35
258,86
264,95

一


GE1
265,25 - 269,99
Box58
267,08
GE1
269,99 - 274,61
BOX59
270,85
GE1
274,61 - 279,28
BOX60
276,38

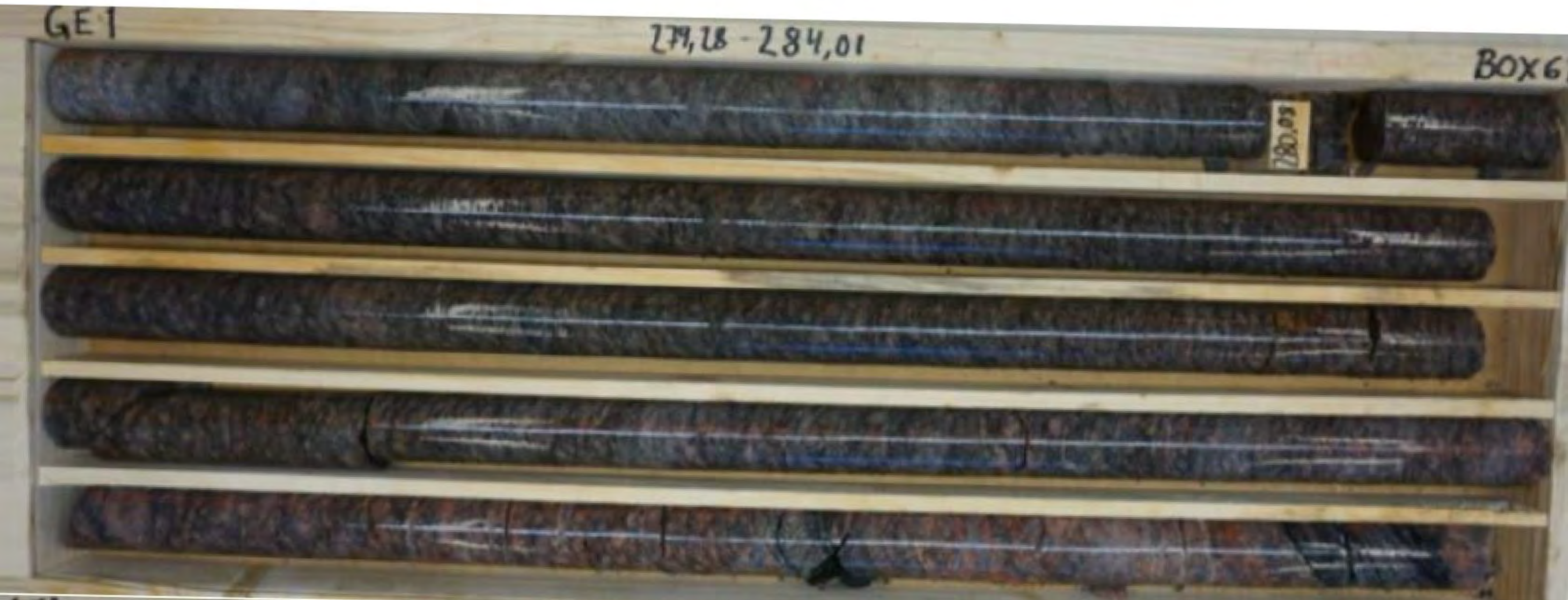
GE1
279,28 - 284,01
BOX6
280,05


GE1
284.01- 289,30
Box62
285,85


GE1
289,30-293,09
Box63
291,00


GE1
293,09– 297,40
BOX64
297,14
GE1
297,40 – 301,98
Box65
298,02
GE1
301,98–306,66
Box 66


GE1
306,66-311,42
Box 67
309,85


GE1
311,42 - 316,17
Box 68
315,85


GE1
316,17 - 320,76
Box 69


GE1
320,76-325,42
BOX 70
321,85
324,85


GE1
325,42-330,15
BOX 71


GE1
330,15 - 334,85
BOX 72
330,85


GE1
334,85 - 339,50
BOX 7
GE1
339,50 - 344,01
BOX 74
GE1
344,01 - 348,55
BOX 75


GE1
348,55 - 353,31
Box 76
351,60
GE1
353,31 - 357,61
Box 77
GE1
357,61 - 362,39
Box 78
357,75

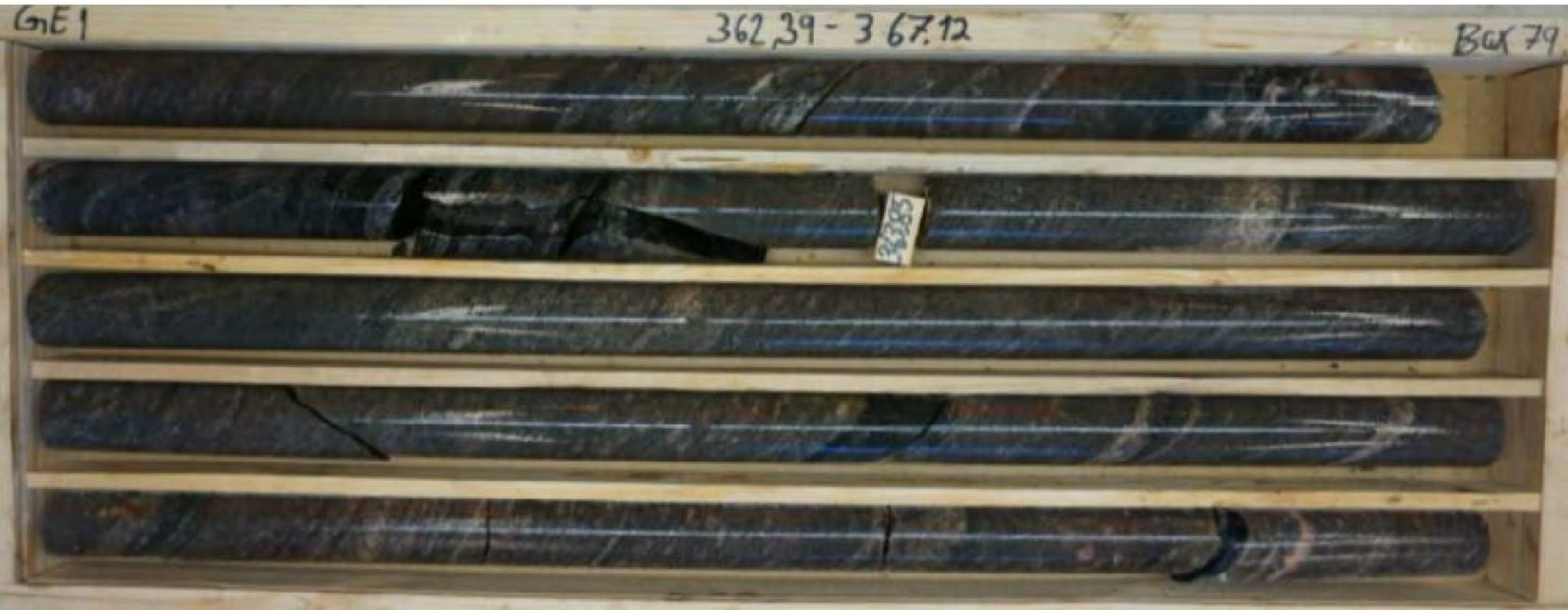
GE1
362,39 - 367,12
Box 79


GE1
367,12 - 371,68
Box 80


GE1
371,68 - 376,62
Box 81


GE1
376,62–381,29
BOX 82
381,27
GE1
381,29–386,09
BOX 83
GE1
386,09-396,75
BOX 84
387,75


GE1
390,75–395,28
Box 85
GE1
395,28–400,16
Box 86
GE1
400,16–404,97
Box 87


GE1
404,97-409,59
405,86
GE1
409,59-414,27
410,57
412,85
GE1
414,27-418,87
BOX 90
417,85

1/37


GE1
418,87 - 423,84
BOX 91
421,25


GE1
423,84-428,63
Box 92
426,85


GE1
428,63 - 433,12
Box 93
432,85

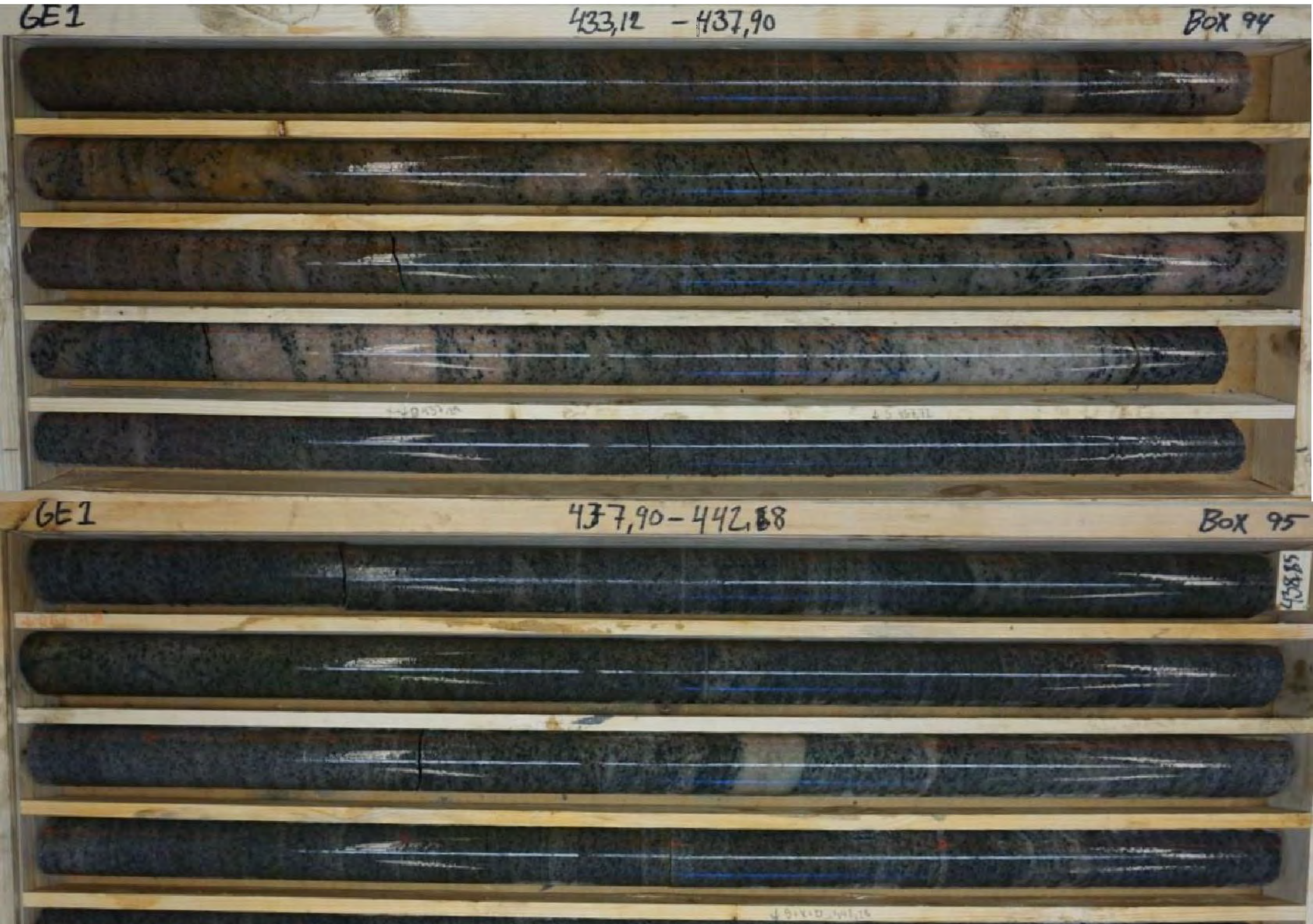
GE1
433,12 - 437,90
Box 94
GE1
437,90-442,68
Box 95
438,85
GE1
442,68-447,42
Box 96
444,38


GE1
447,42 - 451,94
Box 9
448,61
GE1
451,94-456,90
Box 98
453,85
GE1
456,80-461,61
Box 99
459,75

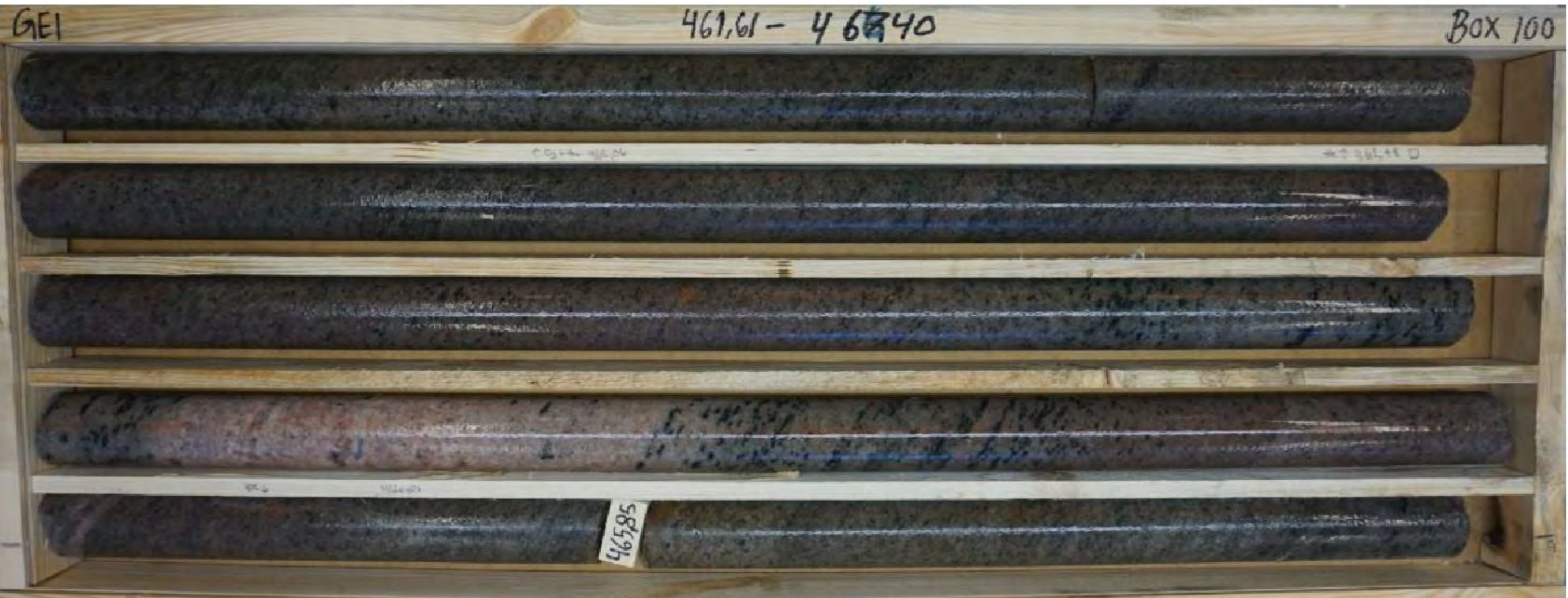
GE1
461,61 – 466,40
Box 100
465,85


GE1
466,40 – 471,12
Box 101


GE1
471,12 – 475,84
Box 102
471,85


GE1
475,84 - 480,57
BOX 103
477,95
GE1
480,57 -485,29
Box 104
483,85
GE1
485,29- 490,04
Box 105
489,85


GE1
490,04-494,80
BOX106
493,55
GE1
494,80 - 499,52
Box 107
498,85
GE1
49952-504,31
BOX108


GE1
504,31-508,93
BOX 10
504,85
GE1
508,93-513,75
BOX 1
510,85
GE1
513,74- 518,43
BOX 111
516,85


GE1
518,43-523,19
BOX 112
522,85
GE1
523,17-527,95
BOX 113
GE1
527,95-532,71
BOX 114
528,85


GE1
532,71-537,43
BOX 11
534,85
GE1
537,43-542,04
BOX 11
538,83
GE1
542,04- 546,75
BOX 117
545,30

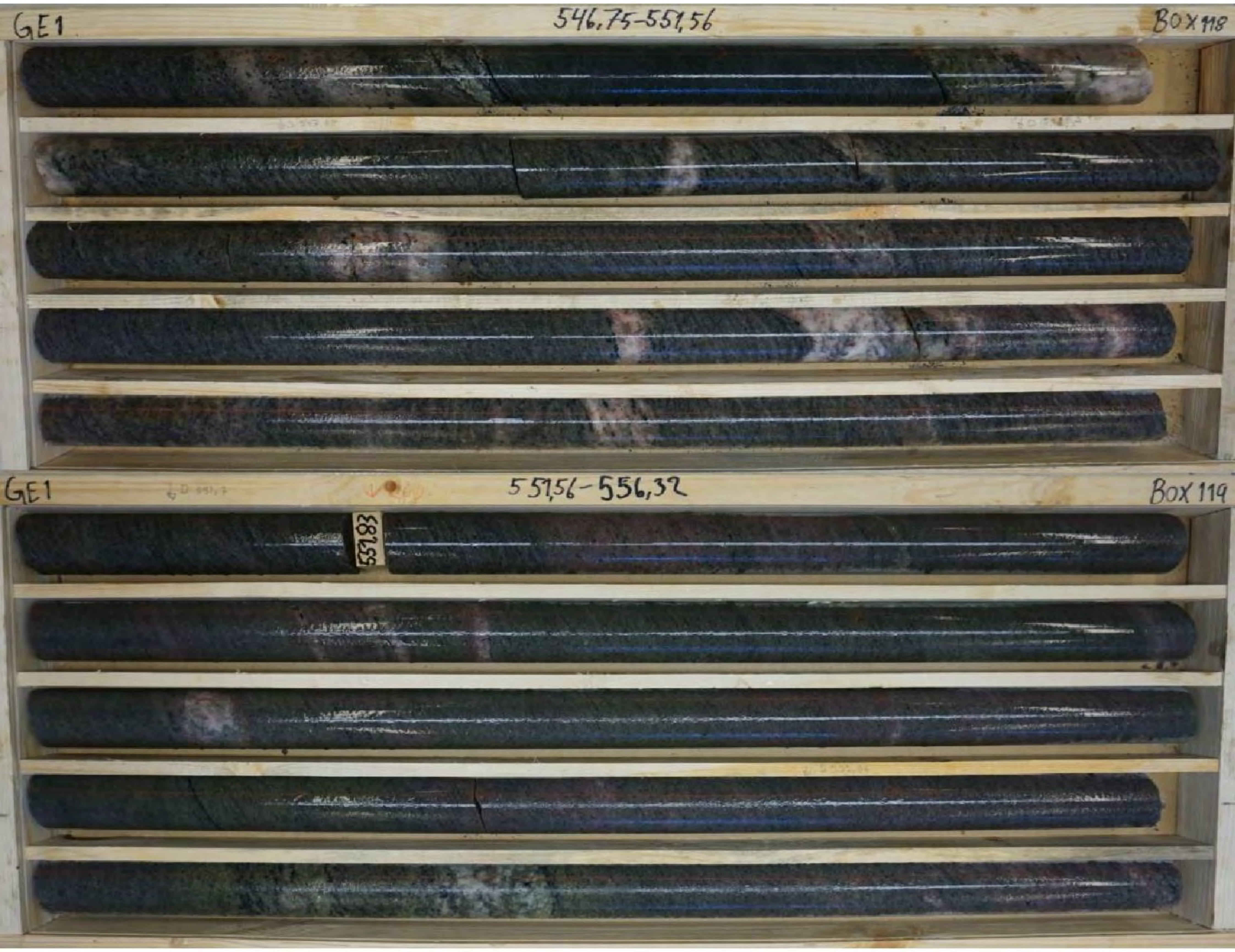
GE1
546,75-551,56
Box 118
GE1
551,56-556,32
Box 119
551,83